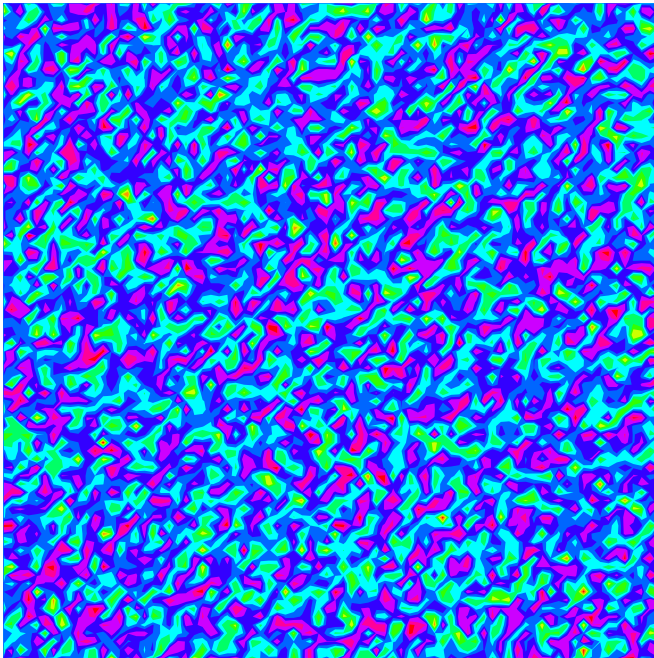


AMPLITUDE AND
PHASE FLUCTUATIONS
IN
HIGH TEMPERATURE
SUPERCONDUCTORS



Philippe Curty

Université de Neuchâtel

Thèse présentée par Philippe Curty
à la Faculté des Sciences
de l'Université de Neuchâtel
pour l'obtention du titre de Docteur ès sciences.

sous la direction du
professeur Hans Beck
de l'Université de Neuchâtel.

Experts:
Prof. Piero Martinoli (Neuchâtel),
Dr Pierbiagio Pieri (Camerino, Italie),
Dr Nicolas Macris (EPFL).

Université de Neuchâtel, 2000 Neuchâtel, Switzerland,
Copyright Philippe Curty, 2003

Preface

The purpose of this thesis is to study amplitude and phase fluctuations in the context of high temperature superconductivity. Since some methods already exist, I have tried to separate clearly standard computations that can be found in articles or books from my own calculations. The latter are to be found in chapter 3 which has been partly published in Physical Review Letters [1], chapter 4 (partly published in Physical Review Letters [2] and reference [3]) and chapter 5. One exception is the CPA method whose introduction is presented in section 5.1. Concerning the notation, bold letters are reserved for vectors and matrices. Indices will be often omitted in order to have a lighter formalism.

Philippe Curty 2003

Contents

| | | |
|----------|--|-----------|
| 1 | INTRODUCTION | 1 |
| 2 | BASIC CONCEPTS | 3 |
| 2.1 | High Temperature Superconductors | 3 |
| 2.1.1 | Historical Overview | 3 |
| 2.1.2 | The Pairing Mechanism | 5 |
| 2.1.3 | The Pseudogap Regime | 6 |
| 2.2 | Ginzburg-Landau and ϕ^4 Models | 9 |
| 2.2.1 | Landau Theory of Phase Transition | 9 |
| 2.2.2 | Fluctuations: Beyond Mean Field | 10 |
| 2.2.3 | Harmonic Approximation and Critical Region | 11 |
| 2.2.4 | Renormalisation Group | 14 |
| 2.3 | Condensed Matter Concepts | 15 |
| 2.3.1 | The Interaction Representation | 15 |
| 2.3.2 | Imaginary Time Formalism | 15 |
| 2.3.3 | Matsubara Formalism and Temperature Green Functions | 17 |
| 2.3.4 | Path Integral in Superconductivity | 18 |
| 2.3.5 | The Hubbard-Stratonovich Transformation | 20 |
| 2.3.6 | Gorkov Equation of Motion | 22 |
| 2.3.7 | Bogoliubov-de Gennes Equations | 25 |
| 2.3.8 | BCS Solution | 26 |
| 2.4 | Monte Carlo Simulations | 27 |
| 2.4.1 | Metropolis Algorithm | 27 |
| 2.4.2 | Metropolis for the Ising Model | 29 |
| 2.4.3 | Exploring Configurations: Ergodicity | 29 |
| 2.4.4 | No Time Reversal Symmetry Breaking: Detailed Balance | 30 |
| 2.4.5 | Metropolis for the GL Model | 30 |
| 2.4.6 | Cluster Algorithm | 32 |
| 3 | VARIATIONAL APPROACH FOR THE GL MODEL | 37 |
| 3.1 | Choosing the Right Variational Approach | 37 |
| 3.2 | Overview | 39 |
| 3.3 | Effective Action | 40 |

| | | |
|----------|--|-----------|
| 3.4 | Self Consistent Approximation | 41 |
| 3.5 | Fluctuations Around the Saddle Point | 43 |
| 3.6 | Validity of the Method | 47 |
| 3.7 | Qualitative Criterion on Amplitude and Vortices | 49 |
| 3.8 | Outline | 50 |
| 4 | THERMODYNAMICS OF HIGH T_c SUPERCONDUCTORS | 51 |
| 4.1 | Motivation | 53 |
| 4.2 | Model and Effective Action | 54 |
| 4.3 | Variational Method | 56 |
| 4.4 | Average Value Method | 57 |
| | 4.4.1 Method | 57 |
| | 4.4.2 Simulations | 60 |
| 4.5 | Specific Heat | 61 |
| | 4.5.1 Normalisation | 61 |
| | 4.5.2 d -wave Symmetry | 62 |
| | 4.5.3 s -wave Symmetry | 63 |
| 4.6 | Spin Susceptibility | 66 |
| 4.7 | Differential conductance | 67 |
| 4.8 | Extracted Phase diagram | 68 |
| 4.9 | Discussion | 69 |
| 5 | COHERENT POTENTIAL APPROXIMATION AND FLUCTUATIONS | 71 |
| 5.1 | CPA for Fixed Amplitude | 71 |
| | 5.1.1 The homogenous Green function and its local expression | 72 |
| | 5.1.2 The Single Site Problem in an Effective Medium | 73 |
| | 5.1.3 The CPA condition | 74 |
| | 5.1.4 CPA Equations for Random Phases | 74 |
| | 5.1.5 The CPA Gap Equation for Fixed Amplitude | 75 |
| | 5.1.6 The Quantum Critical Point of the Gap Equation | 77 |
| 5.2 | CPA for d -wave Pairing | 78 |
| | 5.2.1 Dyson Equation | 79 |
| | 5.2.2 d -wave Differential Operator | 79 |
| | 5.2.3 The Effective Medium d -wave Green Function | 80 |
| | 5.2.4 The Field Dependent CPA d -wave Green Function | 81 |
| | 5.2.5 The CPA Condition | 82 |
| 5.3 | CPA for Random Amplitudes | 82 |
| | 5.3.1 Uniform Distribution | 82 |
| | 5.3.2 Gaussian Distribution | 84 |
| | 5.3.3 Comparison with DMFT | 85 |
| 6 | SUPERCONDUCTORS WITH SHORT RANGE CORRELATIONS | 89 |
| 6.1 | CPA below in Superconducting State | 89 |
| 6.2 | Spectral Properties | 90 |

| | | |
|----------|--|------------|
| 7 | SUPERCONDUCTORS WITH LONG RANGE CORRELATIONS | 95 |
| 7.1 | The Electronic Self-Energy | 95 |
| 7.2 | Phase Correlations Below and Above T_c | 97 |
| 7.2.1 | $T \gg T_c$ | 98 |
| 7.2.2 | $T \ll T_c$ | 98 |
| A | EXPECTATION VALUE OF $\log \mathbf{R}$ | 103 |
| B | GL MODEL AND QUANTUM CHAIN | 105 |
| B.1 | The Transfer Operator | 106 |
| B.2 | Reduction to a $d - 1$ Quantum Problem | 107 |
| C | REMERCIEMENTS :-) | 109 |
| D | LA RECHERCHE ACADÉMIQUE EN SUISSE: QUEL AVENIR? | 111 |

Chapter 1

INTRODUCTION

We begin this work by an overview of selected topics of phase transitions and condensed matter physics, then we have the following chapters:

Chapter 3 is devoted to the study the reciprocal influence between the phase ϕ and the amplitude $|\psi|$ of the complex field ψ in the Ginzburg-Landau (GL) functional. This functional contains two parts: the amplitude part, involving only the amplitude $|\psi|$ and a coupling constant coming from the phase part, and the phase part, XY like, with a coupling constant coming from the amplitude part. The essential result of this chapter is a new approach for solving the GL functional integral by separating amplitude and phase. One important consequence is the possibility of a first order transition (that is a jump of the order parameter) at the transition temperature.

The aim of the chapter 4 is to focus on the problem of the pseudogap phase of underdoped high temperature superconductors. The starting point will be a pairing hamiltonian for fermions like in BCS theory [4]. Using the Hubbard-Stratonovich transformation with a complex pairing field, the main goal will be to take into account both amplitude and phase influence on the electronic properties. One of the results is that the mean amplitude of the pairing field remains large at high temperature: it is never zero because of fluctuations especially in the underdoped regime where the charge carrier density is low. Phase fluctuations are still correlated above T_c until some crossover temperature T_ϕ which is typically 30 % above T_c . Comparison with measured specific heat on underdoped YBCO reproduces the double peak structure: a sharp peak at T_c coming from phase fluctuations and a wide hump above T_c rounded by amplitude fluctuations. The spin susceptibility, related to the amplitude, recovers its normal behaviour near the temperature T^* whereas the orbital magnetic susceptibility, related to the phases, disappears near T_ϕ . All these findings provide additional evidence for the fact that superconductivity and pseudogap have the same origin. The former is primarily related to phases of the pairing field, which order below the transition temperature and whose correlations survive over a limited temperature region above T_c until T_ϕ . The pseudogap regime of underdoped materials then extends to much higher temperatures thanks to the persisting amplitude fluctuations of the pairing field.

Chapter 5 is devoted to the study of the high temperature domain of the pseudogap phase where phases are completely uncorrelated, i.e. above T_ϕ . A method suitable to disordered systems known as CPA (Coherent Potential Approximation) is used to compute the Green function. CPA is extended to d -wave symmetry, and the role of amplitude fluctuations is discussed in a simplified approach. A comparison is made to DMFT results on the attractive Hubbard model showing similar results provided that amplitude fluctuations are included in the CPA approach.

In chapter 6, the CPA calculations is extended below T_c in the presence of a superconducting order parameter.

In chapter 7, the Green function and the self-energy are computed in the Hubbard-Stratonovich transformation below and above the critical temperature T_c by introducing phase correlations.

Chapter 2

BASIC CONCEPTS

In this chapter, some aspects of superconductivity, phase transitions and condensed matter physics are introduced.

2.1 High Temperature Superconductors

2.1.1 Historical Overview

Superconductivity was discovered in 1911 by H. Kamerlingh Onnes in Leiden. He observed that the resistance of Mercury drops to zero below the critical temperature of 4.15 Kelvin. Two years later he found that lead was superconducting below 7.19 Kelvin. A superconductor is then a perfect conductor. In 1933, Meissner and Ochsenfeld discovered the perfect diamagnetism of superconductivity: the magnetic field is completely excluded inside the superconductor. A superconductor is therefore not only a perfect conductor but also a perfect diamagnet.

The first theoretical understanding of superconductivity has been proposed by the brothers Fritz and Heinz London in 1935. Their theory is based on two equations describing the microscopic current and the relation between the magnetic field and the current. These electrodynamic equations allow to explain the Meisner effect, that is the expulsion of the magnetic field from the inner of the superconductor.

The second theoretical approach of superconductivity was advanced in 1950 by Landau and Ginzburg. They proposed a phenomenological free energy depending on a complex field whose modulus is the superfluid density. This theory allows to compute the coherence length ξ of superconductors and the penetration length of the magnetic field λ . The ratio $\kappa = \lambda/\xi$ allows to distinguish between Type I $\kappa \ll 1$ and Type II $\kappa \gg 1$ superconductors. Type II superconductors have a negative surface energy at the interface between the superconductor and the normal metal. Therefore there is a mixed phase where the magnetic field penetrates the inner of superconductor in form of tubes called vortex. The magnetic field is "divided" in many vortices carrying one single magnetic flux in order to minimise the surface energy. One single big vortex would be instable since its interface with the superconductor is smaller than many small vortices.

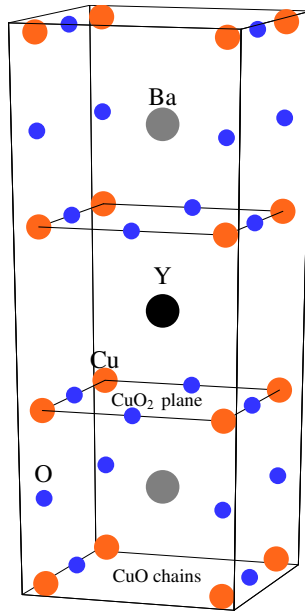


Figure 2.1: Schematic representation of the ceramic $\text{YBa}_2\text{Cu}_3\text{O}_7$ unit cell. The electric current is essentially confined in the two CuO_2 planes above and below the Yttrium atom.

In 1957, John Bardeen, Leon Cooper, and John Schrieffer [4] explained superconductivity at low temperatures for elements and simple alloys by using a microscopic description of the pairing of electrons due to phonons. However, at higher critical temperatures and with cuprates superconductor systems, the BCS theory has subsequently become inadequate to fully explain how superconductivity is occurring.

Another significant theoretical advancement came in 1962 when Brian D. Josephson, a graduate student at Cambridge University, predicted that electrical current would flow between two superconducting materials - even when they are separated by a non-superconductor or insulator. This tunneling phenomenon is today known as the "Josephson effect" and has been applied to electronic devices such as the SQUID, an instrument capable of detecting even the weakest magnetic fields.

Since 1973, the highest critical temperature was 23.3K for the Nb_3Ge . Superconductivity was already observed in some oxides at that time, for example SrTiO_3 had a T_c of 13K. In 1986, Alex Müller and Georg Bednorz [5] found a ceramic compound that was superconducting at the highest temperature then known: 35 K. This ceramic was made of rare earth, copper and oxygen $\text{La}_{1.85}\text{Sr}_{0.15}\text{CuO}_4$. Compounds made of rare earth copper and oxygen are now called *cuprate*. The current world record T_c of 138 K is held by a ceramic of Mercury, Thallium, Barium, Calcium, Copper and Oxygen:

$\text{Hg}_{0.8}\text{Tl}_{0.2}\text{Ba}_2\text{Ca}_2\text{Cu}_3\text{O}_{8.33}$ [6].

2.1.2 The Pairing Mechanism

Although we are not primarily interested in this thesis to study the origin of the pairing mechanism in high T_c superconductors but the consequence of pairing, it is important to have an overview concerning possible pairing mechanism in cuprates, the most common high T_c superconductors. First of all superconducting current in high T_c cuprates is carried by quasiparticles with charge $q = \pm 2e$ depending whether the ceramic has pairs of electrons with negative charge or pairs of holes with positive charge. The problem is the origin of such a pairing. In the BCS approach, the pairing mechanism is due to the exchange of phonons between electrons. It is believed that this mechanism is not responsible for the large T_c of cuprates. However this has not been shown clearly until now, and phonons may be responsible of the pairing in a different mechanism than Cooper pairing.

One of the most probable explanations for the pairing mechanism is based on antiferromagnetism: high T_c cuprates are doped Mott insulators with antiferromagnetic ground state if the stoichiometric doping, i.e. the charge carriers concentration, is very low and a superconducting state at higher doping. Consider now one hole moving on an array with electrons having antiferromagnetic order. Each time the hole is moving from one site to another, it is breaking an antiferromagnetic bond since it replaces an electron. The latter is forced to occupy the site where the hole comes from. One ends up with two electrons showing spins in the same direction which is energetically unfavorable.

We add a second hole. Whenever the first hole has replaced one electron, it forms a domain wall, i.e. two spins having same orientation. This domain wall remains until the second hole comes. The second hole follows the first one in order to "erase" its path. This produces an effective attractive interaction. Of course, one needs a certain number of mobile holes, i.e. a certain doping, in order to have superconductivity.

Why are superconductivity and antiferromagnetism not coexisting? Antiferromagnetism needs fixed electrons sitting at the same site whereas superconductivity needs mobile holes or electrons. One cannot be mobile and fixed at the same time! This is the reason why they occupy different regions of the phase diagram. The question of whether there is an overlap at the transition between superconductivity and antiferromagnetism is still unresolved.

Another pairing mechanism that has been put forward for one dimensional systems like ladders is the super-exchange interaction. In a ladder, at half-filling and high Coulomb repulsion, the ground state is insulator and made of electrons in singlet sitting on the bar of the ladder. The singlet state is the superposition of states $|\uparrow\downarrow\rangle$ and $|\downarrow\uparrow\rangle$, i.e. electrons move virtually from their site to the neighbouring site and come back in a very short time. This interaction is called *super-exchange* since electrons virtually exchange their position in a singlet state. These singlet states have a lower energy compared to a classical antiferromagnetic order. Now if one removes two electrons by adding impurities, one gets two holes in the ladder. The holes will break singlet electron pairs

and increase the energy unless they are sitting on the same bar. Hence an effective attraction is established between the two holes. However, this interesting mechanism has not been generalised yet to 2 or 3 dimensional systems.

2.1.3 The Pseudogap Regime

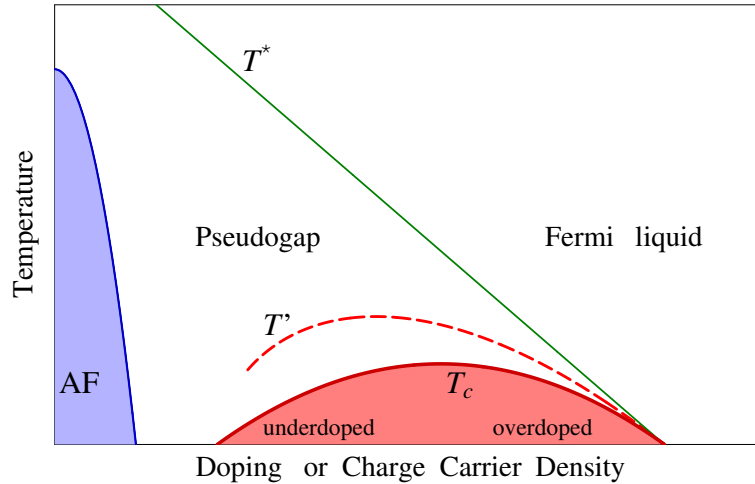


Figure 2.2: Schematic phase diagram of cuprates. The pseudogap region of the copper oxides phase diagram lies between the critical temperature T_c and a temperature T^* that interpolates the antiferromagnetic domain noted by AF. The crossover temperature T' has been reported in several experiments.

In 1989, it was first discovered [7] that cuprate superconductors can have a large region above T_c where physical quantities deviate significantly from the Fermi liquid behaviour up to some temperature T^* which is up to 20 times larger than T_c . This region was later called the *pseudogap* phase since a suppression of spectral weight in the density of states is observed in this regime. In recent years a lot of efforts have been put on the understanding of the pseudogap regime of high temperature superconductors.

The first experiment that revealed anomalous effect above T_c was NMR (Nuclear Magnetic Resonance). Warren *et al* [7] observed a decrease in the magnetic spin susceptibility unlike the constant Pauli susceptibility. They attributed this decrease to a "spin gap" since NMR probes the spin channel. Walstedt *et al* [8] observed that the Knight shift, which is proportional to the magnetic susceptibility, was substantially lowered already at $T = 300\text{K}$ for the underdoped YBCO_{6.7} compound (see figure 2.3).

The second experimental evidence for a pseudogap regime above T_c has been shown in specific heat measurements on YBCO. Loram *et al* [9] in 1993 found a lowering of the specific heat becoming more important in the underdoped regime. The temperature T^* where the specific heat deviates from the normal Fermi liquid behaviour is in agreement

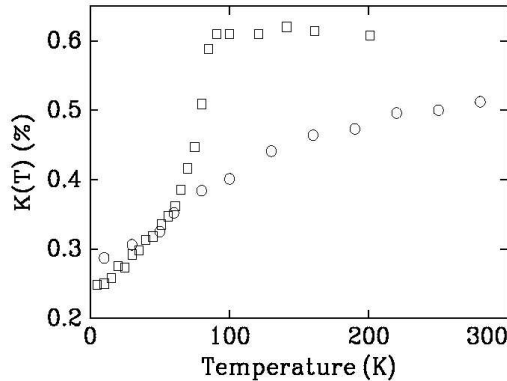


Figure 2.3: Planar ^{63}Cu Knight shift for maximum doping $\text{YBa}_2\text{Cu}_3\text{O}_{6.95}$ (squares) and underdoped $\text{YBa}_2\text{Cu}_3\text{O}_{6.64}$ (circles). The underdoped Knight shift in the normal phase has a strong decrease with respect to the maximum doping shift. Experiments are from reference [8].

with NMR experiments confirming that the pseudogap regime is not an artifact of experiments.

Tunneling experiments are done using a STM (Scanning Tunneling Microscop): a metallic tip is placed above the sample and a voltage is applied between the tip and the sample. The current flows from the sample through the tip. Hence one can recover the density of states, i.e. the number of electrons, as a function of the voltage. Actually the density of states is not measured directly because STM measures the so called I, V curve. The differential conductance dI/dV between a normal metal and a superconductor is directly related to the density of states and the amplitude of the pairing field by the standard formula [10]:

$$\frac{dI}{dV} = -G_{nn} \frac{N_s(\xi)}{N(0)} \frac{\partial f(\xi + eV)}{\partial(eV)} \quad (2.1)$$

where G_{nn} is the differential conductance between two normal metals. Early measurement have been performed by Renner *et al* [11] in Geneva. These results showed a suppression of density of states well above the transition temperature (see figure 2.4), i.e. a pseudogap. These behaviour was seen in $\text{Bi}_2\text{Sr}_2\text{CaCu}_2\text{O}_{8+\delta}$ up to temperature of 300 K in the underdoped regime.

Another experimental setup allows to do tunneling: this is the intrinsic tunneling experiment where tunneling is done inside a layered superconductor between different layers. This experimental method allows to work in a magnetic field. The main result has been found by Krasnov *et al* in year 2000-2001 [12, 13]: they succeed to discriminate the superconducting coherent peaks and the pseudogap by applying a magnetic field that destroys the coherence peak. The pseudogap seems to persists inside the

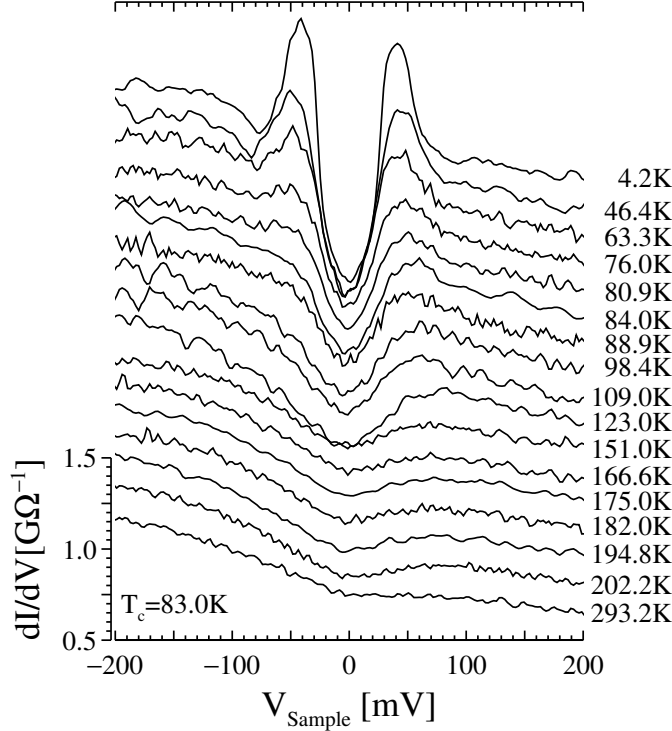


Figure 2.4: Tunneling conductance for underdoped $\text{Bi}_2\text{Sr}_2\text{CaCu}_2\text{O}_{8+\delta}$. A gap-like feature at zero bias is seen to persist in the normal state which is direct evidence of a pseudogap in the tunneling conductance. In the superconducting state a peak develops at ± 45 meV followed by a dip and a broad maximum. The gap frequency does not seem to be temperature dependent.

superconducting region and its size is almost constant.

The pseudogap behaviour has also been seen in ARPES (photoemission). The main result of photoemission is that pseudogap and superconducting gap have the same symmetry: d -wave. On the Fermi surface, the size of the pseudogap changes with the direction. In the plane defined by the momentum k_x and k_y , the pseudogap goes to zero in four directions ($k_x = \pm k_y$). This is a hint for people who believe that superconductivity and the pseudogap have the same origin. For a more complete review on the basic experimental results, one can have a look at the review of T. Timusk and S. Bryan [14].

More recently a second crossover line T' or T_{onset} (see figure 2.5) has been added to the phase diagram of figure 2.2. This line has been measured in Nernst effect [15] and is interpreted as the temperature where vortices start to be correlated. The evidence for an extended temperature interval with vortex-like excitations is strong in this system.

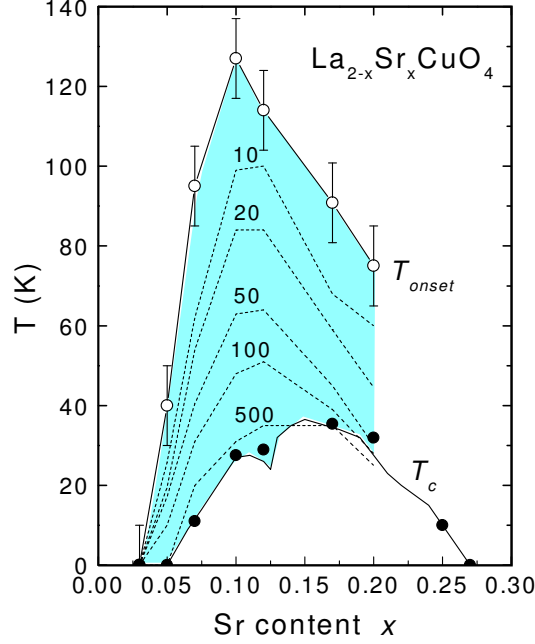


Figure 2.5: The x dependence of T_ν and the contours of the vortex-like Nernst signal in LSCO. The anomalous Nernst signal is measured below the temperature T_{onset} .

2.2 Ginzburg-Landau and ϕ^4 Models

2.2.1 Landau Theory of Phase Transition

The usual Landau theory of phase transitions assumes that it exists a free energy functional depending on a local field which is the order parameter for a phase transition. In general, for a field ψ with n components, the free energy functional can be expanded in power of ψ and $\vec{\nabla}\psi$ near the critical point of the transition where $\psi \approx 0$. For symmetry reasons, the power can be only even since the operation $\psi \rightarrow -\psi$ should not change the free energy. The free energy F reads then:

$$F = \int dV \left(a|\psi|^2 + \frac{b}{2}|\psi|^4 + \frac{c}{2}|(\vec{\nabla} - iq\vec{A})\psi|^2 \right) \quad (2.2)$$

where a , b and c are coefficients that depends on the physical problem. In a temperature driven phase transition, the coefficient a must be of the form $a = a_0(T/T_0 - 1)$ and b and c are constants.

We consider now a complex order parameter ψ in a superconductor. Taking the functional derivative of F with respect to the field ψ^* leads to

$$0 = a\psi + b|\psi|^2\psi + 2c(\vec{\nabla} - iq\vec{A})^2\psi \quad (2.3)$$

Taking the functional derivative of F with respect to the field \vec{A} leads to

$$\mathbf{j}_s = 2c(\vec{\nabla} - iq\vec{A})^2\psi \quad (2.4)$$

where \mathbf{j}_s is the superconducting charge current. Solution of equation (2.3) for the case where the order parameter is constant is simply given by the solution of:

$$(a + b|\psi|^2)\psi = 0 \quad (2.5)$$

This equation has two solutions: $|\psi|^2 = -\frac{a}{b}$ below T_0 and $\psi = 0$ above T_0 . The lowest free energy indicates which solution is correct.

The study of equations (2.3) and (2.4) leads to the definition of Type I and Type II superconductors. Type I have a long zero temperature coherence length ξ_0 and a small zero temperature magnetic penetration depth λ_0 . Typical representatives of Type I are Al or Pb. Type II have a small ξ_0 and a large λ_0 . If one computes the difference between the total energy and the bulk energy, i.e. the surface energy, for a superconductor in a magnetic field, the surface energy is negative for Type II superconductors. The consequence is that Type II superconductors tend to maximise their contact with normal phase and form vortices in a magnetic field. Magnetic vortices are idealised tubes where a quantum magnetic flux penetrates inside the superconductors. The center of the vortex is non-superconducting and therefore each vortex has a contact surface of negative energy. Hence the system maximises the number of vortices, each one carrying a single quantum flux.

2.2.2 Fluctuations: Beyond Mean Field

Ginzburg-Landau Equations (2.3) and (2.4) are mean field solutions of the statistical Ginzburg-Landau model where the action or hamiltonian has the same field dependence like the mean field free energy F . The GL action is:

$$S_{GL} = \int dV \left(a|\psi|^2 + \frac{b}{2}|\psi|^4 + \frac{c}{2}|(\vec{\nabla} - iq\vec{A})\psi|^2 \right) \quad (2.6)$$

The free energy is determined by integrating over all possible configurations of the field ψ according to the canonical ensemble. Therefore one has to compute the partition function

$$Z_{GL} = \int D\psi e^{-\beta S_{GL}} \quad (2.7)$$

This is a infinite dimension integral including gradient terms, that is far from being simple to solve... In the next sections, we will review some of the possible approach to solve the problem of computing Z_{GL} : 1) The harmonic approximation which is simple but not very realistic. 2) The renormalisation group approach which is very general and gives good insights to the nature of the phase transition. 3) Numerical simulations which can be considered as the experimental realisation of the model. If correctly done, they should provide a realistic approximation to the exact solution. However simulations suffer from finite size effect since arrays used for simulations are always finite. They can also suffer from critical slowing down at the phase transition: the system is trapped in a subspace of metastable states and the transition probability to other configurations is almost zero.

2.2.3 Harmonic Approximation and Critical Region

The computation of the GL partition function is impossible to be done exactly. However it is possible to perform a gaussian or harmonic approximation on it, i.e. to suppress the quartic term. The gaussian GL action is therefore

$$S_h = \int dV \left(\tilde{a} |\psi|^2 + \frac{c}{2} |(\vec{\nabla} - iq\vec{A})\psi|^2 \right) \quad (2.8)$$

where $\tilde{a} = a$ for simplest approximation or $\tilde{a} = a + b/2 \langle |\psi|^2 \rangle$ in a Hartree-Fock approximation. The partition function can be solved exactly by expanding the field ψ in plane waves ϕ_n solution of the Schroedinger equation in a magnetic field with a constant potential \tilde{a}

$$\left(\tilde{a} + \frac{c}{2} (\vec{\nabla} - iq\vec{A})^2 \right) \phi_n = E_n \phi_n \quad (2.9)$$

Eigenvalues E_n of this equation are identical to solutions of the harmonic oscillator in 2d for a symmetric gauge.

$$E_n = \hbar\omega \left(\frac{1}{2} + n_x + n_y \right) + \frac{\hbar^2 k_z^2}{2m} + \tilde{a} \quad (2.10)$$

where $\omega = qB$. With

$$\psi = \sum_n c_n \phi_n \quad (2.11)$$

where the summation over k_z is assumed, the action (2.8) becomes then

$$\begin{aligned} S_h &= \int dV \psi^* \left(\tilde{a} + \frac{c}{2} (\vec{\nabla} - iq\vec{A})^2 \right) \psi \\ &= \int dV \sum_m c_m^* \phi_m^* \sum_n c_n E_n \phi_n \\ &= \sum_n E_n |c_n|^2 \end{aligned} \quad (2.12)$$

The partition function can be separated in simple gaussian integrals:

$$\begin{aligned} Z_h &= \int D\psi e^{-\beta S_h} \\ &= \int \prod_n dc_n e^{-\beta \sum_n E_n |c_n|^2} \\ &= \prod_n \int dc_n e^{-\beta E_n |c_n|^2} \\ &= \prod_n \frac{\pi}{\beta E_n} \end{aligned} \quad (2.13)$$

The free energy $F_h = -\beta^{-1} \log(Z_h)$ of the harmonic approximation has then the simple form

$$F_h = \beta^{-1} \sum_n \log(\beta E_n) \quad (2.14)$$

where the constant term is omitted. In the zero field, the free energy is then the sum over vectors k in all directions:

$$F_h(B=0) = \beta^{-1} \sum_{\mathbf{k}} \log \left[\beta \left(\tilde{a} + \frac{\hbar^2 \mathbf{k}^2}{2m} \right) \right] \quad (2.15)$$

In the high field approximation, only the lowest level $n = 0$ is selected since other energy contribution are too high.

$$F_h(\hbar\omega \gg k_B T) \approx \beta^{-1} \sum_{\mathbf{k}_z} \log \left[\beta \left(\frac{1}{2} \hbar\omega + \tilde{a} + \frac{\hbar^2 \mathbf{k}_z^2}{2m} \right) \right] \quad (2.16)$$

Hence a high magnetic field reduces the dimensionality to 1 since all physics is confined to the Lowest Landau Level (LLL) with $n = 0$. It is possible to calculate critical exponents in the harmonic approximation itself but the results are far from the exact solution.

We are now interested in looking for the size of the region around T_c where correlations are so strong that a simple mean field calculation becomes wrong. It is important to understand that we look for a regime with strong correlations, not strong fluctuations. Indeed, fluctuations of a variable are defined by its standard deviation whereas its correlation is only measurable with respect to another variable at a different site for example. We define now the deviation \mathcal{D} between the harmonic approximation and the mean field approach by computing harmonic correlations in the harmonic approximation:

$$\mathcal{D} = \frac{\sum_{ij} (\langle \psi_i^* \psi_j \rangle - \langle \psi_i^* \rangle \langle \psi_j \rangle)}{\sum_i \langle \psi_i^* \rangle^2} \quad (2.17)$$

If there is no correlation, the correlation function is zero, $\mathcal{D} = 0$ and the mean field approximation should be valid. However, if \mathcal{D} is of the order of one, i.e. if correlations are "of the same size" as the order parameter, the mean field theory will break down.

Since we want to use the gaussian approximation to evaluate this coefficient, simple averages $\langle \psi_i^* \rangle$ are equal to the mean field order parameter:

$$\langle \psi_i \rangle = \psi_0 \quad (2.18)$$

The deviation is then

$$\mathcal{D} = \frac{\sum_{ij} \langle \psi_i^* \psi_j \rangle - \psi_0^2}{V \psi_0^2} \quad (2.19)$$

We compute now the correlation in the the continuum notation:

$$\begin{aligned} V^{-2} \int d\mathbf{r} d\mathbf{r}' \langle \psi^*(\mathbf{r}) \psi(\mathbf{r}') \rangle &= V^{-1} \int d\mathbf{r} \langle \psi^*(\mathbf{r}) \psi(0) \rangle \\ &= \frac{1}{V} \sum_{\mathbf{k}} \langle \psi_{\mathbf{k}}^* \psi_{\mathbf{k}} \rangle V \delta_{\mathbf{k},0} \\ &= \frac{k_B T}{a} \end{aligned} \quad (2.20)$$

where we used the result

$$\begin{aligned} \langle \psi_{\mathbf{k}}^* \psi_{\mathbf{k}'} \rangle &= \langle \psi_{\mathbf{k}}^* \psi_{\mathbf{k}} \rangle \delta_{\mathbf{k},\mathbf{k}'} \\ &= \frac{k_B T}{a + \frac{c}{2} k^2} \delta_{\mathbf{k},\mathbf{k}'} \end{aligned} \quad (2.21)$$

The denominator of (2.19) is

$$V\psi_0^2 = V\frac{a}{b} \quad (2.22)$$

And the deviation (2.19) is estimated by

$$\mathcal{D} = k_B T \frac{b}{a^2 V} \quad (2.23)$$

We see that \mathcal{D} is proportional to the inverse of the integration volume. The problem is that we considered correlations over the entire volume V and not only over the correlated volume. The correlation function $\langle \psi^*(\mathbf{r})\psi(0) \rangle$ is only different from zero when $|\mathbf{r}|$ is smaller than the size of the correlation volume ξ . Therefore we replace V by ξ^d where d is the dimension:

$$\mathcal{D} = k_B T \frac{b}{a^2 \xi^d} \quad (2.24)$$

The correlation length can be computed in a mean field calculation. It is the only relevant length scale and its value is $\xi^2 = c/|a|$ for a negative a . We get then:

$$\mathcal{D} = k_B T \frac{b}{c^{d/2}} |a|^{\frac{d-4}{2}} \quad (2.25)$$

We see the appearance of special dimension. Indeed, when $d > 4$ the power of a changes sign. The dimension 4 is a critical dimension where critical properties change. The intuition tells us that a high dimension is highly connected and should be therefore mean field like whereas small dimensions are subject to stronger fluctuations. This intuition is confirmed by this calculation. Near the critical point where $a \rightarrow 0$, $\mathcal{D} \rightarrow \infty$ if the dimension is smaller than 4. That is mean field theory is always wrong because of strong correlations. If the dimension is larger than 4, $\mathcal{D} \rightarrow 0$ and mean field theory is valid.

However, details depends on the value of the coefficients a, b and c . The size of the critical region is defined as the regime where $\mathcal{D} > 1$. For temperature dependent $a = a_0 t = a_0(T/T_c - 1)$, the limit $t_G = (T_G/T_c - 1)$ is then given by $\mathcal{D} = 1$:

$$1 = k_B T \frac{b}{c^{d/2}} |a|^{\frac{d-4}{2}} \quad (2.26)$$

Using $a = a_0 t$, we have

$$t_G = \frac{1}{a_0} \left(k_B T \frac{b}{c^{d/2}} \right)^{\frac{2}{4-d}} \quad (2.27)$$

Using the normalised coefficients, only two parameters remain:

$$\sigma := \varepsilon^2 / \xi_0^2 \quad V_0 := \frac{1}{k_B} \frac{a}{b} \gamma \varepsilon^{d-2} \quad (2.28)$$

where ε is the lattice constant and σ is a coarse grained length controlling amplitude fluctuations. V_0 corresponds to the zero temperature phase stiffness. See chapter 3 for

further explanations. The critical region is then given by:

$$t_G = \left(\frac{T_c}{V_0} \right)^{\frac{2}{4-d}} \sigma^{\frac{2}{4-d}} \quad (2.29)$$

where the temperature T is now taken at the true T_c and not at the original mean field temperature T_0 . The coarse grained parameter σ is considered to be a constant depending on the material. It should lie between 1 and 10. For a classical low temperature superconductor, V_0 is estimated by the charge carrier density is of the order 10^4 and T_c is of the order of 10. Evaluating t_G for this case yields:

$$t_G \sim \left(\frac{T_c}{V_0} \right)^2 \approx 10^{-8} \quad (2.30)$$

Hence the critical region of low temperature superconductors is very small. This explains why a mean field theory like BCS is so successful at explaining their properties. For a high temperature superconductors in the underdoped regime, with quasi 2 dimensional behaviour, we get

$$t_G \sim \left(\frac{T_c}{V_0} \right) \approx 1 \quad (2.31)$$

since $T_c \approx V_0$. This means that for $T_c = 90\text{K}$, one has an absolute critical region of 90 K around T_c . This is of course only a qualitative statement, but showing anyway that a mean field BCS theory cannot apply to this kind of superconductors because of the size of the critical region.

As we shall see in chapter 4, the size of the region where uncorrelated fluctuations are large extends even to a temperature T^* which is up to five times larger than the critical temperature whereas the region of correlations is limited up to 50 % of T_c . This regime where phases are still correlated can be identified with the Ginzburg critical region.

In the next section, we will see how critical exponents can be derived by combining the harmonic approximation and the renormalisation group leading to a much better description of the actual phase transition.

2.2.4 Renormalisation Group

We shall not derive the full RG (Renormalisation Group) method for phase transition but introduce the basic assumptions and the main consequences. RG is based on the assumption that a system is invariant under a scale transformation at the critical point of a second order phase transition. This implies the existence of infinite coherence length ξ . However the transformation between two different scales of the system is not linear in the coupling coefficients of the system but the latter are transformed under functions depending on the particular system.

One of the main result of RG is the universality of second order phase transitions: critical exponents depends only on the dimensionality D of the system and on the number of components n of the order parameter, i.e. its symmetry. Each couple $\{D, n\}$

defines a so called universality class. For example, Josephson Junction Arrays which are $2D$ arrays of superconducting islands must have the same universality class as superfluid 4He confined in $2D$. All other quantities are negligible (irrelevant) since the coherence length ξ is much larger than the microscopic details. This is why a physical system as high T_c cuprates, which is very complex, must have a phase transition belonging to $2DXY$ or $3DXY$ universality class. But in reality, the universality can be hidden due to a very small critical region as in classical superconductors where the size of the critical region is about 10^{-6} K.

For further informations on phase transitions and RG, I refer the reader to the excellent book of N. Goldenfeld [16].

2.3 Condensed Matter Concepts

2.3.1 The Interaction Representation

In the classical Schroedinger formalism operators do not depend on time. It is the wave function that depends on time and evolves in the system. However, it is possible to consider another point of view: operators evolves with time. With such a formalism, the Schroedinger equation is no more an equation for field depending on time, but it becomes an equation for operators evolving in time. Let us define the transformation of an operator c in the interaction representation for an hamiltonian $H = H_0 + V$:

$$c(\tau) = e^{-\tau H_0} c e^{\tau H_0} \quad (2.32)$$

where $\tau = it$ when real time t evolution is considered.

2.3.2 Imaginary Time Formalism

The imaginary time formalism is derived for a system at finite temperature. The "time" is additional coordinate reflecting the quantum nature of observables, i.e. the fact that operators do not commute in general.

We assume a quantum hamiltonian of the form:

$$H = H_0 + V \quad (2.33)$$

where H_0 is a non interacting hamiltonian and V is the interaction part. The problem is here to evaluate the partition function

$$Z = \text{Tr} e^{-\beta H} \quad (2.34)$$

where the symbol Tr denotes the trace, i.e. the sum over all eigenstates of H . Usually the eigenstates of H_0 are known but not those of H . It is therefore preferable to separate H_0 and V . However the commutator $[H_0, V]$ is usually different from zero since they are quantum operators. Therefore it is not possible to factorise the exponential as:

$$e^{-\beta(H_0+V)} \neq e^{-\beta H_0} e^{-\beta V} \quad (2.35)$$

and perform averages $\langle e^{-\beta V} \rangle$ over H_0 . Introducing the interaction representation:

$$V(\beta) = e^{-\beta H_0} V e^{\beta H_0} \quad (2.36)$$

and the operator

$$U(\beta) = e^{\beta H_0} e^{-\beta H}, \quad (2.37)$$

this problem can be overcome by solving the following differential equation:

$$\begin{aligned} \frac{\partial U(\beta)}{\partial \beta} &= \frac{\partial}{\partial \beta} e^{\beta H_0} e^{-\beta H} \\ &= -V(\beta)U(\beta) \end{aligned} \quad (2.38)$$

Integrating this equation with respect to β leads to

$$U(\beta) = 1 - \int_0^\beta \Delta\tau_1 V(\tau_1) U(\tau_1) \quad (2.39)$$

since $U(0) = 1$. τ is called *imaginary time* since the replacement $\tau = it$ leads to the time dependant quantum mechanic at zero temperature. If this equation is iterated, we get:

$$U(\beta) = 1 - \int_0^\beta \Delta\tau_1 V(\tau_1) + (-1)^2 \int_0^\beta \Delta\tau_1 \int_0^{\tau_1} \Delta\tau_2 V(\tau_2) U(\tau_2) \quad (2.40)$$

For an infinite number of iterations, we have:

$$U(\beta) = \sum_{n=0}^{\infty} (-1)^n \int_0^\beta \Delta\tau_1 \int_0^{\tau_1} \Delta\tau_2 \dots \int_0^{\tau_{n-1}} \Delta\tau_n V(\tau_1) V(\tau_2) \dots V(\tau_n) \quad (2.41)$$

We introduce the "time" ordering operator \mathcal{T} which orders operators as:

$$\mathcal{T} [V(\tau_1) V(\tau_2) V(\tau_3)] = V(\tau_1) V(\tau_2) V(\tau_3) \quad (2.42)$$

if $\tau_3 < \tau_2 < \tau_1$. For a multi-dimensional integral, variables $\tau_1, \tau_2, \dots, \tau_n$ can take all order. In fact, there are $n!$ combinations. This gives the identity

$$\begin{aligned} \int_0^\beta \Delta\tau_1 \int_0^{\tau_1} \Delta\tau_2 \dots \int_0^{\tau_{n-1}} \Delta\tau_n V(\tau_1) V(\tau_2) \dots V(\tau_n) = \\ \frac{1}{n!} \int_0^\beta \Delta\tau_1 \int_0^{\tau_1} \Delta\tau_2 \dots \int_0^{\tau_{n-1}} \Delta\tau_n \mathcal{T} [V(\tau_1) V(\tau_2) \dots V(\tau_n)] \end{aligned} \quad (2.43)$$

Therefore, we can formulate $U(\beta)$ as an exponential of V :

$$U(\beta) = \mathcal{T} e^{-\int_0^\beta \Delta\tau V(\tau)} \quad (2.44)$$

Now, we come back to our original problem which was the computation of the partition function. Using the last identity, we have:

$$\begin{aligned} Z &= \text{Tr} e^{\beta H} = \text{Tr} e^{\beta H_0} U(\beta) \\ &= \text{Tr} e^{\beta H_0} \mathcal{T} e^{-\int_0^\beta \Delta\tau V(\tau)} \\ &= Z_0 \langle \mathcal{T} e^{-\int_0^\beta \Delta\tau V(\tau)} \rangle_0 \end{aligned} \quad (2.45)$$

where $Z_0 = \text{Tr} \exp(-\beta H_0)$. We have therefore separated $H_0 + V$, and reduced the problem to compute averages of $V(\tau)$ over the hamiltonian H_0 .

2.3.3 Matsubara Formalism and Temperature Green Functions

The temperature (Matsubara) Green function is defined as

$$G(\mathbf{k}, \tau, \tau') := - \langle \mathcal{T}_\tau c_{\mathbf{k}}(\tau) c_{\mathbf{k}}^+(\tau') \rangle \quad (2.46)$$

where

$$c_{\mathbf{k}}(\tau) = e^{\tau H} c_{\mathbf{k}} e^{-\tau H} \quad (2.47)$$

and τ goes from 0 to β .

The unperturbed Green function corresponds to the grand canonical hamiltonian

$$H_0 = \sum_{\mathbf{k}} (\varepsilon_{\mathbf{k}} - \mu) c_{\mathbf{k}}^+ c_{\mathbf{k}} = \sum_{\mathbf{k}} \xi_{\mathbf{k}} c_{\mathbf{k}}^+ c_{\mathbf{k}} \quad (2.48)$$

The imaginary time evolution of the operator is thus

$$c_{\mathbf{k}}(\tau) = e^{\tau H_0} c_{\mathbf{k}} e^{-\tau H_0} = c_{\mathbf{k}} e^{-\tau \xi_{\mathbf{k}}} \quad (2.49)$$

$$c_{\mathbf{k}}^+(\tau) = e^{\tau H_0} c_{\mathbf{k}}^+ e^{-\tau H_0} = c_{\mathbf{k}}^+ e^{\tau \xi_{\mathbf{k}}} \quad (2.50)$$

where we used the Baker-Hausdorff theorem:

$$e^A c e^A = c + [A, c] + [A, [A, c]]/2! + [A, [A, [A, c]]]/3! + \dots$$

The temperature dependent Green function is:

$$\begin{aligned} G(\mathbf{k}, \tau, \tau') &= - \langle \mathcal{T}_\tau c_{\mathbf{k}} e^{-\tau \xi_{\mathbf{k}}} c_{\mathbf{k}}^+ e^{\tau' \xi_{\mathbf{k}}} \rangle \\ &= -e^{(\tau' - \tau) \xi_{\mathbf{k}}} \langle c_{\mathbf{k}} c_{\mathbf{k}}^+ \Theta(\tau - \tau') + c_{\mathbf{k}}^+ c_{\mathbf{k}} \Theta(\tau' - \tau) \rangle \\ &= -e^{(\tau' - \tau) \xi_{\mathbf{k}}} [(1 - f_{\mathbf{k}}) \Theta(\tau - \tau') + f_{\mathbf{k}} (\Theta(\tau - \tau') - 1)] \\ &= -e^{(\tau' - \tau) \xi_{\mathbf{k}}} [\Theta(\tau - \tau') - f_{\mathbf{k}}] \end{aligned} \quad (2.51)$$

where

$$f_{\mathbf{k}} = \langle c_{\mathbf{k}} c_{\mathbf{k}}^+ \rangle = \frac{1}{e^{\beta \xi_{\mathbf{k}}} + 1} \quad (2.52)$$

is the Fermi distribution. The Fourier transform with respect to the imaginary time introduces the complex frequency ω_n . Setting $\tau' = 0$, we have

$$G(\mathbf{k}, \omega_n) = \int_0^\beta \Delta\tau e^{i\omega_n \tau} G(\mathbf{k}, \tau) \quad (2.53)$$

The unperturbed Green function is therefore:

$$G_0(\mathbf{k}, \omega_n) = -(1 - f_{\mathbf{k}}) \frac{e^{\beta(i\omega_n - \xi_{\mathbf{k}})} - 1}{i\omega_n - \xi_{\mathbf{k}}}$$

Since the frequency are determined by the Fourier condition:

$$\omega_n = (2n + 1)\pi/\beta$$

where n is a positive integer number, we may simplify the Green function and we obtain:

$$G_0(\mathbf{k}, \omega_n) = \frac{1}{i\omega_n - \xi_{\mathbf{k}}} \quad (2.54)$$

The information concerning the temperature dependence goes now through ω . We see that the unperturbed temperature Green function in the Matsubara notation has the same form as the unperturbed zero temperature Green function since the temperature dependence is now hidden in the frequency summation.

2.3.4 Path Integral in Superconductivity

We shall not develop the theory of path integrals in this section but resume the most important results. Path integrals allow to transform a microscopic theory written in second quantisation into a field theory. The fields are either usual complex fields when the second quantised operator are bosonic, but they are Grassmann numbers when dealing with fermionic operators. Grassmann numbers are complex numbers with special commutation relation. Considering two Grassmann number w_i and w_j , we have:

$$w_i w_j + w_j w_i = 0 \quad (2.55)$$

This implies that $w_i^2 = 0$. Any function $f(w)$ can be expanded as

$$f(w) = f(0) + f'(0) w \quad (2.56)$$

since higher order term in z vanish due to the rule $z^2 = 0$. Hence every function $f(w_1, \dots, w_N)$ in Grassmann variable is then written as

$$f(w_1, \dots, w_N) = \sum_{n=0}^N \sum_{i_1 < i_2 < \dots < i_n} C_n(i_1, \dots, i_n) w_{i_1} \cdots w_{i_n} \quad (2.57)$$

where C_n is a complex function of the multi-index i_j . The Grassmann integral over the function $f(z)$ is then defined as:

$$\oint dw f(w) = f'(0) \quad (2.58)$$

Integrating z like a normal number would have given $z^2/2 = 0$, and taking $f(0)$ instead of $f'(0)$ would have break the translational invariance of the integral: $\int dw f(w + \eta) = \int dw f(w)$. The Grassmann integral is then identical to the derivative.

In particular, we have the result

$$\oint dw w = 1 \quad (2.59)$$

The Grassmann integral should be understood as a tool which perform a functional operation. It is not the measure of some volume like the Riemann integral.

The integral over a function $f(w_1, \dots, w_N)$ always reduces in an integral over the product of Grassmann numbers:

$$\oint dw_1 \cdots dw_N f(w_1, \dots, w_N) \sim \oint dw_{j_1} \cdots dw_{j_n} w_{i_1} \cdots w_{i_n} \quad (2.60)$$

where $\{j_1, \dots, j_n\}$ is another set of indices. Using the definition of the Grassmann integral 2.58, the result of the integral is then only different from zero if $\{j_1, \dots, j_n\} = \{i_1, \dots, i_n\}$

An essential result is that the trace of an operator ρ can be replaced by its "integral" over Grassmann numbers. First we have to define the Grassmann state:

$$|w\rangle = e^{-\sum_{\sigma} w_{\sigma} c_{\sigma}^{\dagger}} |0\rangle \quad (2.61)$$

It is then possible to show the following identities:

$$c_{\sigma}|w\rangle = w_{\sigma}|w\rangle \quad \text{and} \quad \langle w|c_{\sigma}^{\dagger} = \langle w|w_{\sigma}^* \quad (2.62)$$

The projection of an operator $f(c_{\sigma}^{\dagger}, c_{\sigma})$ on the Grassmann basis yields:

$$\langle w|f(c_{\sigma}^{\dagger}, c_{\sigma})|w\rangle = e^{-\sum_{\sigma} w_{\sigma} w_{\sigma}^*} f(w_{\sigma}^*, w_{\sigma}) \quad (2.63)$$

Using the identity operator

$$\oint d\mu(w) e^{-\sum_{\sigma} w_{\sigma} w_{\sigma}^*} |w\rangle \langle w| = 1 \quad (2.64)$$

we can express states $|\phi\rangle$ in the Grassmann states basis:

$$|\phi\rangle = \oint d\mu(w) e^{-\sum_{\sigma} w_{\sigma} w_{\sigma}^*} |w\rangle \langle w|\phi\rangle \quad (2.65)$$

We can now transform the trace of an operator on complete set of eigenstates $|n\rangle$ to a Grassmann integral. If we omit the spin indices we have:

$$\text{Tr} A = \sum_n \langle n|A|n\rangle = \oint dw^* dw e^{-w^* w} \langle w|A|w\rangle \quad (2.66)$$

where we used the operator identity $\sum_n |n\rangle \langle n| = 1$. In order to compute the partition function, we have to split the term $\exp(-\beta H)$ in infinitesimal operators $\exp(-\beta H \Delta\tau)$. Working with $\exp(-\beta H \Delta\tau)$ allows to take the trace of each term. The partition function in the canonical ensemble is then:

$$\begin{aligned} Z &= \text{Tr} e^{-\beta H} \\ &= \text{Tr} \left(e^{-\beta H \Delta\tau} \right)^M \\ &= \oint dw^* dw e^{-w^* w} \langle w| \left(e^{-\beta H \Delta\tau} \right)^M |w\rangle \\ &= \oint dw^* dw e^{-w^* w} \langle w| e^{-\beta H \Delta\tau_1} |w_1\rangle \oint dw_1^* dw_1 e^{-w_1^* w_1} \langle w_1| \cdots e^{-\beta H \Delta\tau_M} |w\rangle \\ &= \prod_{m=0}^M \oint dw_m^* dw_m e^{-w_m^* w_m} \langle w_m| e^{-\beta H \Delta\tau_m} |w_{m+1}\rangle \end{aligned} \quad (2.67)$$

where $w_0 := w$ and the anti-periodic boundary condition is $w_{M+1} = -w_0$. Using equation 2.65, we can compute the term

$$\langle w_m | e^{-\beta H \Delta \tau_m} | w_{m+1} \rangle = e^{w_m w_{m+1}} e^{-\beta H(w_m, w_{m+1}^*) \Delta \tau_m} \quad (2.68)$$

Inserting this last result in equation (2.67), we have

$$Z = \prod_{m=0}^M \oint dw_m^* dw_m e^{-\sum_m [\beta H(w_m, w_{m+1}^*) \Delta \tau_m + w_m^* (w_m - w_{m+1})]} \quad (2.69)$$

We can define the action S , taking the limit $M \rightarrow \infty$ yields :

$$S = \int_0^\beta d\tau [H(w(\tau), w^*(\tau)) + w^*(\tau) \partial_\tau w(\tau)] \quad (2.70)$$

2.3.5 The Hubbard-Stratonovich Transformation

This transformation allows to transform a microscopic hamiltonian into an effective field theory by introducing a complex pairing field ψ . We start from the attractive Hubbard model whose hamiltonian is

$$H = - \sum_{\langle i,j \rangle \sigma} t_{ij} c_{i\sigma}^\dagger c_{j\sigma} - U \sum_i c_{i\uparrow}^\dagger c_{i\uparrow} c_{i\downarrow}^\dagger c_{i\downarrow} \quad (2.71)$$

with a hopping t_{ij} between nearest neighbour sites i and j on a square lattice. The negative interaction $-U$ favours the formation of onsite pairs. The Hubbard Stratonovich transformation is based on the identity for an operator \mathbf{O}

$$e^{-a\mathbf{O}^2} = \int_{-\infty}^{\infty} dx e^{-\pi x^2 - 2i\sqrt{a\pi}x\mathbf{O}} \quad (2.72)$$

or for two operators \mathbf{A} and \mathbf{B} :

$$e^{-a\mathbf{A}\mathbf{B}} = \int dz dz^* e^{-\pi|z|^2 - \sqrt{a\pi}(z\mathbf{A} + z^*\mathbf{B})} \quad (2.73)$$

The partition function of the hamiltonian (2.71) is given by:

$$Z = \text{Tr} e^{-\beta(H_0 + V)} \quad (2.74)$$

where H_0 is non interacting part of H . Let us introduce the partition function of the non-interacting part:

$$Z_0 = \text{Tr} e^{-\beta H_0} \quad (2.75)$$

We would like now to express the full partition function as averages over the free hamiltonian H_0 . The operation is not so simple as in the classical case since H and H_0 do not commute. This can be done by using the imaginary time formalism as seen in equation (2.45). The resulting partition function is

$$Z = \text{Tr} e^{-\beta H_0} \mathcal{T}_\tau e^{-\int_0^\beta \Delta \tau V(\tau)} \quad (2.76)$$

Using the Hubbard-Stratonovich transformation, one can express the integral by the integration over the complex field ψ which interact with free electrons:

$$Z = \text{Tr} \int D\psi \mathcal{T}_\tau e^{-\int_0^\beta \Delta\tau S(\tau, \psi)} \quad (2.77)$$

where the time dependent action $S(\tau, \psi)$ is

$$S(\tau, \psi, c) = H_0 + \sum_i \left[\frac{1}{U} |\psi|^2 + \psi c_\uparrow^\dagger c_\downarrow^\dagger + \psi^* c_\downarrow c_\uparrow \right] \quad (2.78)$$

with $c_\sigma = c_\sigma(i, \tau)$ and $\psi = \psi(i, \tau)$.

We introduce now the so-called Nambu spinors which are nothing else than two creation operators written in a two components vectors:

$$\mathbf{s} = \begin{pmatrix} c_\uparrow^\dagger \\ c_\downarrow^\dagger \end{pmatrix} \quad \text{and} \quad \mathbf{s}^\dagger = \begin{pmatrix} c_\uparrow^\dagger \\ c_\downarrow \end{pmatrix} \quad (2.79)$$

where the spinor is now only site and time dependent: $\mathbf{s} = \mathbf{s}(i, \tau)$. The anticommutation rule applies to the fermionic Nambu spinors as well:

$$\{ \mathbf{s}^\dagger(i, \tau), \mathbf{s}(j, \tau') \} = \delta_{i,j} \delta_{\tau, \tau'}$$

We can now write the effective action (2.78) in term of Nambu spinors. If we use the identity:

$$\psi^* c_\uparrow^\dagger c_\downarrow^\dagger + \psi c_\downarrow c_\uparrow = \begin{pmatrix} c_\uparrow^\dagger \\ c_\downarrow \end{pmatrix} \begin{pmatrix} 0 & \psi \\ \psi^* & 0 \end{pmatrix} \begin{pmatrix} c_\uparrow^\dagger \\ c_\downarrow^\dagger \end{pmatrix} = \mathbf{s}^\dagger \Psi \mathbf{s}$$

where the matrix Ψ is defined as: $\Psi = \begin{pmatrix} 0 & \psi \\ \psi^* & 0 \end{pmatrix}$, and the identity:

$$\sum_\sigma c_\sigma^\dagger t_{ij} c_\sigma = \begin{pmatrix} c_\uparrow^\dagger \\ c_\downarrow \end{pmatrix} \begin{pmatrix} t_{ij} & 0 \\ 0 & -t_{ij} \end{pmatrix} \begin{pmatrix} c_\uparrow^\dagger \\ c_\downarrow^\dagger \end{pmatrix} = \mathbf{s}^\dagger \mathbf{T}_{ij} \mathbf{s}$$

where the matrix \mathbf{T}_{ij} is defined as: $\mathbf{T}_{ij} = \begin{pmatrix} t_{ij} & 0 \\ 0 & -t_{ij} \end{pmatrix}$, we have

$$S(\tau, \psi, \mathbf{s}) = \sum_{ij} \mathbf{s}^\dagger \mathbf{T}_{ij} \mathbf{s} + \sum_i \left[\frac{1}{U} |\psi|^2 + \mathbf{s}^\dagger \Psi \mathbf{s} \right] \quad (2.80)$$

Note that the minus sign in \mathbf{T}_{ij}^{22} comes from the anticommutation relation. We can introduce a Kronecker delta function in this effective action by using the equality $\sum_i = \sum_{ij} \delta_{ij}$:

$$S(\tau, \psi, \mathbf{s}) = \sum_i \frac{1}{U} |\psi|^2 + \sum_{ij} \left[\mathbf{s}_i^\dagger (\mathbf{T}_{ij} + \delta_{ij} \Psi) \mathbf{s}_j \right] \quad (2.81)$$

The trace over the fermionic operators can be performed by using Grassmann integral since the action is quadratic, at least formally. For a precise derivation, look at reference [17]. The result is the identity:

$$\text{Tr} e^{\sum_{ij} [s_i^\dagger \mathbf{A}_{ij} s_j]} = \det \mathbf{A} \quad (2.82)$$

where \mathbf{A}_{ij} is in grand canonical ensemble:

$$\mathbf{A}_{ij} = \mathbf{T}_{ij} + \delta_{ij} \Psi + \begin{pmatrix} -\mu \delta_{ij} & 0 \\ 0 & \mu \delta_{ij} \end{pmatrix} = \begin{pmatrix} t_{ij} - \mu \delta_{ij} & \psi \delta_{ij} \\ \psi^* \delta_{ij} & -t_{ij} + \mu \delta_{ij} \end{pmatrix}$$

and $\mathbf{A} = (\mathbf{A}_{ij})_{i=1, \dots, N, j=1, \dots, N}$ where N is the number of sites. Bringing together equation (2.77), (2.81) and (2.82), we find that the partition function is now:

$$Z = \int D\psi \mathcal{T}_\tau e^{-\int_0^\beta d\tau [\sum_i \frac{1}{V} |\psi|^2 + \text{Tr} \log(\mathbf{A})]} \quad (2.83)$$

2.3.6 Gorkov Equation of Motion

The equation of motion for the Green function is derived by writing first the equation of motion for the time dependent operator itself:

$$\frac{\partial c_\downarrow(\tau)}{\partial \tau} = [c_\downarrow(\tau), H] \quad (2.84)$$

Using this identity, one can derive the equation of motion for the field dependent Green function $\mathbf{g}_{lr'}$:

$$\sum_l \begin{pmatrix} t_{rl} + (-\mu + \partial_\tau) \delta_{rl} & \psi_l \delta_{rl} \\ \psi_l^* \delta_{rl} & -t_{rl} + (\mu + \partial_\tau) \delta_{rl} \end{pmatrix} \mathbf{g}_{lr'}(\tau) = \delta_{rr'} \delta(\tau) \mathbb{I} \quad (2.85)$$

Using the fermionic Fourier-Matsubara transformation with respect to space and time τ :

$$\tilde{f}(\mathbf{k}, \omega_n) = \frac{1}{\beta V} \int d\tau \sum_r f(\mathbf{r}, \tau) e^{i\omega_n \tau} e^{-i\mathbf{k} \cdot \mathbf{r}} \quad (2.86)$$

where $\omega_n = (2n + 1)\pi/\beta$ is the Matsubara frequency.

Time Matsubara Transformation

The diagonal time derivative equation transforms as follows:

$$\begin{aligned} \partial_\tau g(\tau) &= \delta(\tau) & | \cdot e^{i\omega_n \tau} \\ \int d\tau e^{i\omega_n \tau} \partial_\tau g(\tau) &= \int d\tau e^{i\omega_n \tau} \delta(\tau) & | \int d\tau \dots \\ i\omega_n g(\omega_n) &= 1 & \end{aligned} \quad (2.87)$$

where part integration has been applied on the left side of the equation. The same operations have to be applied to the off-diagonal field dependent term:

$$\begin{aligned}
\psi(\tau)g(\tau) &= 0 & | \cdot e^{i\omega_n\tau} \\
\int d\tau e^{i\omega_n\tau}\psi(\tau)g(\tau) &= 0 & | \int d\tau\dots \\
\sum_{\omega_m} \int d\tau e^{i\omega_n\tau} e^{-i\omega_m\tau} \psi(\omega_m)g(\tau) &= 0 \\
\sum_{\omega_m} \psi(\omega_m)g(\omega_n - \omega_m) &= 0
\end{aligned} \tag{2.88}$$

where

$$\psi(\omega_m) = \int d\tau \psi(\tau) e^{-i\tau\omega_m},$$

and $\omega_m = 2\pi n'/\beta$ is the bosonic Matsubara frequency. This quantisation of the frequency is due to the periodicity $\psi(\tau + \beta) = \psi(\tau)$.

Space Fourier Transformation

The Fourier transformation is more complicate since the kinetic energy term depends on two space coordinates. Hence a double Fourier transformation has to be applied:

$$\begin{aligned}
\sum_l t_{rl} g_{lr'} - \mu g_{rr'} &= \delta_{rr'} & | \cdot e^{ikr} e^{ik'r'} \\
\sum_l \sum_r e^{ikr} t_{rl} \sum_{r'} e^{ik'r'} g_{lr'} - \mu \sum_{rr'} e^{ikr} e^{ik'r'} g_{rr'} &= \sum_r \sum_{r'} e^{ikr} e^{ik'r'} \\
\sum_l t_{kl} g_{lk'} - \mu g_{kk'} &= \delta_{kk'}
\end{aligned} \tag{2.89}$$

Using the second Fourier transform

$$t_{kl} = \sum_q \varepsilon_{kq} e^{iql} \quad \text{and} \quad g_{lk'} = \sum_{q'} g_{q'k'} e^{iq'l} \tag{2.90}$$

where ε_{kq} is the band dispersion, we get

$$\sum_q \varepsilon_{kq} g_{qk'} = \delta_{kk'}$$

A non local band dispersion is very difficult to treat, hence, assuming that the hopping integral is local, we can replaced ε_{kq} by $\varepsilon_k \delta_{kq}$:

$$\sum_q \varepsilon_{kq} g_{qk'} \rightarrow \varepsilon_k g_{kk'}$$

Hence the diagonal terms of equation (2.85) transform as

$$\sum_l (t_{rl} - \mu \delta_{lr}) g_{lr'} \rightarrow (\varepsilon_k - \mu) g_{kk'} \tag{2.91}$$

Now we apply the same transformations to the off-diagonal terms:

$$\begin{aligned} \psi_r g_{rr'} &= 0 & | \cdot e^{ikr} e^{ik'r'} \\ \sum_r e^{ikr} \psi_r \sum_{r'} e^{ik'r'} g_{lr'} &= 0 \\ \sum_q \psi_q g_{k-q,k'} &= 0 \end{aligned} \quad (2.92)$$

where we have introduced the Fourier transform of ψ :

$$\psi(\mathbf{r}) = \sum_q \psi_q e^{-i\mathbf{q}\cdot\mathbf{r}}$$

Collecting these results, the equation of motion (2.85) can be written in Fourier-Matsubara space:

$$\mathbf{G}_{0,k}^{-1}(\omega_n) \mathbf{g}_{kk'}(\omega_n) + \sum_{q,\omega_m} \mathbf{V}_q(\omega_m) \mathbf{g}_{k-q,k'}(\omega_n - \omega_m) = \delta_{kk'} \quad (2.93)$$

where the inverse unperturbed Green function is

$$\mathbf{G}_{0,k}^{-1}(\omega_n) = \begin{pmatrix} \varepsilon_k - \mu + i\omega_n & 0 \\ 0 & -\varepsilon_k + \mu + i\omega_n \end{pmatrix}$$

and the pairing potential is

$$V(q, \omega_m) = \begin{pmatrix} 0 & \psi_q(\omega_m) \\ \psi_q^*(\omega_m) & 0 \end{pmatrix}.$$

Solving the equation of motion with respect to the Green function $\mathbf{g}_{kk'}(\omega_n)$, we have

$$\mathbf{g}_{kk'}(\omega_n) = \mathbf{G}_{0,k}(\omega_n) \delta_{kk'} - \mathbf{G}_{0,k}(\omega_n) \sum_{q,\omega_m} \mathbf{V}_q(\omega_m) \mathbf{g}_{k-q,k'}(\omega_n - \omega_m) \quad (2.94)$$

The actual Green function \mathbf{G} of the system is then obtained by averaging the function \mathbf{g} over the field ψ :

$$\mathbf{G} = \langle \mathcal{T} c_i(\tau) c_j^\dagger(\tau') \rangle = \frac{1}{Z} \int D\psi \mathbf{g}(\psi) e^{-\beta S[\psi]} \quad (2.95)$$

This can be shown by adding a source field $\sum_i (c_i(\tau) h_i + c_i^\dagger(\tau') h_i^*)$ to the hamiltonian (2.71), and by taking the derivative successively with respect to h_i and h_j^* . Then the Green function is

$$G(i, j, \tau, \tau') = \frac{\partial^2 F}{\partial h_i(\tau) \partial h_j^*(\tau')}$$

In reciprocal space, the average Green function is

$$\langle \mathbf{g}_{kk'}(\omega_n - \omega_m) \rangle = \mathbf{G}_{kk'}(\omega_n - \omega_m) \delta_{\omega_n \omega_m} \delta_{kk'}$$

where δ functions appear since the system is translationally invariant.

The electronic self-energy $\Sigma(\mathbf{k}, \omega_n)$ can also be derived in the framework of the Hubbard-Stratonovich transformation. It is then a function of average of the pairing field:

$$\Sigma(\mathbf{k}, \omega_n) = \Sigma(\mathbf{k}, \omega_n, \langle |\psi|^2 \rangle) \quad (2.96)$$

A detailed derivation of this formula is done in chapter 6.

2.3.7 Bogoliubov-de Gennes Equations

Let's consider a homogeneous system. We follow first de Gennes derivation [18]. The second quantised hamiltonian is given by

$$H = \int d\mathbf{r} \sum_{\alpha} c_{\alpha}^{\dagger}(\mathbf{r}) \left[\frac{\mathbf{p}^2}{2m} \right] c_{\alpha}(\mathbf{r}) - \frac{1}{2} V \int d\mathbf{r} \sum_{\alpha\beta} c_{\alpha}^{\dagger}(\mathbf{r}) c_{\beta}^{\dagger}(\mathbf{r}) c_{\beta}(\mathbf{r}) c_{\alpha}(\mathbf{r}), \quad (2.97)$$

where the field operator $c_{\alpha}(\mathbf{r})$ is a destruction operator for an electron with spin α at position \mathbf{r} . The attraction between electrons is put in the negative potential $-V < 0$. Using the Gor'kov's factorization [19], we get an effective Hamiltonian of the form

$$H_{eff} = \int d\mathbf{r} \left\{ \sum_{\alpha} c_{\alpha}^{\dagger}(\mathbf{r}) \frac{\mathbf{p}^2}{2m} c_{\alpha}(\mathbf{r}) + \psi(\mathbf{r}) c_{\uparrow}^{\dagger}(\mathbf{r}) c_{\downarrow}^{\dagger}(\mathbf{r}) + \psi^*(\mathbf{r}) c_{\downarrow}(\mathbf{r}) c_{\uparrow}(\mathbf{r}) \right\}, \quad (2.98)$$

In order to find the eigenstates and corresponding energies, we perform a unitary transformation

$$\begin{aligned} c_{\uparrow}(\mathbf{r}) &= \sum_n (\gamma_{n\uparrow} u_n(\mathbf{r}) - \gamma_{n\downarrow}^{\dagger} v_n^*(\mathbf{r})), \\ c_{\downarrow}(\mathbf{r}) &= \sum_n (\gamma_{n\downarrow} u_n(\mathbf{r}) + \gamma_{n\uparrow}^{\dagger} v_n^*(\mathbf{r})), \end{aligned} \quad (2.99)$$

where the γ and γ^{\dagger} are quasiparticle operators satisfying the fermion commutation relations

$$\begin{aligned} \{\gamma_{n\alpha}, \gamma_{m\beta}^{\dagger}\} &= \delta_{mn} \delta_{\alpha\beta}, \\ \{\gamma_{n\alpha}, \gamma_{m\beta}\} &= 0. \end{aligned} \quad (2.100)$$

By the transformation (2.99), the effective Hamiltonian may be diagonalized, that is,

$$H_{eff} = E_g + \sum_{n,\alpha} \epsilon_n \gamma_{n\alpha}^{\dagger} \gamma_{n\alpha}, \quad (2.101)$$

where E_g is the ground state energy of H_{eff} and ϵ_n is the energy of the excitation n . Writing the equation of motion for H_{eff} , we obtain the Bogoliubov-de Gennes equations:

$$\begin{aligned}\epsilon u(\mathbf{r}) &= H_{\mathbf{p}}u(\mathbf{r}) + \psi(\mathbf{r})v(\mathbf{r}), \\ \epsilon v(\mathbf{r}) &= -H_{\mathbf{p}}^*v(\mathbf{r}) + \psi^*(\mathbf{r})u(\mathbf{r}),\end{aligned}\quad (2.102)$$

where $H_{\mathbf{p}} = \frac{\mathbf{p}^2}{2m}$. These equations can be written compactly in matrix form

$$\begin{pmatrix} H_{\mathbf{p}} & \psi(\mathbf{r}) \\ \psi^*(\mathbf{r}) & -H_{\mathbf{p}}^* \end{pmatrix} \begin{pmatrix} u \\ v \end{pmatrix} = \epsilon \begin{pmatrix} u \\ v \end{pmatrix}\quad (2.103)$$

In the case of a constant parameter $\psi(\mathbf{r})$ (that is no integral is performed on different path integrals $H_{eff}[\psi(\mathbf{r})]$) the free energy is minimised when

$$\psi(\mathbf{r}) = -V \langle c_{\downarrow}(\mathbf{r})c_{\uparrow}(\mathbf{r}) \rangle. \quad (2.104)$$

$\psi(\mathbf{r})$ is called by the pair potential at the position \mathbf{r} . Substituting Eq. (2.99) into Eq. (2.104) we find

$$\psi(\mathbf{r}) = V \sum_n v_n^*(\mathbf{r})u_n(\mathbf{r})(1 - 2f_n), \quad (2.105)$$

where $f_n = \frac{1}{\exp(\beta\epsilon_n)+1}$. Eq. (2.105) is the self-consistency equation for the pair potential.

2.3.8 BCS Solution

The BCS gap equation of superconductivity can be now easily found, either from equation Bogoliubov-de Gennes equation (2.103) or from Gorkov equation of motion (2.85). We expose now the derivation from equation (2.94). In the BCS approximation the probability distribution $p[\psi(\mathbf{r})]$ of the site dependent pairing field is replaced by a distribution p_0 for the given field ψ_0 :

$$p[\psi(\mathbf{r})] \rightarrow p_0 = \prod_{\mathbf{r}} \delta(\psi_0(\mathbf{r}) - \psi(\mathbf{r}))$$

In Fourier-Matsubara space, the pairing potential is

$$\psi_q(\omega_m) \rightarrow \psi_0 \delta_{kq} \delta_{\omega_m}$$

where k is the reference vector. Using this probability distribution, one can average the equation of motion (2.94) and gets:

$$\mathbf{G}_{kk'}(\omega_n) = \mathbf{G}_{0,k}(\omega_n)\delta_{kk'} - \mathbf{G}_{0,k}(\omega_n)\mathbf{V}_k\mathbf{G}_{k,k'}(\omega_n) \quad (2.106)$$

In matrix notation, we have

$$\begin{pmatrix} \epsilon_k - \mu + i\omega_n & \psi_0 \\ \psi_0^* & -\epsilon_k + \mu + i\omega_n \end{pmatrix} \mathbf{G}_k(\omega_n) = \mathbb{I} \quad (2.107)$$

Inverting the left matrix gives the Green function is

$$\mathbf{G}_k(\omega_n) = \frac{1}{G_{0,11}^{-1}G_{0,22}^{-1} - |\psi_0|^2} \begin{pmatrix} 1/G_{0,22} & -\psi_0 \\ -\psi_0^* & 1/G_{0,11} \end{pmatrix} \quad (2.108)$$

where $G_{0,11}^{-1} = \varepsilon_k - \mu - i\omega_n$ and $G_{0,22}^{-1} = -\varepsilon_k + \mu - i\omega_n$. The self-consistent gap equation is derived from this last equation and by the mean field condition $\psi_0 = -U \sum_{k,\omega_n} G_{12}$:

$$\psi_0 = U \sum_{k,\omega_n} \frac{\psi_0}{G_{0,11}^{-1}G_{0,22}^{-1} - |\psi_0|^2} \quad (2.109)$$

Introducing the reduced energy the $E_k = \sqrt{(\varepsilon_k - \mu)^2 + |\psi_0|^2}$, the gap equation is

$$\psi_0 = U \sum_{k,\omega_n} \frac{\psi_0}{(i\omega_n - E_k)(i\omega_n + E_k)}$$

Performing the Matsubara sum over the frequencies ω_n yields:

$$\psi_0 = -U \sum_k \psi_0 \frac{\tanh(E_k/(2T))}{2TE_k} \quad (2.110)$$

2.4 Monte Carlo Simulations

2.4.1 Metropolis Algorithm

The Monte Carlo procedure explores some configuration space by using random numbers. For example, it is possible to compute integrals by using random numbers. The number $\pi = 3.141\dots$ is obtained by selecting random numbers in a unity square surface containing a disk. Then the ratio between the number of points N_{disk} that lie inside a disk over the total number N_{square} allows to estimate π :

$$\pi := \frac{\text{area of the disk}}{\text{area of the square}} \approx \frac{N_{disk}}{N_{square}}$$

The Metropolis algorithm is a special Monte Carlo algorithm that allows to compute multi-dimensional integrals or sums. Since an integral has many integration variables x_1, \dots, x_n , a given value of the vector $\{x_1, \dots, x_n\}$ is called a configuration.

For the one dimensional integral of a function $f(x)$ on an interval $[a, b]$, it is easy to explore the configuration space by choosing N_0 random numbers uniformly distributed in this interval. However if the integral has n variables, the phase space, i.e. the number of points N necessary to evaluate the integral, grows as

$$N = \underbrace{N_0 \dots N_0}_{n \times}$$

For the Ising model, the variables are two valued spins 1 or -1. Evaluating the exact sum over one spin needs two operations, therefore $N_0 = 2$. This is quite easy! But if one

wants to evaluate the exact sum over only 100 spins then one needs to perform $2^{100} \sim 10^{30}$. On a fast computer with 10^{10} simple operations per second, this would require at least $3 \cdot 10^{12}$ years of computation: 100 times the age of the universe! Therefore one needs a approximate procedure to evaluate such sums or integrals. The idea of the Monte Carlo algorithm for large integral is to explore only configurations that have the largest weight, and to go from one to another by a random Markov chain. One plays at the Casino to evaluate his integral!

Suppose one wants to evaluate the sum:

$$Z = \sum_{x_1, \dots, x_n} f(x_1, \dots, x_n) \quad (2.111)$$

then the Monte Carlo procedure is as follow

1. Start with a random configuration $x_1^{(0)}, \dots, x_n^{(0)}$.
2. Pick up the first variable and assign to it a new random value: $x_1^{(0)} \rightarrow x_1'$.
3. Evaluate the $f_0 = f(x_1^{(0)}, \dots, x_n^{(0)})$ and $f' = f(x_1', x_2^{(0)}, \dots, x_n^{(0)})$.
4. If $f' > f_0$, the new configuration contributes more to the integral or sum than the old one and the new configuration is $x_1^{(1)}, x_1^{(0)}, \dots, x_n^{(0)}$ where $x_1^{(1)} = x_1'$.
If $f' < f_0$, the new configuration x_1' is rejected.
5. Perform points 2) to 5) for all variables $x_i^{(0)}$ with $i = 2, \dots, n$.

This set of operations is one Monte Carlo step per site and is called a *sweep* since all variables have been updated one time. To have a correct estimation of the sum, one would need more sweeps, typically 10000 to 10^{10} are used for 1000 variables.

However this Monte Carlo procedure assumes that one can explore all configurations. That is one is never trapped in a local maximum where changes in the configuration would yield only smaller values of f . If the Monte Carlo procedure encounters a local maximum, then the procedure stops and it is impossible to explore other configurations with higher value of f .

To escape from local maxima, one needs to accept a certain number of configurations with smaller value of f . This is the Metropolis version of the Monte Carlo procedure. The point 4) of the Monte Carlo procedure becomes then

4') If $f' > f_0$ then $x_1^{(1)} = x_1'$ as in the simple Monte Carlo method. If $f' < f_0$ then one accepts the move $x_1^{(1)} = x_1'$ with a certain probability p : first pick up a random number r between between 0 and r_{max} . If $r < f'/f_0$ the move is accepted otherwise it is rejected. The condition $r < f'/f_0$ means that the move is "not too bad" since small values of f'/f_0 have less chances to be accepted than values just below unity. We want to accept bad moves, but not too many...

The number r_{max} fixes how many moves in average are accepted with "bad" configurations. A 20% rate of bad moves is a typical strategy to escape from local maxima. One still has 80% of good moves to explore better configurations.

2.4.2 Metropolis for the Ising Model

In the Ising model, the hamiltonian on the real space lattice is given by

$$H = -J \sum_{\langle i,j \rangle} s_i s_j \quad (2.112)$$

where the classical spins s_i can have the value ± 1 and the sum is performed over all nearest neighbours sites $\langle i,j \rangle$. J is a coupling constant. Therefore the partition function is the sum over all configurations $\{s_i = \pm 1\}$:

$$Z = \sum_{s_i = \pm 1} e^{\beta J \sum_{\langle i,j \rangle} s_i s_j} \quad (2.113)$$

where $\beta = 1/T$ is the inverse temperature. Since one updates only one spin at each Monte Carlo step, the difference in $f = \exp(-\beta H)$ between to configurations with only one spin being different at site k is:

$$\frac{f'}{f_0} = e^{\beta J (s'_k - s_k) \sum_{\bar{k}} s_{\bar{k}}} \quad (2.114)$$

where sites \bar{k} are nearest neighbours of k . It is therefore very simple to test the condition $f' < f_0$ in a model with nearest neighbour interactions since all other contributions cancel. The Metropolis Monte Carlo procedure for updating one array (= one sweep)

1. Start with a random configuration $s_1^{(0)} = \pm 1, \dots, s_n^{(0)} = \pm 1$.
2. Pick up the first variable and assign to it the opposite value: $s_1^{(0)} \rightarrow s'_1 = -s_1^{(0)}$.
3. Evaluate f'/f_0 .
4. If $f'/f_0 > 1$ then $s_1^{(1)} = s'_1$. If $f'/f_0 < 1$ then one accepts the move if a random number r between 0 and 1 satisfies $r < f'/f_0$.
5. Perform points 2) to 5) for all spins $s_i^{(0)}$ with $i = 2, \dots, n$.

2.4.3 Exploring Configurations: Ergodicity

Not all algorithms exploring configurations in phase space are able to give an estimation of an integral. Consider for example the Metropolis algorithm for the Ising model at very high temperature. Since all configurations have the same weight, one has $f' = f_0$ and the condition $r < f'/f_0$ is always satisfied. Hence, at each Monte Carlo step, the spin will be reversed. The Markov chain is then

$$A \rightarrow B \rightarrow A \rightarrow B \rightarrow \dots$$

where A and B are two configurations having all spins with opposite sign. The problem is that the algorithm remains in the subspace $\{A, B\}$ of configuration space: it is non

ergodic and the result will be false. It is therefore very important to prove the ergodicity of an algorithm by showing that there is a finite probability to go from one configuration σ to any other configuration ϱ :

$$p(\sigma \rightarrow \varrho) > 0 \quad (2.115)$$

2.4.4 No Time Reversal Symmetry Breaking: Detailed Balance

The detailed balance condition tells us on average the system goes from a state σ to a state ϱ in the same rate as from ϱ to σ . In other words, the system has no preferred direction in phase space. If one compares the simulation time with a real time, the detailed balance condition is equivalent to say that there is no time reversal symmetry breaking. Any path in the configuration space have the same transition rate R weighted by the probability p_σ to start with the configuration σ :

$$p_\sigma R(\sigma \rightarrow \varrho) = p_\varrho R(\varrho \rightarrow \sigma) \quad (2.116)$$

If we work in the canonical ensemble, the equilibrium distribution is the Boltzmann distribution:

$$p_\sigma \sim e^{-\beta E_\sigma} \quad (2.117)$$

Hence, the detailed balance condition (2.116) reads:

$$\frac{R(\sigma \rightarrow \varrho)}{R(\varrho \rightarrow \sigma)} = \frac{p_\varrho}{p_\sigma} = e^{-\beta(E_\varrho - E_\sigma)} \quad (2.118)$$

2.4.5 Metropolis for the GL Model

The complex Φ^4 or Ginzburg-Landau (GL) model is the statistical version of the Landau mean field theory and vice-versa. The action S of the GL model has the same form as the free energy 2.2 in the mean field Landau theory.

$$S[\psi] = \int d^d r \left[at |\psi|^2 + \frac{b}{2} |\psi|^4 + \frac{\gamma}{2} |\nabla \psi|^2 \right] \quad (2.119)$$

The partition function Z in the canonical ensemble is the sum over all possible configuration of the complex field ψ

$$Z = \int D^2 \psi e^{-\beta S[\psi]} \quad (2.120)$$

There are three main differences with respect to the Ising model:

1. The field ψ is continuous in space.
2. The size or amplitude of the field is not fixed but is determined by the potential $at |\psi|^2 + \frac{b}{2} |\psi|^4$.

3. ψ is complex and belongs to XY universality class. An XY spin or field is a planar vector with unity modulus.

On the lattice, with lattice spacing ε , we normalise the hamiltonian by setting

$$R^2 = |\psi|^2/(a/b), \quad \text{and} \quad \vec{u} = \vec{r}/\xi_0$$

where $\xi_0^2 = \gamma/a$ is the mean field correlation length at zero temperature. The normalised action is then:

$$S = k_B V_0 \left(U_R + \sum_{\langle ij \rangle} |\psi_i - \psi_j|^2 \right) \quad (2.121)$$

where

$$U_R := \sum_{i=1}^N [\sigma (tR_i^2 + R_i^4/2)].$$

We have now only three independent parameters: V_0, σ, T_0 . $\sqrt{\sigma} = \varepsilon/\xi_0$ is the coarse graining parameter and its value is typically between 3 and 10. That is one needs an array of lattice constant $3 - 10\xi_0$ to define an average ψ starting from a microscopic model.

The Metropolis Monte Carlo procedure for updating one array (= one sweep) is:

1. Start with a random configuration $\psi_1^{(0)}, \dots, \psi_n^{(0)}$, where ψ is complex $|\psi| < 1$.
2. Pick up the first variable and move it as: $\psi_1^{(0)} \rightarrow \psi_1' = \psi_1^{(0)} + \psi\psi$ where $\psi\psi$ is random complex number whose size is lower than a limit $L\psi$.
3. Evaluate the f'/f_0 .
4. If $f'/f_0 > 1$ then $s_1^{(1)} = s_1'$. If $f'/f_0 < 1$ then one accepts the move if a random number r between 0 and 1 satisfies $r < f'/f_0$.

Writing the Monte Carlo procedure in C code for a two dimensional $n \times n$ lattice gives the following program:

```

/* loops over sites */
for (i=0;i<n;i++){
for (j=0;j<n;j++){

    /* periodic boundary conditions: coordinates of the 4 neighbours sites of site (i,j) */
    ineg=(i+n-1) % n; jpos=(j+1) % n;
    jneg=(j+n-1) % n; ipos=(i+1) % n;

    /*The trial field x at site (i,j) is the old one psi plus a random fluctuation: */
    x[0] = psi[i][j][0] + (drand48()- 0.5) * 2 * Lim;

```

```

x[1] = psi[i][j][1] + (drand48()- 0.5) * 2 * Lim;

/* difference between the old and the trial configuration */
for (l=0;l<2;l++){ ds[l] = x[l]-psi[i][j][l];
stot[l] = psi[ineg][j][l]+ psi[i][jneg][l]+
psi[ipos][j][l]+ psi[i][jpos][l] ;};

/* difference between old and new Ginzburg-Landau potentials*/
R2 = psi[i][j][0]*psi[i][j][0]+psi[i][j][1]*psi[i][j][1];/* amplitude square*/
Uold = (4*c+a)*R2 + b* R2*R2 /2.;
R2 = x[0]*x[0]+x[1]*x[1];
Unew = (4*c+a)*R2 + b* R2*R2 /2.;

/*transition probability p = f'/f0 */
p=exp(-(Uold-Unew-2*c*(ds[0]*stot[0]+ds[1]*stot[1]))*Vo/T);

/*condition for updating */
if( p < drand48() )
{ for (l=0;l<2;l++) {spin[i][j][l] = x[l];};
};

}};/* end of loops over sites*/

```

where `drand48()` yields a random number between 0 and 1.

2.4.6 Cluster Algorithm

The Metropolis algorithm changes only one spin after the other ignoring updates of larger structures. The idea of the cluster algorithm is to perform cluster flip instead of spin flip. Consider a snap shot of an Ising simulation, one sees that near the phase transition there are many clusters of spins having the same orientation. The size of these clusters becoming comparable with the size of the system at the critical temperature T_c . Hence, these clusters are the "natural" structures of the phase transition, and it is much faster to explore the phase space by going from one cluster configuration to another instead of flipping single spins.

The first realisation of a cluster algorithm has been done by Swendsen and Wang in 1987 for the Ising model. In the Swendsen and Wang cluster algorithm, all clusters are flipped at each step. Here we want to explain the Wolff algorithm derive by Uli Wolff in 1989 where only one cluster is flipped at each step.

To introduce this algorithm we use the ferromagnetic Ising model.

$$H = -J \sum_{\langle i,j \rangle} s_i s_j \quad (2.122)$$

Consider an array containing some clusters of spins with same orientation and pick up one cluster at random. If we flip that cluster, the energy change will be only on the frontier of the cluster. Suppose one has N_c spins in the cluster with L bonds between the border of the cluster and other spins of the array, all these bonds have positive energy J and will have negative energy $-J$ after the cluster flip. The energy change ΔE is then

$$\Delta E = -2LJ \quad (2.123)$$

The probability for going from one configuration σ to the another σ' by flipping the cluster is then

$$p_{\sigma \rightarrow \sigma'} = \frac{p_{\sigma}}{p_{\sigma'}} = e^{-\beta \Delta E} = e^{\beta 2LJ} \quad (2.124)$$

The problem is the following: if one flips the entire cluster at each step then one will never explore then entire phase space since one will end up with one big cluster filling all the array.

To achieve ergodicity it is necessary to put some disorder by introducing temperature in the system: that is to construct clusters with impurities. If one flips imperfect cluster with a small number of spin with opposite sign in it, one can explore all the configuration space. How to achieve such a cluster? Let us construct a cluster from the first spin, called the *seed* for obvious reasons. First we pick up one spin at random and we look for neighbours having the same orientation. All neighbours with same orientation are added in the cluster with a probability p_{add} .

In order to find an expression for p_{add} , we use the *detailed balance* condition from equation (2.118). If we flip a cluster with different oriented spins, one has to break m bonds of similarly oriented spins. The probability of not adding this m spins is $(1 - p_{add})^m$. Note that we flip the cluster spin by spin. Now we consider the reverse operation on the same cluster. one has now n spins with similar orientations ($n = L - m$ where L is the number of spins at the edge of the cluster). When one breaks this bonds, the probability of not adding them to the cluster is $(1 - p_{add})^n$.

The probability $P(\mu \rightarrow \nu)$ of going from a configuration μ to a configuration ν can be separated in two operations:

1. one has a selection probability $S(\nu|\mu)$ that the algorithm will generate a configuration ν when starting from a configuration μ .
2. Then one has an acceptance $A(\mu \rightarrow \nu)$ rate for going from the configuration μ to the configuration ν .

Therefore the probability $P(\mu \rightarrow \nu)$ is

$$P(\mu \rightarrow \nu) = S(\nu|\mu) A(\mu \rightarrow \nu) \quad (2.125)$$

The detailed balance condition(2.118) is then

$$\frac{P(\mu \rightarrow \nu)}{P(\nu \rightarrow \mu)} = \frac{S(\nu|\mu) A(\mu \rightarrow \nu)}{S(\mu|\nu) A(\nu \rightarrow \mu)} = e^{-\beta(E_{\nu} - E_{\mu})} \quad (2.126)$$

In our problem, the probability of selecting the configuration ν with n bonds broken is

$$S(\nu|\mu) = (1 - p_{add})^n \quad (2.127)$$

We do not consider the other bonds since their probability is the same by going from μ to ν or from ν to μ . Therefore

$$\frac{P(\mu \rightarrow \nu)}{P(\nu \rightarrow \mu)} = (1 - p_{add})^{m-n} \frac{A(\mu \rightarrow \nu)}{A(\nu \rightarrow \mu)} = e^{-\beta(E_\nu - E_\mu)} \quad (2.128)$$

The energy difference between the two configurations is given by

$$E_\nu - E_\mu = -2Jn + 2Jm = 2J(m - n) \quad (2.129)$$

In order to have the highest acceptance rate, we can choose p_{add} as:

$$p_{add} = 1 - e^{-2\beta J} \quad (2.130)$$

With this choice we can set $A(\mu \rightarrow \nu) = A(\nu \rightarrow \mu) = 1$: that is every move is accepted. We have therefore a simple and efficient algorithm which satisfies the detailed balance condition.

Cluster algorithms are very efficient in reducing the critical slowing down during the simulation time near a critical temperature. They are however less efficient at high temperatures than a Metropolis algorithm since one has to check all neighbours at each step even if clusters are formed of one spin in average.

I do not present here the algorithm for planar spins (XY models) and we refer the reader to the original article of Uli Wolff [20] and for the Φ^4 model to the article of R. C. Brower [21]. However I show the listing of the implementation in C code for the Ginzburg-Landau cluster algorithm:

Cluster Monte Carlo for the phase

D is the dimension.

$size$ is the dimension of the array.

$clus$ is the cluster $size^D$ array, it is composed of 0 (the spin is not in the cluster) and 1 (the spin is in the cluster).

$seed$ is the starting point of the cluster.

```

/*choose a random seed to start the cluster*/
for (l=0;l < D;l++) seed[l] = rand() % size;

/*the starting cluster is empty */
for (k=0;k < size;k++)for (p=0;p < size;p++) clus[k][p]=0;;

clus[seed[0]][seed[1]] = 1; /*the seed is added to the cluster */
nvo[0][0] = seed[0];
nvo[0][1] = seed[1]; /*spins added at the previous loop*/

```

```

r = drand48()* 2 * 3.1415926535897; /*random number*/

/*choose a random complex number z defining the cluster orientation*/
z[0]= cos(r); z[1]= sin(r);

/*mc is the number of spins in the cluster, i.e. the number of 1*/
mc=1; mo=1; mcOld=0;

/*Perform loops until no new spin can be added: the size of the cluster is constant*/
while( mc!=mcOld ){ mcOld=mc;
  m=0;
  for (k=0;k < mo ;k++){
    i = nvo[k][0];/*position of spin added at the previous loop*/
    j = nvo[k][1];
    ipos = (i+1) % size; /*position of the neighbour modulo size*/
    jpos = (j+1) % size;
    ineg = (i+size-1) % size;
    jneg = (j+size-1) % size;
    r1 = spin[i][j][0]*z[0]+spin[i][j][1]*z[1];
    if (r1<0) sis = -1; else sis =1;/*orientation of the spin in direction z*/

    /*if the neighbour of the new spin is not already in the cluster*/
    if (clus[ipos][j]!=1){
      r2 = (spin[ipos][j][0]*z[0] + spin[ipos][j][1]*z[1]); /*compute the scalar product*/
      if (r2<0) sig = -1; else sig = 1; if( sis == sig ){ /*if the orientation the in z*/
        if ( drand48() < 1-exp(-4*c*r1*r2*Vo/T)){ /*probability of adding the new spin*/
          nv[m][0] = ipos; nv[m][1] = j; m=m+1;/*the position of the new spin is stored*/
          clus[ipos][j] = 1; mc=mc+1;}};/*the spin is added in the cluster*/

      ...
      /* update all neighbours of spin {i,j} using this procedure*/
      ...

      s[0] = spin[i][j][0];
      s[1] = spin[i][j][1];

      /*flip the spin that has been added in the cluster*/
      for (l=0;l<n;l++) {spin[i][j][l] = s[l] - 2*r1*z[l];};

    };/*end of loop over the spins that have been added at the last loop nvo*/

    /*store the position of the spin that have been added*/
    for (p=0;p<m;p++)nvo[p][0]= nv[p][0];
    nvo[p][1]= nv[p][1];}; mo=m; /*mo is the old cluster size*/
  }
}

```

} **/ end of while */*

Chapter 3

VARIATIONAL APPROACH FOR THE GL MODEL

The d -dimensional complex Ginzburg-Landau (GL) model is solved according to a variational method by separating phase and amplitude. This approach allows to find an approximate solution for the partition function including all phase fluctuations and gaussian fluctuations of the amplitude. The GL transition becomes first order for high superfluid density because of effects of phase fluctuations. We discuss its origin with various arguments showing that, in particular for $d = 3$, the validity of our approach lies precisely in the first order domain.

3.1 Choosing the Right Variational Approach

From the usual point of view, a self-consistent approach consists in fixing a variable or a more elaborated function like a Green function and looking for the minimum of the free energy with respect to it. However, we want to show here that the choice of the variable to be fixed is not innocent. For example, one can look for the minimum of a function $f(x)$ with respect to x or with respect to $a = x^2$ by defining $f'(a) = f(\sqrt{a})$. In this example, the result is identical for both methods. However, in the problem of computing an integral, results can be very different as I show for the following simple example. Let us consider the probability distribution

$$p(r) = e^{-r^2} \quad (3.1)$$

where $r > 0$. We would like to compute the mean-value of r by computing the integral

$$\langle r \rangle = \frac{\int_0^\infty dr r e^{-r^2}}{\int_0^\infty dr e^{-r^2}} \quad (3.2)$$

Evaluating directly the integrals gives the exact result:

$$\langle r \rangle = \frac{1/2}{1/\sqrt{\pi}} = \frac{1}{\sqrt{\pi}} \approx 0.56.$$

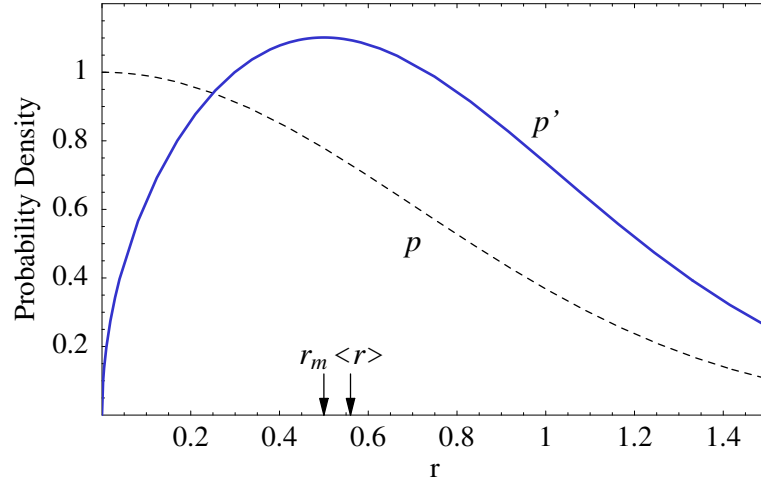


Figure 3.1: The probability density is more symmetric with respect to $\langle r \rangle$ for $p'(r)$ than for $p(r)$.

Now we would like to look for approximate solution of this integral by estimating where is the maximum contribution of the function $p(r) = e^{-r^2}$. $p(r)$ is maximal for $r_m^{(0)} = 0$ and our estimate of the average value could be $\langle r \rangle = r_m^{(0)} = 0$ which is of course completely wrong. Why are $\langle r \rangle$ and r_m so different? This is due to asymmetry of the probability distribution with respect to r_m . Indeed, any symmetric distribution with respect to its maximum will have $\langle r \rangle = r_m$ like the gaussian distribution $\exp(-x^2)$ where $x \in]-\infty, \infty[$. The difficulty is therefore to find the right variable in order to have the most symmetric distribution with respect to its maximum. Then an estimate of averaged values is done by a variational scheme. In our example, it is possible to express the probability distribution in term of a new variable $u = \sqrt{r}$. The normalisation factor is

$$\int_0^\infty dr e^{-r^2} = \int_0^\infty du 2u e^{-u^4} \quad (3.3)$$

The new probability distribution is $p'(u) = 2u e^{-u^4}$ and it can be expressed in the variable r :

$$p'(r) = 2\sqrt{r} e^{-r^2} \quad (3.4)$$

$p'(r)$ is obviously more symmetric with respect to its average value than $p(r)$, see figure 3.1. Indeed the maximum of $p'(r)$ lies at $r_m = 1/2$ and gives the estimate for $\langle r \rangle$:

$$\langle r \rangle \approx r_m = 0.5 \quad (3.5)$$

which is not to fare from the exact result 0.56. This estimation is much better than the one of the naive approach since the first guess was $\langle r \rangle = 0$. The transformation $u = r^2$ has been chosen but there are other transformations leading to better results.

We have shown the importance of choosing the correct representation for a one dimensional integral. This will be also relevant for multi-dimensional integrals. When

doing a variational approach with respect to the amplitude of a complex field, it is therefore important to check the symmetry of the probability distribution. This can be done by including the Jacobian of the transformation from cartesian to polar coordinates in the potential as we will see in the next chapters.

3.2 Overview

Ginzburg-Landau free energy functionals involving a n -component space and time dependent field have been widely used in order to describe different types of phase transitions in a semi-phenomenological way. The case $n = 2$, corresponding to a complex field ψ , applies in particular to superconductivity, superfluidity, metal-insulator transitions or to magnetic systems with moments that are confined to a plane (XY moments). For such particular applications, the coefficients determining the functional can be derived from appropriate microscopic models. For superconductors, this was originally done by Gorkov [22] and has been refined since by numerous authors [23]. In its simplest form, the GL functional involves a time independent field and thus describes (classical) thermodynamic and static phenomena of superconductors. For the description of dynamic phenomena, charging effects [24] or pairing fluctuations in strong coupling superconductors [23], one needs the generalisation to a time dependent field.

An important aspect of the case $n = 2$ is the interplay between variations of amplitude $|\psi|$ and phase ϕ of the corresponding complex field $\psi = |\psi|e^{i\phi}$. In various approximate treatments, such as the mean field approximation or the Hartree decoupling of terms involving higher powers of ψ , the field is treated as a whole, without separating amplitude and phase. More accurate studies of the static GL problem, like the renormalisation group approach [25, 26] focusing in particular on the region near the phase transition, show that the amplitude has no critical behaviour and is irrelevant at the transition. The phase transition scenario should then correspond to the one of the XY model with the same dimensionality. In the framework of the ε -expansion [27, 28], for $d = 3$, the transition is second order and seems to have the same critical exponents as the XY model. On the other hand, Bormann and Beck [29] have shown that amplitude fluctuations, even though not being critical by themselves, might alter the cooperative phenomenon occurring with phases, in particular in dimension 2. Like the XY model, corresponding to a fixed value of the amplitude, the $2d$ GL model can be mapped onto a Coulomb gas describing vortex-antivortex pairs. As soon as one allows for amplitude variations, these topological excitations become energetically more favorable. Taking into account gaussian amplitude fluctuations, Bormann and Beck [29] have shown that the system may be driven into a regime where - according to Minnhagen's phase diagram [30] - a first order transition replaces the usual Kosterlitz-Thouless scenario.

As far as superconductors are concerned, BCS theory [4] predicts that the transition between the normal state and the superconducting state is a second order phase transition. However, it is well known that fluctuations can change the order of the transition. For example, fluctuations of the magnetic field change the GL-BCS transition to a first

order transition for type I superconductors [31]. The three state Potts model in two dimensions is an opposite example: mean field theory predicts a first order transition, whereas the actual transition is continuous. So the question of the order of the transition in the GL model, as well as the more detailed mutual influence between phase and amplitude, is still an open problem.

The aim of this chapter is to show the reciprocal influence between phase and amplitude by separating self-consistently, from the outset, the GL functional into two parts: the amplitude part and the phase part.

3.3 Effective Action

According to Ginzburg-Landau theory, we define the effective hamiltonian functional

$$H[\psi] = \int d^d r \left[at |\psi|^2 + \frac{b}{2} |\psi|^4 + \frac{\gamma}{2} |\nabla \psi|^2 \right] \quad (3.6)$$

where a , b and γ are coefficients independent of the temperature derived from a microscopic model. $t = T/T_0 - 1$ is the reduced temperature and T_0 is the mean field critical temperature. We now introduce the amplitude $|\psi|$ and the phase ϕ of the field $\psi = |\psi|e^{i\phi}$. On the lattice, with lattice spacing ε , we normalize the hamiltonian by setting $R^2 = |\psi|^2/(a/b)$, $\vec{u} = \vec{r}/\xi_0$, where $\xi_0^2 = \gamma/a$ is the mean field correlation length at zero temperature. The normalized hamiltonian is then:

$$H[R, \phi] = k_B V_0 \left(H_R + \sum_{i=1}^N R_i^2 f_i \right) \quad (3.7)$$

where

$$f_i := \sum_{j=1}^d [1 - \cos(\phi_i - \phi_j)] \quad (3.8)$$

and

$$H_R := \sum_{i=1}^N \left[\sigma (tR_i^2 + R_i^4/2) + (\nabla R_i)^2 / 2 \right]. \quad (3.9)$$

where $\nabla R_i := \sum_j \vec{e}_j (R_i - R_j)$. j points to the nearest neighbours of i and \vec{e}_j is a unit vector in direction j . We have set $R_i R_j = R_i ((R_j - R_i) + R_i) \approx R_i^2$ in the XY part of the hamiltonian. Indeed, the term $R_i (R_j - R_i)$ is not important for the present discussion because our approach will be reliable when amplitude fluctuations are small compared to phase fluctuations. Only two parameters, that are in competition, remain:

$$\sigma := \varepsilon^2 / \xi_0^2 \quad V_0 := \frac{1}{k_B} \frac{a}{b} \gamma \varepsilon^{d-2}$$

σ controls amplitude fluctuations. V_0 corresponds to the zero temperature phase stiffness. V_0 is proportional to the superfluid density a/b and controls the general critical

behaviour. When V_0/T_0 is large, the critical region is small and the material behaves according to mean field theory (as BCS superconductors). When V_0/T_0 is of the order of 1, phase fluctuations become very large and give an upper bound for the critical temperature [32]. Thermodynamic properties of the system are parametrized by the temperature T in the Boltzmann factor but also by the temperature $t = T/T_0 - 1$ inside the hamiltonian $H[\psi]$.

Let us write the partition function in polar coordinates:

$$Z = \int_0^{2\pi} D\phi \int_0^\infty DR e^{-\beta H_{eff}}$$

where the effective hamiltonian H_{eff} is

$$H_{eff} = k_B V_0 \left[H_R + \sum_i \left(R_i^2 f_i - \frac{T}{V_0} \log R_i \right) \right] \quad (3.10)$$

We keep the factor R of the Jacobian, $R D\phi DR$, and take it in the exponential giving a contribution $\log R$ to the potential. This incorporates the fact that small values of R have a small statistical weight, due to the volume element in phase space, into the Boltzmann factor of the canonical ensemble.

3.4 Self Consistent Approximation

We compute now the partition function by integrating only the phase. For this purpose, we will drop the integration on R_i and search for the minimum of the free energy with respect to R . The partition function becomes then:

$$Z \approx \int_0^{2\pi} D\phi e^{-\beta H_{eff}}$$

The minimum of the free energy $F = -k_B T \log Z$ is given through the equation $\delta F / \delta R_i = 0$. Assuming that the gradient of the amplitude is zero, we have

$$\sigma (tR^2 + R^4) - \frac{T}{2V_0} + R^2 f(K) = 0 \quad (3.11)$$

where we have multiplied the equation by $R/2$. $f(K) = \langle f_i \rangle$ is the expectation value within the XY model of f_i with a dimensionless coupling $K = \frac{V_0}{T} R^2$. Since the average should not depend on the site, we can write:

$$\langle f_i \rangle = \left\langle \frac{1}{N} \sum_i f_i \right\rangle \quad (3.12)$$

Therefore the energy of the XY system is:

$$f(K) = \frac{1}{Z_{XY}} \int D\phi \left(\frac{1}{N} \sum_i f_i \right) e^{-K \sum_{\langle i,j \rangle} [1 - \cos(\phi_i - \phi_j)]} \quad (3.13)$$

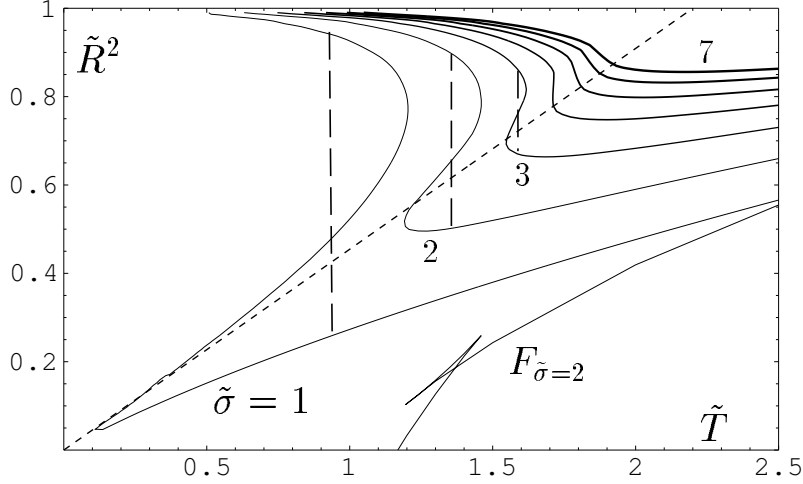


Figure 3.2: **Reduced mean amplitude as a function of the reduced temperature for $d = 3$ for different values of $\tilde{\sigma}$.** The slanting dashed line shows the XY transition ending at $\tilde{T}_c = \omega_{3d} = 2.2$ ($\tilde{\sigma} \rightarrow \infty$). The vertical dashed lines indicate the temperature where the first order transition arises. The free energy $F_{\tilde{\sigma}=2}$ for $\tilde{\sigma} = 2$ is also shown (in arbitrary units).

and $Z_{XY} = \int D\phi e^{-K \sum_{\langle i,j \rangle} [1 - \cos(\phi_i - \phi_j)]}$ Although K has the same value at each lattice site and does not explicitly adapt to the vortex structure of the phase field, the average energy of the latter still determines the value of K through the minimalisation of the free energy F . In this work, we use Monte Carlo simulations to evaluate the function $f(K)$ which is the energy of the XY model [33]. The critical temperature T_c is reached when the coupling K equals the critical constant $1/\omega$:

$$1 = \omega K_c = \omega \frac{V_0}{T_c} \langle R^2 \rangle (T_c) \quad (3.14)$$

where $\omega = 0, 0.9, 2.2$ (for $d = 1, 2, 3$ respectively) is the bare XY critical temperature on a square lattice with unit coupling constant $K = 1/T$.

The solution of equation (3.11) is plotted in figure 3.2 for $d = 3$. We use a normalization which is independent of the temperature t :

$$\tilde{R}^2 = R^2/(-t), \quad \tilde{T} = T/(-tV_0), \quad \tilde{\sigma} = -t\sigma. \quad (3.15)$$

The free energy F is calculated using the formula:

$$F = \int dR \frac{\partial F}{\partial R}, \quad (3.16)$$

and has three branches. The crossing point of the two lower branches determines the location of the first order transition, marked by a vertical dashed line. The consequence

is a first order transition for

$$\tilde{\sigma}_c = -\sigma t_c \lesssim 4.5, \quad (3.17)$$

i.e. the mean amplitude R^2 jumps at T_c . For $d = 2$, we have also a first order transition for $\tilde{\sigma}_c \lesssim 1.25$. For $d = 1$, there is no transition.

A good approximation for the critical temperature due to phase fluctuations is given by (3.14) with $\langle R^2 \rangle = -t_c$:

$$t_c \approx -T_c/(\omega V_0) \quad (3.18)$$

Combining this last equality and (3.17), the first order transition occurs then for $\sigma T_c/V_0 \lesssim C$ where $C = \omega 4.5 \approx 9.9$ for $d = 3$.

3.5 Fluctuations Around the Saddle Point

What are the influence of amplitude fluctuations around the saddle point that we found? Do they destroy the first order transition or not? In order to answer this question, we include harmonic amplitude fluctuations in our computation. We separate phase and amplitude, introduce three variational parameters and derive two self consistent equations for these parameters.

The effective potential

$$U_{eff} := \sigma \left(t R_i^2 + \frac{1}{2} R_i^4 \right) - \frac{T}{V_0} \log R_i \quad (3.19)$$

of the effective hamiltonian (3.10) has only one minimum for all temperatures. So one can expect that a gaussian approximation for the amplitude gives a good approximation for all temperatures. We want also to get an hamiltonian with no direct coupling between phase and amplitude, but with effective constants that keep the memory of their interaction. The idea is then to separate phase and amplitude as:

$$R_i^2 f_i \quad \rightarrow \quad R_i^2 \langle f_i \rangle + \langle R_i^2 \rangle f_i \quad (3.20)$$

Therefore, we set the **trial hamiltonian**:

$$H_t[R, \phi] = \sum_i [B (R_i - R_0)^2 + \frac{1}{2} (\nabla R_i)^2 + A f_i] \quad (3.21)$$

Using the Bogoliubov inequality, we have $F \leq F_t + \langle H_{eff} - H_t \rangle_t = \tilde{F}$, where F is the free energy and $\langle \dots \rangle_t$ is the canonical average with respect to H_t . The right hand side is thus to be minimized with respect to the constants A , R_0 and B to give the best approximation of F . We introduce also the local amplitude fluctuation $\eta_i = R_i - R_0$. The derivative of \tilde{F} with respect to these parameters gives three equations:

$$A = \langle R^2 \rangle = R_0^2 + \langle \eta^2 \rangle \quad (3.22)$$

$$[\sigma(t + 3\langle \eta^2 \rangle) + \langle f \rangle] R_0^2 + \sigma R_0^4 - \frac{T}{V_0} \frac{R_0}{2} \frac{\partial \langle \log R \rangle}{\partial R_0} = 0 \quad (3.23)$$

$$\sigma(t + 3\langle \eta^2 \rangle) + \langle f \rangle - B + 3\sigma R_0^2 - \frac{T}{V_0} \frac{\partial \langle \log R \rangle}{\partial B} = 0 \quad (3.24)$$

where all indices t and i are dropped. $\langle \log R_i \rangle$ is computed by a cumulant expansion, see Appendix A, and gives:

$$\langle \log R \rangle = \langle \log(R_0 + \eta) \rangle \approx \log(R_0) + \log \left[1 - \frac{1}{2} \frac{\langle \eta^2 \rangle}{R_0^2} - \frac{5}{8} \left(\frac{\langle \eta^2 \rangle}{R_0^2} \right)^2 \right] \quad (3.25)$$

Putting the last result into equations (3.23) and (3.24) yields:

$$[\sigma(t + 3\langle \eta^2 \rangle) + \langle f \rangle] R_0^2 + \sigma R_0^4 - \frac{T}{2V_0} g(R_0, B) = 0 \quad (3.26)$$

$$\sigma(t + 3\langle \eta^2 \rangle) + \langle f \rangle - B + 3\sigma R_0^2 - \frac{T}{2V_0} R_0 g(R_0, B) = 0 \quad (3.27)$$

where

$$g(R_0, B) = 1 + \left[\frac{\langle \eta^2 \rangle}{R_0^2} + \frac{5}{2} \left(\frac{\langle \eta^2 \rangle}{R_0^2} \right)^2 \right] \frac{1}{1 - \frac{1}{2} \frac{\langle \eta^2 \rangle}{R_0^2} - \frac{5}{8} \left(\frac{\langle \eta^2 \rangle}{R_0^2} \right)^2} \quad (3.28)$$

The mean square amplitude fluctuation, which depends only on B , is

$$\langle \eta^2 \rangle = \frac{1}{Z_{harm}} \int_{-R_0}^{\infty} D\eta \eta^2 e^{-\beta \sum_i [B \eta^2 + \frac{1}{2} (\nabla \eta)^2]} \quad (3.29)$$

where

$$Z_{harm} = \int_{-R_0}^{\infty} D\eta e^{-\beta \sum_i [B \eta^2 + \frac{1}{2} (\nabla \eta)^2]} \quad (3.30)$$

Using the Fourier transform of η , and assuming that amplitude fluctuations are small, we can extend the lower bound $-R_0$ to $-\infty$, and get the result:

$$\langle \eta^2 \rangle = \frac{T}{V_0} 1/V \sum_{|\mathbf{k}| < \Lambda} \frac{1}{2} \frac{1}{B + k^2/2} \quad (3.31)$$

Λ is the reduced cut-off parameter and is computed on the first Brillouin zone.

Equation (3.26) reduces to equation (3.11) when the additional amplitude fluctuations are zero: $\langle \eta^2 \rangle = 0$. The phase diagram is approximately the same as the one without amplitude integration, except that the critical temperature is smaller due to the additional harmonic amplitude fluctuations. Solving equations (3.26) and (3.27), I found that the transition is first order for $\sigma \lesssim 9.9 V_0/T_c$ for $d = 3$.

For $d = 1$, the inclusion of harmonic amplitude fluctuations suppresses the first order transition (strong fluctuations prevent the system to adopt one of the two minima of the free energy). In figure 3.3, we can see a plot of $\langle R^2 \rangle$ compared to the exact solution proposed by Scalapino, Sears and Ferrel [34] who used a transfer integral to solve the $1d$ Ginzburg-Landau model (see appendix B for a generalisation of this method: equivalence between the d -dimensional Ginzburg-Landau model and the single particle quantum double-well in $d - 1$ dimension). For this comparison, we set $T/V_0 = \sigma = 1$. The upper curve (thin line) is computed with $f(K) = 0$. The dots show the solution of equations (3.26) and (3.27) with a $f(K)$ computed exactly. We can see the influence

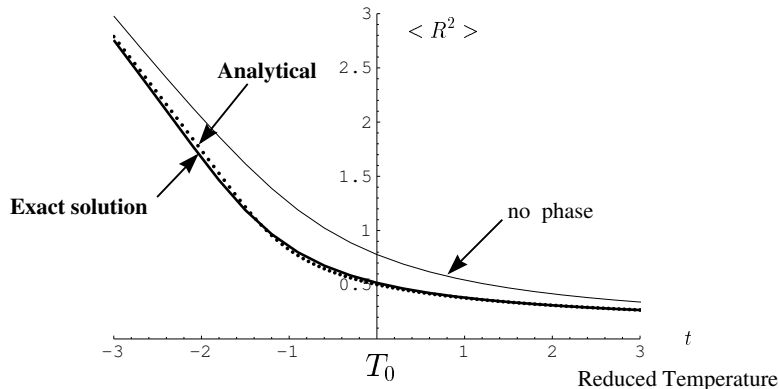


Figure 3.3: **Expectation value of R^2 for $d = 1$.** The points show the solution of equations (3.26) and (3.27). We see here how the phase "moves" the amplitude to lower temperatures due to the effective temperature $t + f(K)$.

of the phase on the amplitude. The phase moves the amplitude towards the left.

Considering equation (3.26), one sees that the effective reduced temperature t_{eff} (i.e. the factor that multiplies R_0^2) is

$$t_{eff} = t + 3\langle\eta^2\rangle + \frac{\langle f_i \rangle}{\sigma} \quad (3.32)$$

There are two additional contributions: the first, $3\langle\eta^2\rangle$, comes from amplitude fluctuations and the second, $\langle f_i \rangle/\sigma$, from the phase. Both terms are positive so that they move the amplitude towards lower values. In other words, amplitude and phase fluctuations induce an effective positive shift in temperature: they act as a heating of the system.

In figure 3.4, in $d = 2$ we compare the result of equation (3.26) and (3.27) to cluster Monte Carlo simulations for the domain where the transition is smooth. Although, the agreement is not so good as in 1 dimension, all essential features are present: the transition temperature is almost correct and the amplitude has the same behaviour as in simulations.

In figure 3.5, comparison is made for the case where the transition is first order. However, simulations show no first order transition but only a cusp near T_c which is the sign of the interplay between phase and amplitude. How can we explain this discrepancy? Two answers are possible:

1. the first order transition is present and simulations are trapped in a local minima of the energy.

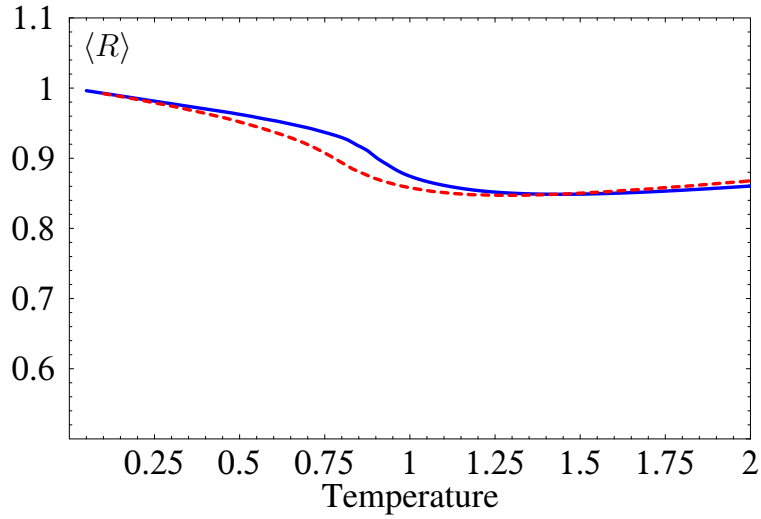


Figure 3.4: Comparison between Monte Carlo simulations (dashed line) and the variational approach (full line) in the continuous regime $\tilde{\sigma} = 4$ in $d = 2$. Note the relative good agreement between the two methods.

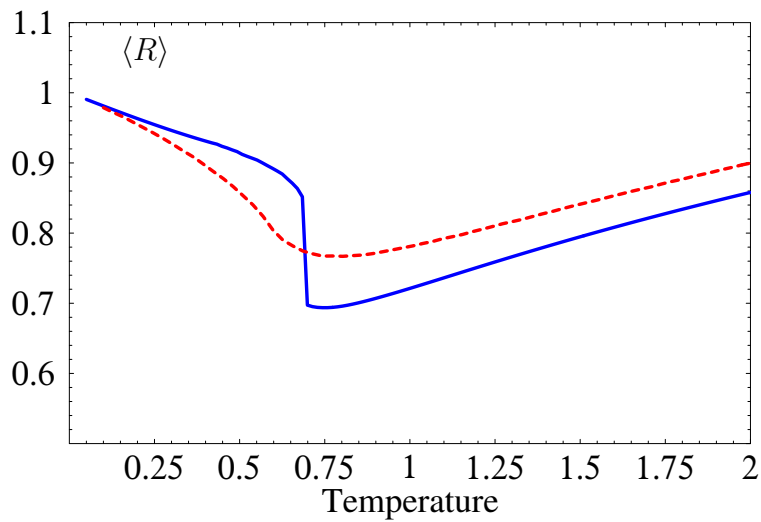


Figure 3.5: Comparison between Monte Carlo simulations (dashed line) and the variational approach (full line) in the first order regime $\tilde{\sigma} = 1$ in $d = 2$. There is no first order transition seen in Monte Carlo simulations.

2. The transition is smooth and the first order nature of the transition signals the breakdown of the analytical approach.

We cannot answer to that question but we will give some hints that indeed a first order transition could be possible. The fact that simulations cannot show the first order transition is possibly due to the existence of many local minima in the free energy. Going from one to another minima requires a special algorithm more sophisticated than a simple Monte Carlo sampling. Indeed, it is very unlikely to explore all the configuration space by adapting one spin after the other. The cluster algorithm does not help further to explore first order phase transitions.

In the Ginzburg-Landau model, simulations on small systems cannot help since there is no special symmetry. Indeed, in the Potts or Ising models, one has a fundamental symmetry in the system. Ising spins can be all up or all down in the ground state. There is a coexistence of two phases, and the probability distribution of these phases is present already for very small systems. Hence, one can analyse the system size dependence of these phases in order to find the order of the phase transition: if both phases remain when increasing the system size, then the transition is first order. If only one phase survives then the transition is second order or higher. Concerning the GL model, there is no fundamental symmetry which could help to find a first order transition since the symmetry is continuous. In our calculations, it is the cooperation between phase and amplitude which is responsible for the second minimum in the free energy. This second minimum is only present at large system sizes and needs a complex dynamics to exist. Therefore it is very difficult to predict whether Monte Carlo simulations are good enough to show this phenomenon.

3.6 Validity of the Method

A remarkable thing is the fact that a negative σ produces a first order transition ([33] p.340). Therefore, the critical line which is believed until now to separate the region $\sigma < 0$ and $\sigma > 0$ is pushed in the region with $\sigma > 0$ by phase fluctuations. The limiting case $\sigma < 0$ is then consistent with a first order transition for $\sigma \lesssim 9.9 V_0/T_c$. We mention here that a variational approximation due to Halperin *et al* [31] for gauge field fluctuations yields an equation that is very similar to equation (3.11) except that our function $f(K) = \langle f_i \rangle$ due to phase fluctuations is replaced by the expectation value $\langle \vec{A}^2 \rangle$. For $d = 3$, magnetic fluctuations of the gauge field \vec{A} produce a first order transition and move the critical point into the positive σ region. The domain of validity is also in the small σ region as for our approach.

We now show that the origin of the first order transition of equations (3.26) and (3.27) is not due to the approximation itself and that the domain of validity of the approximation is precisely in the first order domain for $d = 3$. We establish a quantitative criterion by comparing the size of the critical gaussian region according to the Ginzburg criterion with the critical temperature due to phase fluctuations. The Ginzburg criterion [16] measures the importance of correlated gaussian fluctuations that are mainly

| Dimension | Criterion | Domain of validity |
|-----------|---------------------------|--------------------|
| 1 | $0 \ll 1$ | everywhere |
| 2 | $1/2 \ll 1$ | ? |
| 3 | $\sigma T_c/(2V_0) \ll 1$ | first order domain |
| 4 | $0 \ll 1$ | everywhere |
| >4 | $2V_0/(\sigma T_c) \ll 1$ | continuous domain |

Table 3.1: Validity of the approximation given by criterion (3.34).

due to the amplitude, i.e. they are negligible if

$$|t| \gg t_G := \left(\frac{T_c}{2V_0} \right)^{\frac{2}{4-d}} \sigma^{\frac{d-2}{4-d}}$$

where t_G defines the critical region. $|t_c|$ from equation (3.18) is a measure of the importance of phase fluctuations since it is coming from XY calculations. Our approach is then valid when (amplitude) fluctuations are dominated by phase fluctuations, i.e. when

$$|t_c| \gg t_G. \quad (3.33)$$

Setting $\omega \approx d - 1$ which is almost the correct XY critical temperature, we get the criterion:

$$\frac{d-1}{2} \left(\sigma \frac{T_c}{2V_0} \right)^{\frac{d-2}{4-d}} \ll 1 \quad (3.34)$$

The results of criterion (3.34) for different dimensions are listed in table 3.1.

For $d = 1$, the criterion is in agreement with our results which are almost identical to the exact solution [34]. For $d = 2$, the criterion is not clear. The approximation is reliable precisely in the first order domain for the $3d$ case ($\sigma T_c/V_0 \ll 1$), and everywhere for $d = 4$. For $d > 4$, the domain of validity is in the continuous domain. Therefore, we conclude that the first order transition is not a consequence of the approximation for $d = 3$, whereas a doubt remains for $d = 2$.

The first order transition is due to the fact that the energy of vortices can be lowered by a reduced value of the amplitude, which is energetically favorable when the potential energy of the amplitude is sufficiently soft. In this case, the usual transition scenario, given by an unbinding of topological excitations, seems to be replaced by a sudden proliferation of the latter. Such a process may be difficult to describe within the renormalisation group ε -expansion where the interplay between amplitude and phase is not explicitly taken into account. The first order transition found, for example, in [28] is related to the cubic anisotropy in the fourth order coupling rather than to the interplay between amplitude and phase for the isotropic model treated here. A similar scenario has been found by Minnhagen *et al.* [30] for the $2d$ Coulomb gas. They show that a large vortex fugacity $y = \exp(-\beta\gamma|\psi|^2\pi^2/2)$ can lead to a discontinuous transition produced by a proliferation of vortices, whereas small fugacity causes the

usual Kosterlitz-Thouless transition. When $\tilde{\sigma}$ is small, our scenario corresponds to the case of large vortex fugacity. The mean amplitude can become much smaller than the one of the XY model (see figure 1 where $\tilde{R} = 1$ corresponds to the XY model). For large $\tilde{\sigma}$ ($\tilde{R} \approx 1$), the KT transition is recovered. Our result ($\tilde{\sigma}_c \approx 1.25$) is in good agreement with the one of Bormann and Beck [29] who found a first order transition for $\tilde{\sigma} \lesssim 1$.

For real superconductors, σ is of the order of 1. Therefore, superconductors with low T_c/V_0 could have a first order transition. A candidate for a possible observation would be a $3d$ superconductor with a critical region t_G that is not too small but still in the first order domain. In the BCS limit, the transition becomes very weakly first order such that there is no contradiction with the continuous behaviour of BCS superconductors. Underdoped cuprates are quasi 2 dimensional and have a low V_0/T_c . Their transition is then XY-like, whereas overdoped cuprates, that are almost $3d$ and have a large V_0/T_c , could have an observable first order transition. It is, however, interesting to remark that measurements of the entropy change ΔS at the vortex lattice melting transition of $\text{Bi}_2\text{Sr}_2\text{CaCu}_2\text{O}_8$ [35] have shown a dramatic increase in ΔS per vortex when the zero field transition is approached. This could be a hint that the superconducting transition remains first order even in zero field.

3.7 Qualitative Criterion on Amplitude and Vortices

The following derivation is based on the relation between amplitude and vortices. We would like to motivate the decrease of the amplitude when σ is small as it is seen in figure 3.2. Although it is not possible to find the nature of the transition, this argument can help us to understand how the amplitude adapts itself to vortices and vice-versa.

In the XY model, the energy of vortices is directly proportional to the dimensionless coupling constant K . In the GL model, K is not constant in the sense that it can locally choose a better value to minimize the energy of vortices. Of course the lowest value of K is 0 for the pure XY model. However, in the GL model, $K = R_i^2 V_0/T$ cannot go to zero because of the presence of the potential $U_{GL} = tR^2 + 1/2R^4$. There are two tendencies: on one side, the amplitude wants to decrease to lower the energy of the vortices. On the other side, the amplitude wants to increase to reach the minimum of U_{GL} . Quantitatively, we should have a first order like transition or a strong decrease for the amplitude when the gain of energy due to the lowering of R in the vortices is bigger than the cost for climbing the wall of the potential U_{GL} for all amplitudes.

We try to derive a quantitative criterion based on one vortex. We compute the difference of reduced energy between the minimum $R_0^2 = -t$ of U_{GL} and $R = 0$. For the d dimensional case, the energy difference ΔE_V for a vortex core of vorticity 1 is:

$$\Delta E_V = E_V(R = 0) - E_V(R = R_0) = -N_b R_0^2 (1 - \cos \pi/2) = -t N_b$$

where N_b is the number of bonds in the vortex core. The energy difference ΔE_R for

the GL potential is:

$$\Delta E_R = U_{GL}(R=0) - U_{GL}(R=R_0) = -N_s \sigma (tR_0^2 + 1/2R_0^4) = N_s \sigma t^2 / 2$$

where N_s is the number of sites in the vortex core. So we can set the criterion for a strong decrease of the amplitude. It occurs when

$$|\Delta E_V| > |\Delta E_R|$$

i.e. for

$$\tilde{\sigma} = \sigma |t| < 2 \frac{N_b}{N_s}$$

If we take the formula $N_b = N_s d / 2$, valid for a cubic vortex core, we get the inequality

$$\tilde{\sigma} < d =: \tilde{\sigma}_c$$

In variational phase-amplitude separation approach, we have found a first order transition when $\tilde{\sigma} = \sigma |t|$ is smaller than

$$\tilde{\sigma}_c^{(1d)} = 0 \quad \tilde{\sigma}_c^{(2d)} = 1.25 \quad \tilde{\sigma}_c^{(3d)} = 4.5$$

In both case, $\tilde{\sigma}_c$ increases with the dimension. This argument shows that the comparison between E_V and E_R leads to define to different regimes: if $\tilde{\sigma}$ is small then amplitudes are soft and decreases. If $\tilde{\sigma}$ is large amplitude tends to be more rigid.

3.8 Outline

In this chapter, we have investigated the thermodynamic properties of the classical Ginzburg-Landau (GL) model. It is determined by two model parameters, σ and V_0 . σ governs the strength of amplitude fluctuations and V_0 the overall strength of fluctuations of the complex GL field. We have treated the model by a variational approximation which takes into account the coupling between phase and amplitude through effective coupling constants. Minimizing the corresponding variational free energy leads to a set of self-consistent modified GL equations containing phase and amplitude fluctuations. The behaviour of the GL transition changes when the ratio $\sigma/(V_0/T_c)$ is varied: for $\sigma \lesssim C V_0/T_c$ the transition is of first order with $C = 9.9$ for $d = 3$ and $C = 2.2$ for $d = 2$.

For $d = 3$, we showed that phase fluctuations dominate the transition in the first order domain and amplitude fluctuations can be neglected. We thus conclude that a first order transition is indeed a valid scenario for the GL model, once the amplitude of the field can sufficiently adapt in order to lower the total energy of the system.

Chapter 4

THERMODYNAMICS OF HIGH T_c SUPERCONDUCTORS

Based on a pairing mechanism between electrons, the pseudogap regime is described by taking into account amplitude and phase fluctuations of the pairing field. In the underdoped regime especially, the averaged amplitude of the pairing field is of the order of the zero temperature gap ψ_0 up to room temperature. Above some crossover temperature T_ϕ larger than the critical temperature T_c , the pseudogap region is only determined by the amplitude whereas phase fluctuations are only important near T_c up to T_ϕ . Hence the pseudogap phase has two distinct regimes: a phase dominated below T_ϕ , and an amplitude dominated above T_ϕ where phases are random. Our calculations show very good quantitative agreement with specific heat and magnetic susceptibility experiments. We find that the mean field temperature T_0 has a similar doping dependence compared to the pseudogap temperature T^* , moreover the characteristic pseudogap energy scale E_g is given by the average amplitude above T_ϕ .

In underdoped cuprates, it is commonly believed that the main problem is to identify the pairing mechanism. However it seems that large correlated fluctuations are equally important. This is motivated by the Ginzburg criterion: the critical region is of the order of T_c itself in these materials (see section 2.2.3). Strong microscopic correlations are present in both BCS classical superconductors and high temperature superconductors: they cannot be treated by perturbation theory. Hence the pairing mechanism which produces pairs in cuprates could have the same origin as in BCS theory, i.e. due to phonon exchange between electrons. The day one identifies the pairing mechanism of high T_c , one will presumably not be able to compute observables like specific heat or spin susceptibility since the finite temperature theory will rely on BCS theory. Finding the pairing mechanism of high T_c cuprates is more related to the Cooper problem. To do a complete superconductivity theory, one has to find the pairing mechanism and to take into account thermal fluctuations and correlations of the pairing field as well.

One of the most intriguing problems in high temperature superconductivity is the

presence of a region above the critical temperature T_c and below a temperature T^* where observable quantities deviate from Fermi liquid behaviour. This region is called pseudogap region [36, 14] because it contains effects similar to superconductivity like a partial suppression of electronic density of states.

The origin of such a pseudogap above T_c is unclear. There are four major approaches concerning its theoretical understanding: the first is based on the formation of incoherent Cooper pairs above T_c . Phase order [32, 37] or Bose condensation [23] would then establish superconductivity at T_c . The second assumes that the pseudogap is induced by anti-ferromagnetic fluctuations [38]. The third approach is based on spin-charge separation where spins bind together to form spin-singlets and the energy needed to split them apart leads to the formation of a "spin-gap" [39]. The fourth assumes the existence of a quantum critical point [40] but the latter has never been observed. However, these approaches seem to be unable to describe specific heat and magnetic susceptibility. The main aim of this chapter is to show that various experimental observations

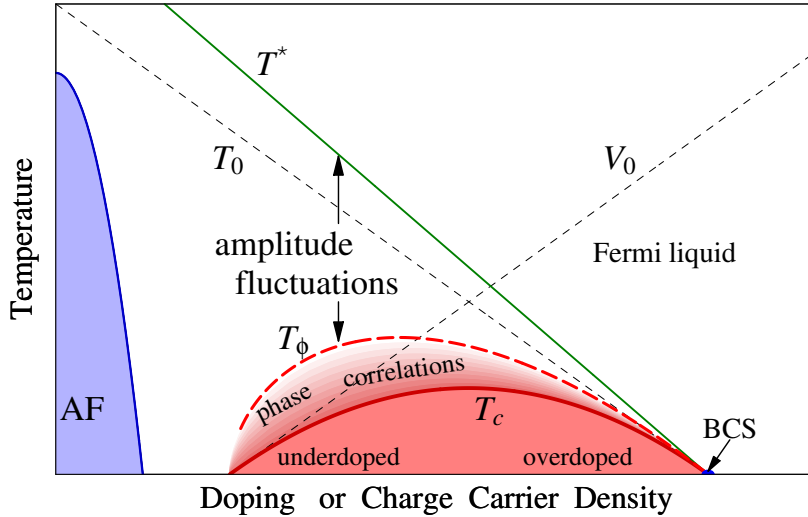


Figure 4.1: Schematic phase diagram of cuprates. The pseudogap region of the copper oxides phase diagram lies between the critical temperature T_c and a temperature T^* that interpolates the antiferromagnetic domain noted by AF. The temperature T' has been reported in several experiments and its meaning will be explained in this chapter.

can indeed be interpreted in terms of fluctuations of the pairing field $\psi = |\psi|e^{i\phi}$, and that two temperature regions have to be distinguished (see Fig. 4.1): for a relatively small temperature interval $T_c < T < T_\phi$ the phase of ψ is still correlated in space over some correlation length ξ (the Kosterlitz-Thouless correlation length in $2d$) whereas the amplitude $|\psi|$ is almost constant. Thus, in this regime, observables are governed by correlated phase fluctuations described by the XY-model. For $T_\phi < T < T^*$, phases of ψ are essentially uncorrelated (ξ is on the order of the lattice constant), but $|\psi|$ is still non-zero, signaling independent fluctuating local pairs. This explains the wide hump seen in specific heat experiments [36], the depression of the spin susceptibility [41] and

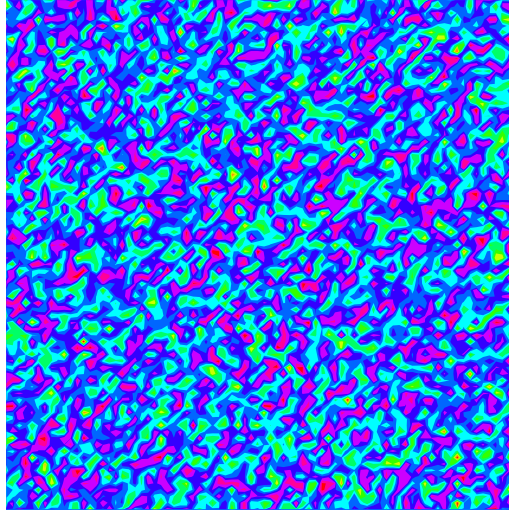


Figure 4.2: Amplitude of the pairing field above T_c on a 80×80 array by cluster Monte Carlo simulations: blue is for large amplitude and red low amplitude.

the persistence of the pseudogap for $T < T^*$. Moreover, a magnetic field that destroys this pseudogap has to break fluctuating pairs and must therefore be much higher than the one which suppresses phase coherence and thus superconductivity [42].

Our approach has a major difference with the Emery and Kivelson phase fluctuations scenario [32] of the pseudogap regime: our calculations show that phase fluctuations influence the pseudogap only up to a temperature T_ϕ which is much smaller than T^* . Above T_ϕ , observables are thus only determined by the amplitude of the pairing field.

The existence of a temperature intermediate between T_c and T^* has also been mentioned by Devillard and Ranninger [43]: using a Boson-Fermion description of pairing in cuprates, they find that uncorrelated pairing of electrons leads to the opening of a pseudogap at T^* . These pairs acquire well behaved itinerant features at T_B^* , leading to partial Meissner screening, and thus to diamagnetic susceptibility, and Drude-type behaviour of the optical conductivity. As a function of lattice anisotropy (and thus of doping) T_B^* has the same tendency as T_c , whereas the higher temperature T^* has the opposite trend. Although in ref [43] T_B^* is related to the temperature where the pair life time becomes long, it could be identified with our T_ϕ .

4.1 Motivation

Our approach is based on the phenomenological attractive Hubbard model. In order to make this choice clearer for the reader, I compare this approach to the famous Newton's law relating force and acceleration. There are two approaches concerning this law:

1. Ontological approach: one tries to find what is the true nature of the constant m that relates force and acceleration. It is a very hard task to predict the value of the mass *a priori*.
2. Phenomenological approach: one supposes that the constant m exists and one solves the equation

$$\text{force} = m \text{ acceleration}$$

The strength of this method lies on the confidence in the assumption. The mass m is then determined by comparison with experiments.

In the attractive Hubbard model approach, one is not interested to know what is the real nature of the attractive coupling between fermion, but one is interested in describing the properties of superconductors and to make predictions. It is like solving Newton's law without knowing where the mass comes from. When one compares his results to experiments, then one should be able to estimate the value of the coupling constant.

The ontological approach of high temperature superconductors tries to find out what is the real nature of the attraction between fermions. This is a difficult goal, and results are up to now too uncertain. Which pairing mechanism is the right one? antiferromagnetism, spin singlets or phonons? or something else. Here the phenomenological approach allows to estimate the value of the attraction, and should be a help to those who want to find the value of the attraction from first principles: both approaches must yield the same value.

4.2 Model and Effective Action

We base our calculations on a d -wave attractive Hubbard model

$$H = - \sum_{\langle i,j \rangle \sigma} t c_{i\sigma}^\dagger c_{j\sigma} - U \sum_i Q_d^\dagger(i) Q_d(i) \quad (4.1)$$

with a hopping t between nearest neighbour sites i and j on a square lattice. The interaction favours the formation of onsite d -wave pairs since

$$Q_d^\dagger(i) = \sum_j D_{ij} Q_{ij}^\dagger \quad (4.2)$$

where $D_{ij} = 1, (-1)$ for i being the nearest neighbour site of j in horizontal (vertical) direction.

$$Q_{ij}^\dagger = (c_{i\uparrow}^\dagger c_{j\downarrow}^\dagger - c_{i\downarrow}^\dagger c_{j\uparrow}^\dagger) / \sqrt{2} \quad (4.3)$$

is an operator creating a singlet pair on neighbouring sites. Decoupling the interaction with the help of a Stratonovich-Hubbard transformation, the partition function $Z = \text{Tr} e^{-\beta H}$ is then

$$Z = Z_n \int D^2\psi \left\langle \mathcal{T} e^{-\int_0^\beta d\tau \sum_i \left(\frac{1}{\nu} |\psi|^2 + \psi Q_d^\dagger(i) + \text{hc} \right)} \right\rangle_{H_n}$$

where

$$\psi = \psi(i, \tau) = |\psi(i, \tau)| e^{i\phi(i, \tau)}, \quad (4.4)$$

and $H_n = -\sum_{\langle i, j \rangle \sigma} t c_{i\sigma}^\dagger c_{j\sigma}$ is the non-interacting part. The trace over the fermionic operators can be evaluated yielding

$$Z = \int D^2\psi e^{-\int_0^\beta d\tau [\sum_i \frac{1}{\beta} |\psi|^2 + \text{Tr} \ln G]}. \quad (4.5)$$

Here G is a Nambu matrix of one-electron Green functions for fermions interacting with a given, space and time dependent pairing field $\psi(i, \tau)$. The Green functions are solution of Gorkov's equations (see [44]).

Expanding (4.5) in power of $\vec{\nabla}\psi$, Z can be written as a functional integral involving an action $S[\psi]$ for a field ψ that changes slowly in space and that can be taken time-independent:

$$S[\psi] = S_0(|\psi|) + S_1(\vec{\nabla}\psi) \quad (4.6)$$

where S_0 is a local functional of ψ :

$$S_0(\langle |\psi| \rangle) = (V \langle |\psi| \rangle^2 / U) - \frac{2}{\beta} \sum_q \log[2 \cosh \beta E_q / 2] \quad (4.7)$$

and $S_1 = c \int d^3r |\vec{\nabla}\psi|^2 / 2$ can be considered as the deformation or kinetic energy where c is a constant.

Now we would like to compute thermodynamic observables such as energy $U = \langle S \rangle_S$, specific heat and spin susceptibility. The point is that we want to keep the XY universality class of the transition together with the fermionic character of the system: in the limit of high density or weak interaction, the superconductor should be described by a BCS like mean field theory whereas in the low density limit with strong interaction the transition becomes XY like. Our goal is to derive a theory that describes these two regimes and, of course, the intermediate regime.

Our main strategy will be to neglect amplitude correlations since simulations show that they are weak between different sites i, j : $\langle |\psi|_i |\psi|_j \rangle - \langle |\psi|^2 \rangle \approx 0$ since the amplitude is always positive and cannot show any critical behaviour. In this spirit, two different approaches are possible:

1. The amplitude is fixed but still temperature dependent, and is determined by a suitable variational equation. Here the remaining fluctuations are those from the XY model, and the amplitude weight coming from the Jacobian of the cartesian to polar coordinates transformation.
2. The energy is expanded around the average amplitude. Higher powers of amplitude fluctuations are neglected. Here the local coupling between phase and amplitude is kept, and amplitude are allowed to fluctuate.

4.3 Variational Method

The integration of the partition function can be expressed in polar coordinates using the transformation:

$$D\psi = \prod_i \int_{-\infty}^{+\infty} d\psi_i d\psi_i^* = \prod_i \int_0^{+\infty} d|\psi_i| |\psi_i| \int_0^{2\pi} d\phi_i \quad (4.8)$$

Rewriting the free energy F in terms of a constant amplitude $|\psi|$ yields

$$F = -\frac{1}{\beta} \log \int D\phi e^{-\beta(S_0(|\psi|) - \log(|\psi|)V/\beta + S_1)}$$

where the Jacobian $|\psi_i|$ of the polar transformation is put into the exponential, and V is the volume. Taking the derivative of F with respect to $|\psi|$ and equating it to zero leads to the self-consistent equation:

$$\frac{\partial S_0(|\psi|)}{\partial |\psi|} - \frac{V}{\beta |\psi|} + c |\psi| \langle |\vec{\nabla} e^{i\phi}|^2 \rangle_{S_1} = 0. \quad (4.9)$$

Evaluating equation (4.9) and multiplying it with $|\psi|/2$

$$|\psi|^2 \left[\frac{1}{U} - \frac{1}{W} \int_{-\mu}^{W-\mu} d\xi \frac{\tanh\left(\frac{\sqrt{\xi^2 + |\psi_k|^2}}{2T}\right)}{\sqrt{\xi^2 + |\psi_k|^2}} \right] - \frac{1}{2\beta} + |\psi|^2 \langle |\vec{\nabla} e^{i\phi}|^2 \rangle_{S_1} = 0. \quad (4.10)$$

The first term, called the amplitude contribution, leads to the BCS gap equation if other contributions are neglected. The second comes from the Jacobian and implies that the amplitude is never zero. The third term is the expectation value of the energy U_{xy} in the XY model with a constant dimensionless coupling K

$$K = \frac{V_0}{T} \frac{|\psi|^2}{|\psi_0|^2}. \quad (4.11)$$

where V_0 is the zero temperature phase stiffness, and $|\psi_0|$ is the zero temperature amplitude. This contribution characterises the influence of the phase fluctuations. $U_{xy}(K)$ is a monotonic decreasing function with an inflexion point at T_c . Solutions of equation (4.10) are reliable for all temperatures except for $T \ll T_c$. However they are only expected to be accurate at T_c if the average amplitude is large and not varying too much with temperature.

This variational approach is similar to the one of chapter 3. Hence it has a first order transition in the overdoped regime, i.e. when T_0 is of the order of the critical temperature T_c . Because the first order transition seems to be too large, we only compare our results for the underdoped regime where it is absent.

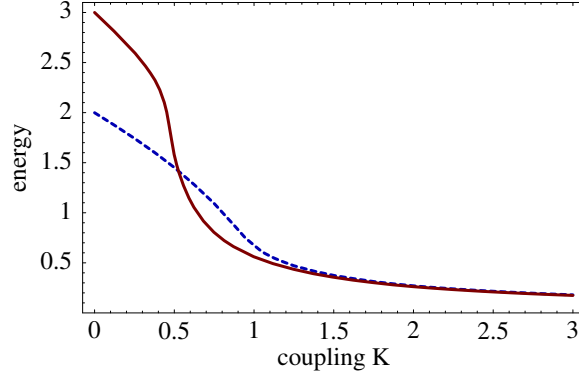


Figure 4.3: Energy in the XY model as a function of the coupling K defined in equation (4.11). The continuous line is for 3 dimensions and dashed is for 2 dimensions. Note that the phase transition occurs near the cusp.

4.4 Average Value Method

4.4.1 Method

Since simulations show that amplitude correlations are weak, we can expand the energy around the average amplitude where it is not coupled to the phase. The energy is then

$$U = \langle S \rangle_S \approx S_0(\langle |\psi| \rangle) + \langle S_1 \rangle_S \quad (4.12)$$

Here, $S_0(\langle |\psi| \rangle)$ is the first term of an expansion of the average $\langle S_0(|\psi|) \rangle$ around $\langle |\psi| \rangle$.

$$\begin{aligned} \langle S \rangle_S &= \left\langle S_0(\langle |\psi| \rangle) + c_1(|\psi| - \langle |\psi| \rangle) + c_2 \frac{(|\psi| - \langle |\psi| \rangle)^2}{2} + \dots \right\rangle \\ &= S_0(\langle |\psi| \rangle) + \sum_{n=1}^{\infty} \frac{c_n}{n!} \langle (|\psi| - \langle |\psi| \rangle)^{2n} \rangle \\ &= S_0(\langle |\psi| \rangle) + \sum_{n=1}^{\infty} c_n \frac{(2n+1)!!}{n!} (\langle |\psi|^2 \rangle - \langle |\psi| \rangle^2)^n \end{aligned} \quad (4.13)$$

since amplitude fluctuations around their average value can be considered as gaussian, see chapter 3 and appendix A. Higher corrections term are proportional to powers of the square of the standard deviation $\langle |\psi|^2 \rangle - \langle |\psi| \rangle^2$. Although amplitude fluctuations are large, the standard deviation is half of the average amplitude, powers of $\langle |\psi|^2 \rangle - \langle |\psi| \rangle^2$ are very small compared to the average amplitude itself. This is why we only take the first term of the expansion which already yield the interesting physics. Additional terms would just add more fluctuations.

For simplicity, averages are computed using a normalised Ginzburg-Landau action S_{GL} (see [1]) whose potential part U_{GL} is equal to the first two terms of the expansion

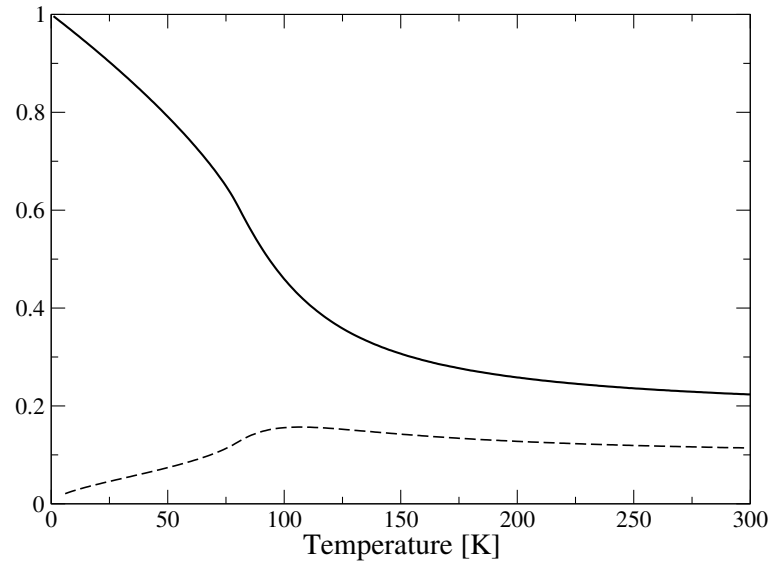


Figure 4.4: Average amplitude (thick line) and the corresponding standard deviation (dashed line). Parameters are $V_0 = 215$, $T_0 = 140$. Note that T_c is about 80K whereas the amplitude remains non zero at least up to 300K.

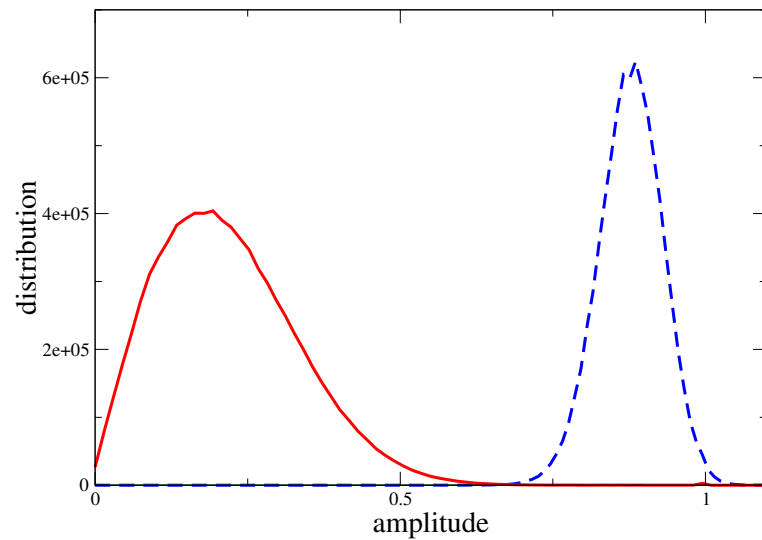


Figure 4.5: Amplitude distribution for $T = 300\text{K}$ (thick line) and $T = 30\text{K}$ (dashed line). Parameters are $V_0 = 215\text{K}$, $T_0 = 140\text{K}$. Note the broadening of the amplitude distribution at high temperature, i.e the increase of fluctuations, compared to the low temperature distribution where the distribution is narrower.

of S_0 with respect to $\beta|\psi|$:

$$S_{GL}[\psi] = k_B V_0 \int d^3r (U_{GL} + S_1) \quad (4.14)$$

where

$$U_{GL} = \eta^2 (t|\tilde{\psi}|^2 + \frac{1}{2}|\tilde{\psi}|^4), \quad (4.15)$$

and $t \approx T/T_0 - 1$ is the reduced temperature, $\tilde{\psi} = \psi/|\psi(T=0)|$ is the reduced field, T_0 is the mean field BCS pairing temperature. S_{GL} is normalised with a lattice spacing ε .

$$\eta := \varepsilon/\xi_0,$$

where ξ_0 is the mean field correlation length at zero temperature, and V_0 is the zero temperature phase stiffness. Contrary to the variational method, amplitude and phase are still *locally* coupled through S_1 . The energy becomes

$$U \approx S_0(\langle|\psi|\rangle_{GL}) + \langle S_1 \rangle_{GL} \quad (4.16)$$

where

$$S_0(\langle|\psi|\rangle) = (V \langle|\psi|\rangle^2 / U) - \frac{2}{\beta} \sum_q \log[2 \cosh \beta E_q / 2]$$

corresponds the BCS free energy for which the gap value is determined by the GL average. The quasi-particle energy is $E_q = [(\varepsilon_q - \mu)^2 + \langle|\psi|\rangle^2 \cos^2(2\theta)]^{1/2}$ where μ is the chemical potential. The d -wave symmetry manifests itself by the angle dependent amplitude $|\psi| \cos(2\theta)$ where θ is the angle in k space with respect to k_x direction. The value of η depends on the coarse-graining procedure and is fixed for each sample. Observables are not very sensitive to changes in η .

Both approaches are valid below and above the critical temperature T_c which is the temperature where the phase stiffness becomes zero. However the average value method gives good results for all values of T_0 and V_0 whereas the variational method works better in the underdoped regime, i.e. for $V_0 < T_0$.

It is important to notice that the amplitude is fluctuating although it is fixed to its averaged value in observables. In figure 4.4, the average amplitude and its standard deviation are shown. One can note that the latter is approximately half of the averaged amplitude. Since the amplitude distribution around its average value is almost gaussian, the probability density $p(|\psi|)$ has the following form:

$$p(|\psi|) \approx e^{-\frac{(|\psi| - \langle|\psi|\rangle)^2}{\langle|\psi|\rangle}} \quad (4.17)$$

This means that the amplitude has values ranging from 0 to $2\langle|\psi|\rangle$, and this is related the large value of $\langle|\psi|\rangle$.

4.4.2 Simulations

Computer simulations of the statistical ensemble $\{\psi\}$ under the action S_{GL} have been done using a standard Monte Carlo procedure to update amplitude $|\tilde{\psi}|$ and a Wolff [20] algorithm for the phase ϕ in the same way as for the real Φ^4 model [21]. Typically 10^4 sweeps are needed to obtain good statistics. I have used a small network of eight Linux workstations with AMD processors (800 Mhz to 1.66 Ghz). The network is connected via an NFS Network File System in order to have all informations and results on one disk.

Since the fitting procedure is done completely automatically, one has to simulate first the Ginzburg-Landau action (2.6) for all possible parameters a and b . This can be done by using a script language like *bash*. When the script is started, then simulations are started on each workstation. The procedure is as follows:

1. start the initial script. (create a new directory, compile the program, move the executable into the new directory)
2. the initial script starts a second script on each workstation separately.
3. the second script creates a directory whose name is given by the parameter b , then launches the executable and simulations are performed for different a .
4. go to point 3) for a certain set of parameters b .

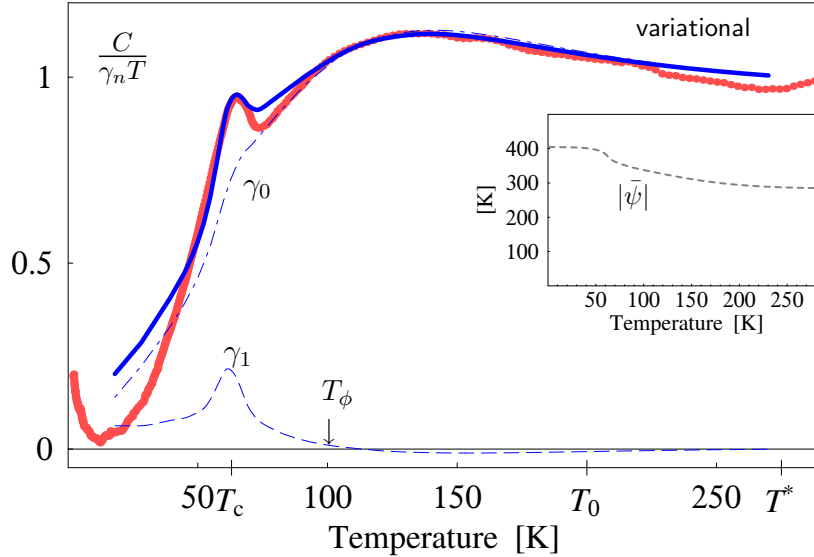


Figure 4.6: The reduced specific heat γ from the variational method (thick), which is the sum of the gradient γ_1 (dashed) and amplitude γ_0 (dotted-dashed) contributions, reproduces measurements of $\text{YBa}_2\text{Cu}_3\text{O}_{6.73}$ (points). *Inset:* The dashed line is the temperature dependent amplitude $|\bar{\psi}|$ from equation (4.10).

4.5 Specific Heat

In both approaches, the specific heat C is the sum of the amplitude C_0 and the gradient C_1 contributions. Defining the reduced specific heat $\gamma = C/(\gamma_n T)$, we have

$$\gamma = \gamma_0 + \gamma_1 \quad (4.18)$$

where γ_1 is divided by T_c instead of T since S_1 is classical and does not satisfy the third law of thermodynamic. The amplitude contribution is:

$$\gamma_0 = \frac{C_0}{\gamma_n T} = -2U \sum_k \frac{\partial f_k}{\partial T} \partial \psi \quad (4.19)$$

where ψ is replaced by $|\bar{\psi}|$ in the variational approach and by $\langle |\psi| \rangle$ in the average value approach. The amplitude specific heat can be calculated by using the entropy. C_0 is the derivative of the entropy times the temperature:

$$C_0 = -T \frac{\partial S}{\partial T} \quad (4.20)$$

where the entropy S for a fermionic system in the presence of a gap $|\psi|$ is a universal function of the ratio $|\psi|/T$:

$$S(|\psi|/T) = \sum_k f_k \log(f_k) \quad (4.21)$$

where the Fermi distribution is $f_k = \frac{1}{e^{-\beta(E_k - \mu)} + 1}$ and the energy E_k is $E_k = \sqrt{\xi_k + |\psi|^2}$. By using the entropy, it is not necessary to perform the sum over k each time one wants to evaluate the specific heat. It is then sufficient to take the derivative of the entropy.

4.5.1 Normalisation

γ_0 is 1 at high temperature since it is divided by the Sommerfeld constant γ_n . The phase contribution is normalised as:

$$\frac{C_1}{\gamma_n} = \frac{k_B}{\xi_0^3 \gamma_n} \frac{C_\phi^{(s)}}{N k_B} \quad (4.22)$$

where C_1 is the specific heat per volume $V = N \xi_0^3$, and $C_\phi^{(s)}/(N k_B)$ is the specific heat per number of lattice sites coming from the simulations. Experiments give $\gamma_n \approx 26 \text{ mJ K}^{-1} \text{ mol}^{-1} = 252 \text{ J K}^{-1} \text{ m}^{-3}$. For the fit of Fig. 4.6, using the reasonable value $\xi_0 \approx 16 \text{ \AA}$, we get the dimensionless constant $\alpha = k_B/(\xi_0^3 \gamma_n) \approx 13.5$.

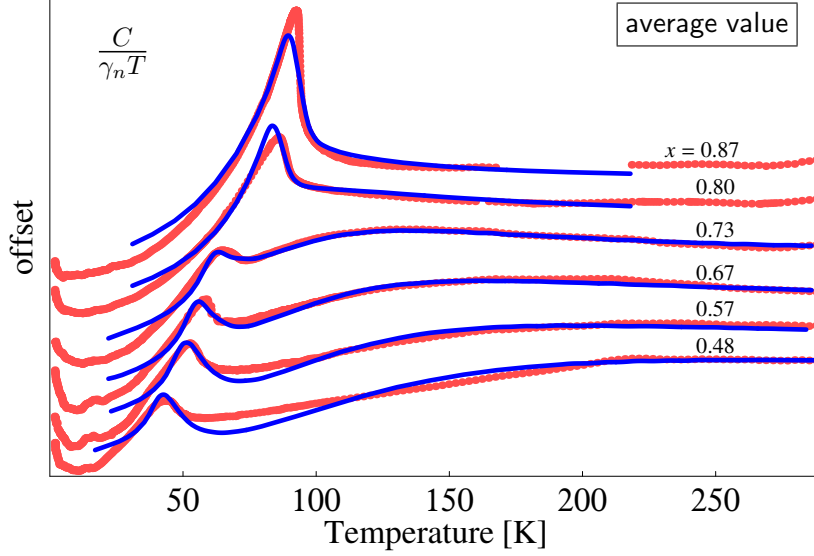


Figure 4.7: $\text{YBa}_2\text{Cu}_3\text{O}_{6+x}$ specific heat for different oxygen dopings x compared to the average value method.

4.5.2 d -wave Symmetry

Variational Method

The specific heat C is now

$$\gamma = \gamma_0 (|\bar{\psi}|) + \gamma_1 \quad (4.23)$$

where the amplitude $|\bar{\psi}|$ is now solution of the amplitude equation (4.10) The dimensionless constant is $\alpha \approx 13.5$.

In Fig. 4.6 the experimental specific heat of $\text{YBa}_2\text{Cu}_3\text{O}_{6.73}$ [36] is fitted using the variational method reproducing the double peak structure: a sharp peak below T_ϕ coming from phase fluctuations and a wide hump below T^* rounded by amplitude fluctuations. The crossover temperature T_ϕ , where phases become random, corresponds to the temperature where γ_1 is less than approximately 2% of the normal specific heat. In amplitude equation (4.10), a 2 dimensional density of states $D(\varepsilon) = 1/W$ is used with $W = 5000\text{K}$, $\mu = 0.25W$ and $U = 959\text{K}$. These parameters gives $T_0 \approx 200\text{K}$ and $\psi_0 \approx 2.14T_0$ in agreement with experiments [45]. The other parameters are $V_0 = 72\text{K}$ and $\eta = 5$.

Average Value Method

Following equation (4.16), the specific heat is given by

$$\gamma = \gamma_0 (\langle |\psi| \rangle_{GL}) + \gamma_1 \quad (4.24)$$

where γ_1 is divided by T_c instead of T since S_{GL} is a classical action and does not satisfy the Nernst theorem. The average value method is compared to specific heat

| Doping | T_c [K] | V_0 [K] | T_0 [K] | α |
|--------|-----------|-----------|-----------|----------|
| 0.92 | 92.9 | 261.9 | 124.3 | 13.7 |
| 0.87 | 93.7 | 178.0 | 143.3 | 14.3 |
| 0.80 | 88.8 | 121.8 | 158.9 | 10.6 |
| 0.73 | 69.3 | 111.0 | 177.6 | 13.7 |
| 0.67 | 60.8 | 88.9 | 193.0 | 18.1 |
| 0.57 | 55.9 | 76.1 | 213.5 | 20.6 |
| 0.48 | 47.7 | 57.6 | 241.5 | 16.0 |
| 0.43 | 31.5 | 37.3 | 251.2 | 9.0 |

Table 4.1: Extracted parameters from the fits of YBCO specific heat. (see 4.7).

obtained for different doping in Fig. 4.7. For underdoped systems $x < 0.80$ we use simulations in $d = 2$. For the more overdoped, $x \geq 0.80$, simulations are done in $d = 3$. The parameter η is fixed to 3. Parameters V_0 and T_0 extracted from the fits are shown in the phase diagram of Fig. 4.13 and in table 4.1. Values of the phase specific heat normalisation constant α range from 10 to 20. The fitting procedure is done completely automatically by a random walk in the parameter space $\{V_0, T_0, \alpha\}$, until the error between experimental data and the fit is minimal. As usual, a local minimum can be reached by using this procedure, and one can be trapped in this minimum. However, when the dimension of the parameter space is 3 as in our case, different local minima can be easily excluded and the best fit can be achieved.

4.5.3 *s*-wave Symmetry

The measured **specific heat** of $\text{YBa}_2\text{Cu}_3\text{O}_{6.76}$ [36] is compared to our results for the *s*-wave symmetry in Fig. 4.9 by using the average value method.

We took the following values for the two parameters: $T_0 = 235K$ is of the order of T^* , $V_0 = 108K$ is of the order of T_c . For the size of ψ we took the BCS *d*-wave relation: $\psi(T = 0) = 2.14T_0$ since it seems to be more in agreement with experiments [45] than the BCS relation of $\psi(T = 0) = 1.76T_0$. This choice plays only a little quantitative role. The mean amplitude, standard deviation and phase stiffness are presented in Fig. 4.10 for the same parameters as in Fig. 4.9. The correlation length ξ is of the order the lattice constant of unity 1 when the temperature T_ϕ is reached. Considering Fig. 4.9, we see that an *s*-wave computation fits equally well experiments as the *d*-wave in Fig. 4.7. Hence, we cannot decide which symmetry is favored by looking at specific heat data. *s*-wave and *d*-wave symmetries are essentially different at low temperatures. *d*-wave specific heat has an algebraic increase with temperature whereas *s*-wave specific heat has an exponential behaviour. Therefore the *s*-wave contribution is smaller at low temperature than the *d*-wave. However, a lower *s*-wave contribution can be compensated by changing parameters T_0 and V_0 . Some people like Alex Müller have pushed forward the idea that the inner of the superconductor has *s*-wave symmetry whereas the

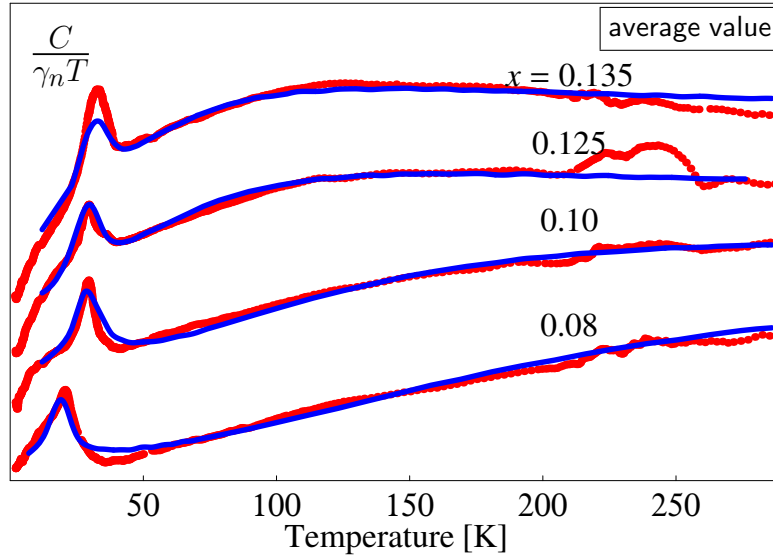


Figure 4.8: Underdoped $\text{La}_{2-x}\text{Sr}_x\text{CuO}_4$ specific heat for different strontium dopings x compared to the d -wave average value method.

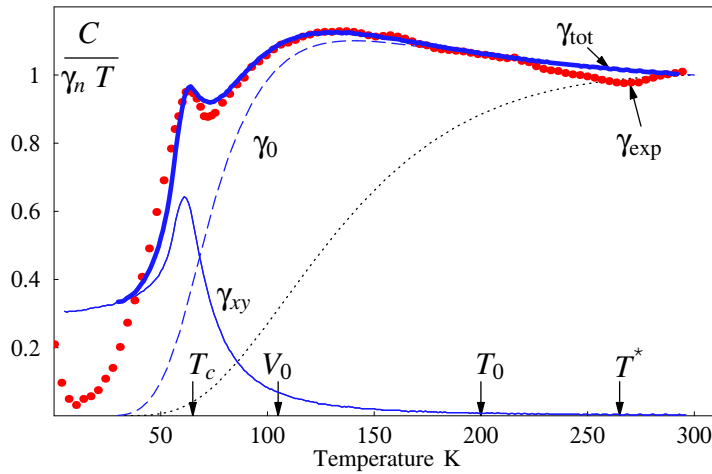


Figure 4.9: Measurements (points) of the specific heat of $\text{YBa}_2\text{Cu}_3\text{O}_{6.76}$ divided by $\gamma_n T$. The total s -wave specific heat (thick blue) is the sum of the critical XY contribution (thin blue) and the amplitude contribution (dashed blue). If the amplitude of the gap were constant of size $2.14T_0$, the contribution would be the dotted black line.

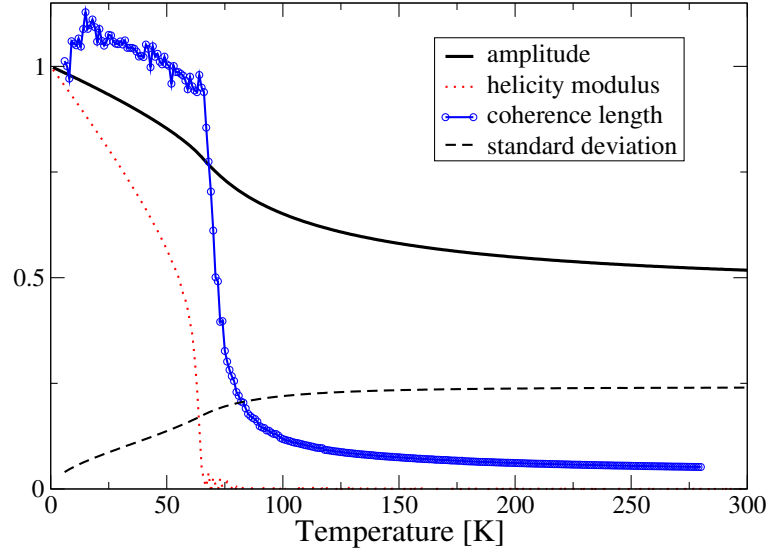


Figure 4.10: The average amplitude $\langle |\tilde{\psi}| \rangle$ (thick) is large even above T_c whereas the coherence length ξ vanishes rapidly above T_c . The standard deviation $\sqrt{\langle |\psi|^2 \rangle - \langle |\tilde{\psi}| \rangle^2}$ (dashed line) is large and almost constant. The phase stiffness Γ_x in x direction (dotted red) jumps from $2/\pi$ to zero at T_c . Lattice size: $N = 80^2$. Parameters are $T_0 = 235$ K, $V_0 = 108$ K, $\eta^2 = 8$.

d -wave symmetry is only present at the surface of the superconductor where ARPES or tunneling experiments are done. Low temperature specific heat which measures bulk properties could decide what is the real bulk symmetry of high T_c cuprates.

4.6 Spin Susceptibility

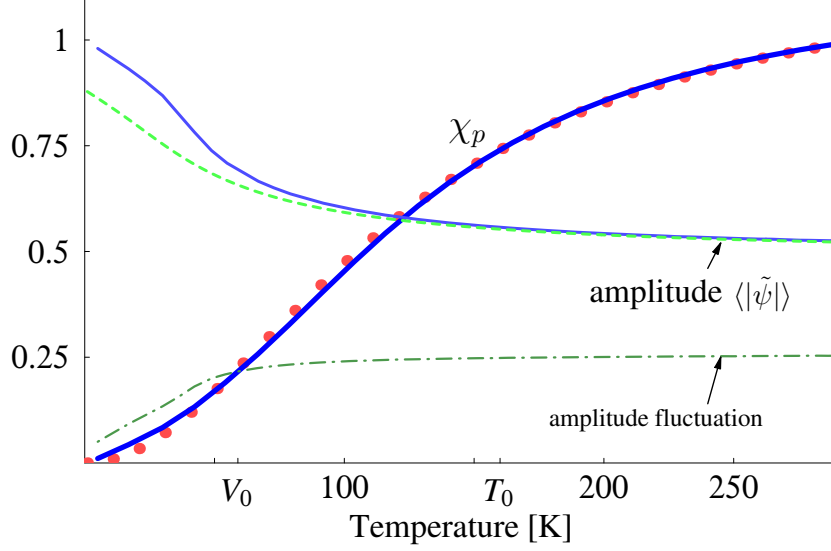


Figure 4.11: The measured spin susceptibility of $\text{YBa}_2\text{Cu}_3\text{O}_{6.63}$ (points) divided by χ_0 is well fitted by the theoretical (thick) susceptibility χ_p . The dotted-dashed line is standard deviation of the average amplitude.

The magnetic susceptibility χ has two contributions: the paramagnetic spin susceptibility χ_p and the orbital diamagnetic susceptibility χ_d . χ_p has been measured by Takigawa *et al* [41] on powder $\text{YBa}_2\text{Cu}_3\text{O}_{6.63}$ using Cu and O NMR experiments. The contribution coming from phases is negligible because NMR probes essentially the presence of pairs which is related to the amplitude. Therefore, the χ_p is given by the amplitude contribution

$$\chi_p = \frac{\chi_0}{2T} \int_0^{2\pi} \frac{d\theta}{2\pi} \int_0^\infty d\varepsilon \cosh^{-2} \frac{\sqrt{\varepsilon^2 + \langle |\psi| \rangle^2 \cos^2(2\theta)}}{2T} \quad (4.25)$$

where the amplitude $\langle |\psi| \rangle$ is averaged over S_{GL} . χ_0 is the Pauli spin susceptibility. In Fig. 4.11, we compare the result of equation (4.25) and Takigawa's measurements on powder $\text{YBa}_2\text{Cu}_3\text{O}_{6.63}$. Using $\eta = 3$, the best fit yields $T_0 = 159.2\text{K}$, $V_0 = 59.3\text{K}$. The competition between amplitude and thermal energy enters into the spin susceptibility (4.25) by the ratio $\langle |\psi| \rangle/T$. The temperature T_ϕ where phases start to influence the thermodynamics is here defined by the temperature where $\langle |\psi| \rangle$ deviates from approximately 2% of the average amplitude computed for random phases. This temperature is found above T_c at $T \approx 90\text{K}$.

The orbital diamagnetic susceptibility χ_d in underdoped $\text{YBa}_2\text{Cu}_3\text{O}_{6.60}$ shows marked fluctuations effects up to about 15 K above the transition temperature. In a fluctuating GL approach [46], the response to a magnetic field can be related to phase fluctuations due to vortices. For $T > T'_\phi$, fluctuations are so strong that χ_d vanishes.

4.7 Differential conductance

The differential conductance between a normal metal and a superconductor is directly related to the density of states and the amplitude of the pairing field by the standard formula [10]:

$$\frac{dI}{dV} = -G_{nn} \sim \frac{N_s(\xi)}{N(0)} \frac{\partial f(\xi + eV)}{\partial(eV)} \quad (4.26)$$

where G_{nn} is the differential conductance between two normal metals. The reduced energy is $\xi = \varepsilon - \mu$. The s -wave density of states is according to BCS theory:

$$N_s(\xi) = |\xi| / \sqrt{\xi^2 - \langle |\psi| \rangle^2} \quad (4.27)$$

Of course, $N_s(\xi) = 0$ if $|\xi| < \langle |\psi| \rangle$.

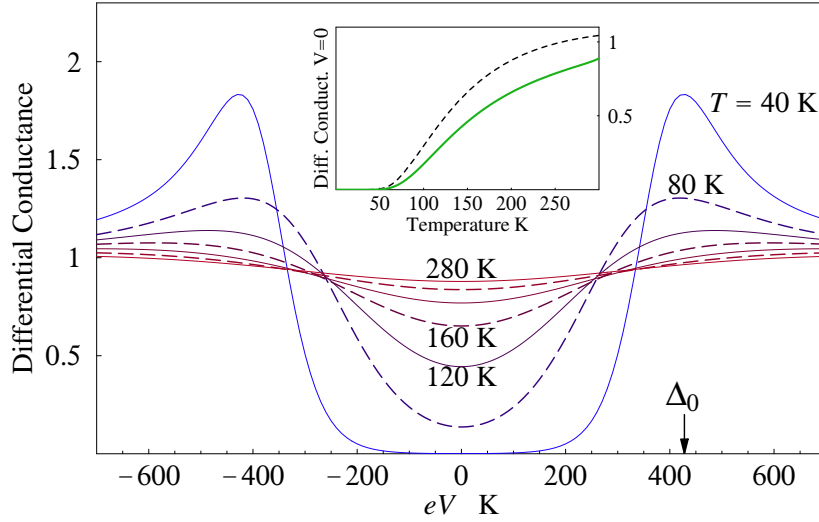


Figure 4.12: The differential conductance of equation (4.26) shows a pseudogap, i.e. a partial suppression of the density of states, up to temperatures near $T^* \approx 300$. Inset: the differential conductance (green curve) at $V = 0$ recovers its normal behaviour near T^* . The low temperature approximation of equation (4.28) is shown by the dashed line.

In Fig. 4.12, the s -wave differential conductance normalised with G_{nn} is presented using the same parameters as in Fig. 4.11 for temperatures from 20 K to 300 K with 40 K intervals. One can see that the width of the differential conductance is proportional to the amplitude $\langle |\psi| \rangle$, and that the gap fills up due to thermal energy. The low temperature differential conductance at $V = 0$ is approximately given by [10]:

$$\frac{dI}{dV}(V = 0) \approx G_{nn} \sqrt{\frac{2\pi |\psi|}{T}} e^{-|\psi|/T} \quad (4.28)$$

These results are in agreement with scanning tunneling microscopy on $\text{Bi}_2\text{Sr}_2\text{CaCu}_2\text{O}_8$ of Renner *et al* [11] where it is observed that the pseudogap gradually fills up whereas

its width remains constant. Do phase fluctuations contribute to the pseudogap? Yes but only up to V_0 where the correlation length ξ is of the order of the lattice spacing as seen in Fig. 4.10. As shown by Eckl *et al* [47], an amplitude of size $2T_0$ maintains a pseudogap in the density of states up to T^* whereas phase effects disappear near T_c .

4.8 Extracted Phase diagram

Values for T_0 , V_0 and T_ϕ extracted for the specific heat in Fig. 4.7 are reported in Fig. 4.13. T_1 is the temperature where $C_\phi/\gamma_n = 2\%$. T_ϕ is computed in the same way as shown in Fig 2 but for average amplitudes used for specific heat fits. The energy scale E_g of the pseudogap is defined here as the amplitude at $T = 200\text{K}$: $E_g = \langle |\psi| \rangle_{T=200\text{K}}$. E_g shows the same doping dependence as the one found by Loram and Tallon [48]. However E_g is not due to some hidden critical point, but is related to the average amplitude in the pseudogap regime. It is remarkable that phase correlations above T_c grow

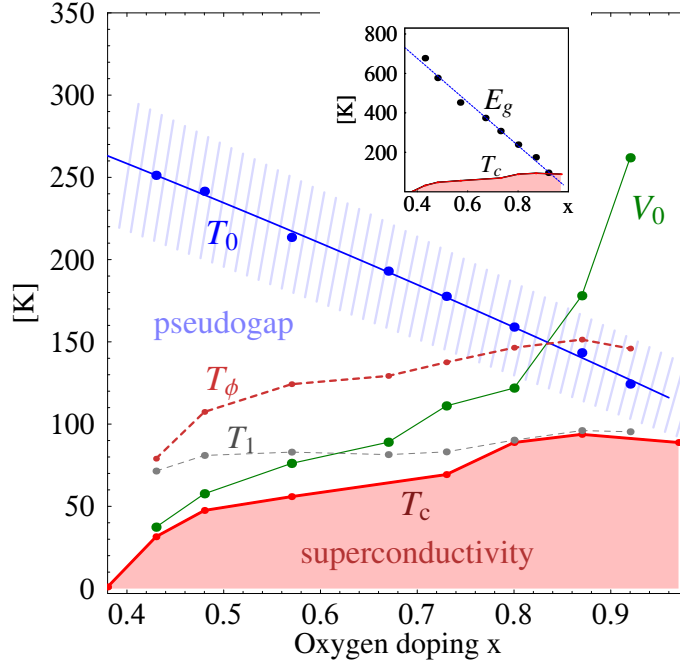


Figure 4.13: Phase diagram of $\text{YBa}_2\text{Cu}_3\text{O}_{6+x}$. Effects of amplitudes are large in the quasi uncorrelated pseudogap region (below T_0) of the copper oxides phase diagram, whereas phase correlations remain important only below T_ϕ . The T_1 line marks where the gradient specific heat disappears. The temperature T^* , where γ and χ_d cross over to normal behaviour, is located in the hatched area. *Inset*: the pseudogap energy scale E_g .

rapidly in the underdoped regime following the T_ϕ line, and reduce when approaching the overdoped regime. T'_ϕ lines are similar to Nernst effect results [15], whereas the gra-

dent specific heat seems to disappear more rapidly. This latter doping dependence is more in agreement with the phase diagram derived in Hall effect experiments [49].

4.9 Discussion

We have described the role of amplitude and phase in the emergence of the pseudogap region of underdoped high temperature superconductors. Phase coherence disappears completely near a temperature T_ϕ above T_c , and therefore, for $T > T_\phi$, the pseudogap region is dominated by amplitude fluctuations. We find that the mean field temperature T_0 has a similar doping dependence as T^* , signaling that the pseudogap region is due to independent fluctuating pairs. The energy scale E_g of the pseudogap is also derived. The large value of E_g in the underdoped domain is due to a finite T_0 and large amplitude fluctuations. At maximum doping, T_0 remains of the order of T_c but amplitude fluctuations are much weaker. Therefore E_g vanishes linearly upon approaching maximum doping.

Comparison with measured specific heat on underdoped YBCO reproduces the double peak structure: a sharp peak below T_ϕ coming from phase fluctuations and a separate wide hump below T^* rounded by the amplitude. The spin susceptibility, related to the amplitude, recovers its normal behaviour near T^* whereas the orbital magnetic susceptibility, related to phases, disappears near T_ϕ . These considerations are independent of the underlying pairing mechanism, and any microscopic theory inducing pairing should lead to similar conclusions.

A main difference between overdoped and underdoped superconductors is the "separation" between amplitude and phase: in the overdoped regime, contributions of amplitude and phase are superimposed at T_c producing only one peak in the specific heat for example. In the underdoped regime, phase correlations remain near T_c and still produce a small peak whereas amplitude fluctuations extend to much larger temperature producing a separate hump between T_c and T^* .

All these findings provide additional evidence for the fact that superconductivity and pseudogap have the same origin. The former is primarily related to phases of the pairing field, which order below the transition temperature and whose correlations survive over a limited temperature region above T_c . The pseudogap regime of underdoped materials then extends to much higher temperatures thanks to the persisting amplitude fluctuations of the pairing field.

Chapter 5

COHERENT POTENTIAL APPROXIMATION AND FLUCTUATIONS

In the previous chapter, we have treated the attractive Hubbard model in the low energy approximation where the field has small variations from one site to another. It is possible to have a phase transition and the derived action is similar to BCS free energy but needs to be averaged over amplitude and phase fluctuations.

We are now interested to start from the completely disordered phase, i.e. at high magnetic field or at high temperature. To attack this problem, we extend the Coherent Potential Approximation (CPA) which has been applied by Gyorffy [44] to Gorkov equations for the first time.

5.1 CPA for Fixed Amplitude

CPA is usually referred as a "mean field" approximation for disordered systems. Here we want to solve the Bogoliubov-de Gennes-Gorkov equation which have no disorder but a fluctuating complex pairing field. This field can be treated as a disordered field where electrons scatter. The basic aim of CPA is then to find a Green function describing the homogenous medium. In order to do this, the local homogenous Green function is set equal to the average local one site Green function which is solution of the one site problem. The average is taken over the pairing field.

We begin with an s -wave attractive four fermions Hamiltonian on the lattice:

$$H = \sum_{ij\sigma} t_{ij} c_{i\sigma}^{\dagger} c_{j\sigma} - U \sum_i c_{i\uparrow}^{\dagger} c_{i\uparrow} c_{i\downarrow}^{\dagger} c_{i\downarrow} \quad (5.1)$$

where $H_n = \sum_{ij\sigma} t_{ij} c_{i\sigma}^{\dagger} c_{j\sigma}$ is the non-interacting part and $U > 0$. Operators $c_{i\sigma}^{\dagger}$ and $c_{i\sigma}$ are the usual fermion creation and fermion annihilation operators. We apply now the Hartree-Fock-Gorkov decoupling to the hamiltonian (5.1) which gives the following

equation.

$$\sum_l \mathbf{g}^{-1}(i, l; z) \mathbf{g}(l, j; z) = \delta_{ij} \mathbb{I} \quad (5.2)$$

where

$$\mathbf{g}^{-1}(l, i, z) = \begin{pmatrix} t_{il} + (z - \mu) \delta_{il} & \psi_i \delta_{il} \\ \psi_i^* \delta_{il} & -t_{il} + (z + \mu) \delta_{il} \end{pmatrix} \quad (5.3)$$

where ψ_j is the complex pairing field. z is the complex frequency. μ is the chemical potential. \mathbb{I} is the identity matrix:

$$\mathbb{I} = \begin{pmatrix} 1 & 0 \\ 0 & 1 \end{pmatrix} \quad (5.4)$$

Equations (5.2) are solved for a certain choice of the field ψ_j . ψ_j are either

- given by the statistical weight $e^{-\beta H}$.
- solution of a self-consistent equation (BCS for example)

5.1.1 The homogenous Green function and its local expression

We start from the effective medium equation in space whose solution is the effective Green function $\mathcal{G}(l, j)$.

$$\sum_l \begin{pmatrix} (z + \mu - \Sigma_{11}(z))\delta_{il} - t_{il} & 0 \\ 0 & (z - \mu - \Sigma_{22}(z))\delta_{il} - t_{il} \end{pmatrix} \mathcal{G}(l, j) = \delta_{ij} \mathbb{I} \quad (5.5)$$

The coherent potential or effective self-energy Σ acts like a "mean field" of all electrons. The effective self-energy Σ is only frequency dependent since we want $\mathcal{G}(l, j)$ to be an effective medium Green function. In reciprocal space, the effective medium Green function $\mathcal{G}(k, z)$ is:

$$\tilde{\mathcal{G}}(k, z) = \begin{pmatrix} \frac{1}{z - \xi_k - \Sigma_{11}(z)} & 0 \\ 0 & \frac{1}{z + \xi_k - \Sigma_{22}(z)} \end{pmatrix} \quad (5.6)$$

where $\Sigma_{ab}(z)$ are the ab component of the unknown self-energy matrix. The tilde means "in Fourier space". The local Green function $\mathcal{G}(r, r')$, where the frequency dependence is omitted, is given by the Fourier transform at site $r = r'$:

$$\mathcal{G}(r, r) = \int d^3k \tilde{\mathcal{G}}(\mathbf{k}, z) e^{i\mathbf{k}(\mathbf{r}-\mathbf{r}')} |_{\mathbf{r}=\mathbf{r}'} = \int d\varepsilon D(\varepsilon) \tilde{\mathcal{G}}(k, z) \quad (5.7)$$

where $D(\varepsilon)$ is the density of states. In our computations, we assume a quasi 2 dimensional constant density of states: $D(\varepsilon) = 1/W$ where W is the bandwidth. The local Green function \mathcal{G}_{11} is then given by:

$$\mathcal{G}_{11}(z) = \frac{1}{W} \int_0^W d\varepsilon \tilde{\mathcal{G}}_{11}(k, z) = f(\Sigma_{11}, z) \quad (5.8)$$

where

$$f(\sigma, z) = \frac{1}{W} \log \left(\frac{z + \mu - \sigma - W}{z + \mu - \sigma} \right). \quad (5.9)$$

\mathcal{G}_{22} is related to \mathcal{G}_{11} as

$$\mathcal{G}_{22}(z) = f(\Sigma_{22}, z) = f(-\Sigma_{11}(-z), -z) \quad (5.10)$$

5.1.2 The Single Site Problem in an Effective Medium

We look now for the solution of equation (5.2) where the particular site r is the only site where ψ_r remains and all other sites are controlled by the homogenous Green function:

$$\psi_j \rightarrow \psi_r \delta_{jr} \quad (5.11)$$

The reduced impurity potential

$$\tilde{\mathbf{V}}_{\mathbf{r}} = \begin{pmatrix} 0 & \psi_r \\ \psi_r^* & 0 \end{pmatrix} - \begin{pmatrix} \Sigma_{11} & 0 \\ 0 & \Sigma_{22} \end{pmatrix} \quad (5.12)$$

adds an impurity field ψ_r and subtracts the effective medium self-energy at site r . Equation (5.2), where electrons evolve in an effective medium represented by $\mathcal{G}^{-1}(i, l)$ and are scattered by the reduced impurity potential $\tilde{\mathbf{V}}_{\mathbf{r}}$, becomes:

$$\sum_l \left[\mathcal{G}^{-1}(i, l) + \tilde{\mathbf{V}}_{\mathbf{r}} \delta_{rl} \right] \mathbf{g}(l, j) = \delta_{ij} \mathbb{I} \quad (5.13)$$

The Dyson representation of this equation is

$$\mathbf{g}(i, j) = \mathcal{G}(i, j) + \sum_l \mathcal{G}(i, l) \tilde{\mathbf{V}}_{\mathbf{r}} \delta_{rl} \mathbf{g}(l, j) \quad (5.14)$$

Equation (5.14) for the particular site r becomes then

$$\mathbf{g}(r, r) = \mathcal{G}(r, r) + \mathcal{G}(r, r) \tilde{\mathbf{V}}_{\mathbf{r}} \mathbf{g}(r, r) \quad (5.15)$$

Solving this equation for $\mathbf{g}(r, r)$, we get the impurity Green function

$$\begin{aligned} \mathbf{g}(r, r) &= \left[\mathbb{I} - \mathcal{G}(r, r) \tilde{\mathbf{V}}_{\mathbf{r}} \right]^{-1} \mathcal{G}(r, r) \\ &= \mathbf{D} \mathcal{G}(r, r) \end{aligned} \quad (5.16)$$

where we define the matrix \mathbf{D} as:

$$\mathbf{D} = [\mathbb{I} - \mathcal{G}(r, r) \tilde{\mathbf{V}}_{\mathbf{r}}]^{-1} \quad (5.17)$$

We get for \mathbf{D} :

$$\mathbf{D} = \begin{pmatrix} 1 + \mathcal{G}_1 \Sigma_1 & -\mathcal{G}_1 \psi_r \\ -\mathcal{G}_2 \psi_r^* & 1 + \mathcal{G}_2 \Sigma_2 \end{pmatrix}^{-1} \quad (5.18)$$

where $\mathcal{G}_\alpha = \mathcal{G}_{\alpha\alpha}$ and $\Sigma_\alpha = \Sigma_{\alpha\alpha}$. Inversion gives then

$$\mathbf{D} = \frac{\begin{pmatrix} 1 + \mathcal{G}_2 \Sigma_2 & \mathcal{G}_1 \psi_r \\ \mathcal{G}_2 \psi_r^* & 1 + \mathcal{G}_1 \Sigma_1 \end{pmatrix}}{(1 + \mathcal{G}_1 \Sigma_1)(1 + \mathcal{G}_2 \Sigma_2) - \mathcal{G}_1 \mathcal{G}_2 |\psi|^2} \quad (5.19)$$

5.1.3 The CPA condition

The CPA condition is: the local Green function (GF) $\mathbf{g}(r, r)$ averaged over the field distribution ψ_j is set equal to the local effective Green function $\mathcal{G}(r, r)$:

$$\underbrace{\langle \mathbf{g}(r, r) \rangle_{\psi_r}}_{\text{average local GF}} = \underbrace{\mathcal{G}(r, r)}_{\text{effective local GF}} \quad (5.20)$$

Using the result of equation (5.16), the condition reads:

$$\langle [\mathbb{I} + \mathcal{G}(r, r)\mathbf{V}]^{-1} \rangle_{\psi_r} = \mathbb{I} \quad (5.21)$$

Bringing together the CPA condition (5.21) and the expression (5.19) for \mathbf{D} , we get

$$\left\langle \frac{\begin{pmatrix} 1 + \mathcal{G}_2 \Sigma_2 & -\mathcal{G}_1 \psi_r \\ -\mathcal{G}_2 \psi_r^* & 1 + \mathcal{G}_1 \Sigma_1 \end{pmatrix}}{(1 + \mathcal{G}_1 \Sigma_1)(1 + \mathcal{G}_2 \Sigma_2) - \mathcal{G}_1 \mathcal{G}_2 |\psi_r|^2} \right\rangle_{\psi_r} = \mathbb{I} \quad (5.22)$$

This last result yields the four complex CPA equations.

5.1.4 CPA Equations for Random Phases

Ginzburg-Landau simulations show that phases are completely uncorrelated above T_ϕ but a finite amplitude $\langle |\psi| \rangle$ remains. Hence the question arises whether a true (pseudo)gap remains in the density of states when no correlations are present. We have applied the coherent potential approximation (CPA) to the Bogoliubov-DeGennes equations, as it was described by Gyorffy *et al* [44].

Using a finite amplitude and a uniform probability distribution p_i for the phase at each site, the total probability P of a configuration is then:

$$P = \prod_l p(\psi_l) \quad (5.23)$$

where $p(\psi_l) = 1/(2\pi)$ is a uniform distribution where phases are random and amplitude are fixed.

The two off-diagonal equations imply that the order parameter must be zero. This is in agreement with the *local* CPA condition which states that there is no correlation between sites. Therefore we are left with the two equations:

$$\left\langle \frac{1 + \mathcal{G}_2 \Sigma_2}{(1 + \mathcal{G}_1 \Sigma_1)(1 + \mathcal{G}_2 \Sigma_2) - \mathcal{G}_1 \mathcal{G}_2 |\psi|^2} \right\rangle_{\psi_r} = 1 \quad (5.24)$$

$$\left\langle \frac{1 + \mathcal{G}_1 \Sigma_1}{(1 + \mathcal{G}_1 \Sigma_1)(1 + \mathcal{G}_2 \Sigma_2) - \mathcal{G}_1 \mathcal{G}_2 |\psi|^2} \right\rangle_{\psi_r} = 1 \quad (5.25)$$

Neglecting amplitude fluctuations, i.e. the amplitude is fixed, and solving for Σ_1 and Σ_2 we have the following equations:

$$\Sigma_1 = \frac{\langle |\psi|^2 \rangle \mathcal{G}_2}{1 + \Sigma_2 \mathcal{G}_2} \quad (5.26)$$

$$\Sigma_2 = \frac{\langle |\psi|^2 \rangle \mathcal{G}_1}{1 + \Sigma_1 \mathcal{G}_1} \quad (5.27)$$

We have computed the density of states, see Fig. 5.1, for quarter filling $\mu = 0.25W$

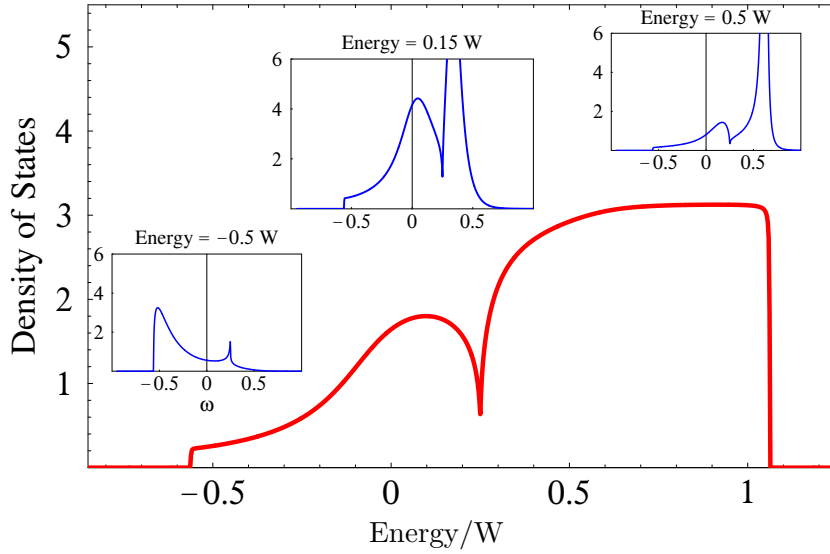


Figure 5.1: Density of states in the CPA approach for $|\psi_0| = 0.24W$ and $\mu = 0.25W$ in the "pseudogap" phase. **Insets:** Spectral functions for k : $\xi_k = -0.5W, 0.15W, 0.5W$. Note the broadening of the spectral function below the chemical potential.

and a pairing amplitude

$$|\psi_0| := \sqrt{\langle |\psi|^2 \rangle} = 0.24W.$$

We have found a pseudogap although phases are completely uncorrelated. Even a full gap can be established if ψ_0 overcomes a critical value $|\psi_c|$, i.e. if $|\psi| > |\psi_c|$. At half-filling this critical amplitude is $|\psi_c| \approx 0.33$

5.1.5 The CPA Gap Equation for Fixed Amplitude

The first attempt to derive an amplitude equation in the CPA has been done in reference [44]. When multiplying the complex field ψ by its complex conjugate ψ^* , one gets the local amplitude square $|\psi|^2$. Using a BCS like equation for ψ

$$\psi = -\frac{U}{\beta} \sum_n G_{12}(r, r), \quad (5.28)$$

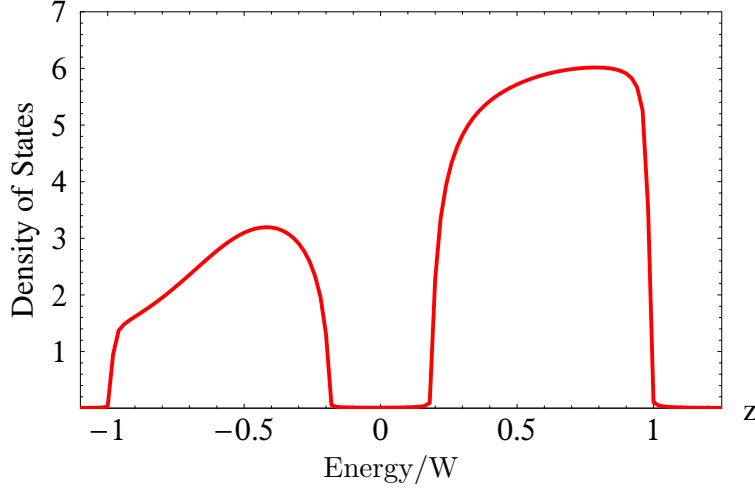


Figure 5.2: Density of states in the CPA approach for $|\psi| = 0.5W$ and $\mu = 0.25W$ in the gap phase. Note that the effective gap is less than half of the parameter ψ .

one can compute $\psi\psi^*$ and gets an equation for $|\psi|^2$:

$$|\psi|^2 = \frac{U^2}{\beta^2} \sum_n G_{12}(r, r) \sum_m G_{21}(r, r) \quad (5.29)$$

Considering equation (5.16), the Green function $G_{12}(r, r)$ and $G_{21}(r, r)$ are related to the matrix \mathbf{D} :

$$\begin{aligned} G_{12}(r, r) &= \langle g_{12}(r, r) \rangle = \langle D_{12} \mathcal{G}_2 \rangle \\ G_{21}(r, r) &= \langle g_{21}(r, r) \rangle = \langle D_{21} \mathcal{G}_1 \rangle \end{aligned} \quad (5.30)$$

The anomalous part is then related to the order parameter in the mean field approximation:

$$\psi(r) = -\frac{U}{\beta} \sum_n G_{12}$$

Using this equation and its complex conjugate, and equation (5.19), we have

$$\begin{aligned} |\psi|^2 &= \frac{U^2}{\beta^2} \sum_n D_{12} \mathcal{G}_2 \sum_m D_{21} \mathcal{G}_1 \\ &= \left(\frac{U}{\beta} \sum_n \frac{\mathcal{G}_1 \mathcal{G}_2}{(1 + \mathcal{G}_1 \Sigma_1)(1 + \mathcal{G}_2 \Sigma_2) - \mathcal{G}_1 \mathcal{G}_2 |\psi|^2} \right)^2 |\psi|^2 \\ &= \left(\frac{U}{\beta} \sum_n \frac{\mathcal{G}_1 \mathcal{G}_2}{1 + \mathcal{G}_1 \Sigma_1} \right)^2 |\psi|^2 \end{aligned} \quad (5.31)$$

where we used the CPA conditions (5.26) and (5.27). $|\psi|^2$ is present on both sides of the equation and can be simplified to get the equation:

$$1 = - \left| \frac{U}{\beta} \sum_n \frac{\mathcal{G}_1 \mathcal{G}_2}{1 + \mathcal{G}_1 \Sigma_1} \right| \quad (5.32)$$

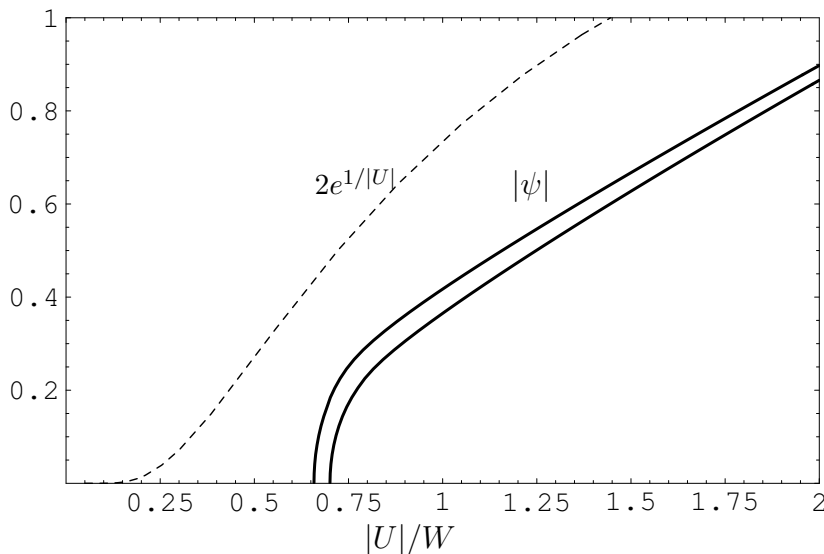


Figure 5.3: The amplitude $|\psi|$ from equation (5.32) for $\mu = 0.5$, left curve, and for $\mu = 0.25$ right curve. The dashed line is the BCS solution.

In figure 5.3, the solution of equation (5.32) is plotted for two different values of the chemical potential $\mu = 0.25$ and $\mu = 0.5$. Since we work at zero temperature, this corresponds respectively to quarter-filling and half-filling. Contrary to DMFT solution [50], the critical point U_c diminishes with increasing density. The main difference between CPA and DMFT is at small U when $\psi = 0$ for CPA. In this regime the CPA has free electrons whereas DMFT already takes into account interaction effects of U . Since CPA is a single site like theory, the critical point $U_c = W/\log(4)$ where ψ starts growing is independent of μ .

5.1.6 The Quantum Critical Point of the Gap Equation

Using the CPA gap equation for $|\psi|$, we look for the first point where $|\psi|$ is different from 0 at zero chemical potential and zero temperature. Indeed there is a critical point in the $\{U, \mu\}$ phase diagram. For values lower than a certain U_c no amplitude different from zero can be solution of equation (5.32). For $U > U_c$, one finds a non-zero amplitude. Since the all calculation is done at zero temperature, U_c is a quantum critical with respect to the control parameter U .

Considering equation (5.32), we have to compute the function X :

$$X = - \int_0^W d\varepsilon_1 \int_0^W d\varepsilon_2 T \sum_n \mathcal{G}_1(z) \mathcal{G}_2(z) \quad (5.33)$$

where $\mathcal{G}_1(z) = (z - \varepsilon_1 + \mu)$ and $\mathcal{G}_2(z) = (z + \varepsilon_1 - \mu)$. The Mastubara sum for $z = z_n = \pi T(2n + 1)$ and $n \in -\infty, \dots, -1, 0, 1, \dots, \infty$ and gives:

$$X = \int_0^W d\varepsilon_1 \int_0^W d\varepsilon_2 \frac{\tanh\left(\frac{\varepsilon_1 - \mu}{2T}\right) + \tanh\left(\frac{\varepsilon_2 - \mu}{2T}\right)}{2(\varepsilon_1 - \mu + \varepsilon_2 - \mu)} \quad (5.34)$$

At zero temperature $T = 0$, X is simply:

$$\begin{aligned} X &= -\frac{1}{W^2} \int_0^W d\varepsilon_1 \int_0^W d\varepsilon_2 \frac{1}{(\varepsilon_1 - \mu + \varepsilon_2 - \mu)} \\ &= -\frac{2}{W^2} (\mu \log(-2\mu) + (W - 2\mu) \log(W - 2\mu) + (\mu - W) \log(2W - 2\mu)) \end{aligned}$$

Taking the limit $\mu \rightarrow 0$ gives the simple formula:

$$X = \frac{\log(4)}{W} \quad (5.35)$$

and the critical coupling where $|\psi|$ becomes different from zero is

$$\boxed{U_c = \frac{W}{\log 4} \approx 0.721 W} \quad (5.36)$$

This new analytical result is in agreement with Gyorffy's numerical result $U_c \approx 0.8W$ [44].

We will see in the next section that this point should not be considered as a phase transition but as an instability since the amplitude $|\psi|$ is never zero due to quantum fluctuations.

5.2 CPA for d -wave Pairing

In the previous section, we have introduced a field ψ with an isotropic s -wave symmetry, i.e. ψ does not depend on the particular choice of the wave vector \mathbf{k} . Since we know that experiments of photoemission on cuprates have shown the d -wave symmetry of the gap and the pseudogap ψ , it is important to extend CPA to the d -wave case. Usually, this is done by replacing the field ψ by an angle dependent field $\psi(\theta)$:

$$\psi(\mathbf{k}) = \psi_0 f(\theta) \quad (5.37)$$

where the angle dependent function $f(\theta)$ is

$$\begin{aligned} f(\theta) &= 1 && \text{for } s\text{-wave} \\ f(\theta) &= \cos(2\theta) && \text{for } d\text{-wave} \end{aligned}$$

since d -wave symmetry in k -space is $\psi(\mathbf{k}) = \psi_0 \frac{(k_x^2 - k_y^2)}{k^2}$.

5.2.1 Dyson Equation

The d -wave symmetry can be shown by starting from the Gorkov equation in its continuum version:

$$\int d^d x \begin{pmatrix} h_1(z, \mathbf{x}) \delta(\mathbf{r} - \mathbf{x}) & \psi(\mathbf{r} - \mathbf{x}) \\ \psi^*(\mathbf{r} - \mathbf{x}) & h_2(z, \mathbf{x}) \delta(\mathbf{r} - \mathbf{x}) \end{pmatrix} \mathbf{g}(\mathbf{x}, \mathbf{r}', z) = \mathbb{I} \delta(\mathbf{r} - \mathbf{r}') \quad (5.38)$$

The field dependent local Green function $\mathbf{g}(\mathbf{r}, \mathbf{r}', z)$ is the solution of the one impurity problem in the presence of the local effective medium Green function

$$\mathcal{G}^{-1}(\mathbf{r}, \mathbf{r}', z) = \sum_{\mathbf{k}} e^{i\mathbf{k}(\mathbf{r}-\mathbf{r}')} \begin{pmatrix} \frac{1}{z - \xi_{\mathbf{k}} - \Sigma_{11}}(z) & 0 \\ 0 & \frac{1}{z + \xi_{\mathbf{k}} - \Sigma_{22}}(z) \end{pmatrix}$$

The Dyson form of (5.59) is then

$$\mathbf{g}(\mathbf{r}, \mathbf{r}') = \mathcal{G}(\mathbf{r}, \mathbf{r}') + \int dx \int dx' \mathcal{G}(\mathbf{r}, \mathbf{x}') \tilde{\mathbf{V}}(\mathbf{x} - \mathbf{x}') \mathbf{g}(\mathbf{x}, \mathbf{r}') \quad (5.39)$$

where $\tilde{\mathbf{V}}(\mathbf{x} - \mathbf{x}')$ is the reduced impurity pairing potential in real space:

$$\tilde{\mathbf{V}}(\mathbf{x} - \mathbf{x}') = \begin{pmatrix} -\Sigma_{11}(z)\delta(x - x') & \psi(\mathbf{x} - \mathbf{x}') \\ \psi^*(\mathbf{x} - \mathbf{x}') & -\Sigma_{22}(z)\delta(x - x') \end{pmatrix} \quad (5.40)$$

5.2.2 d -wave Differential Operator

If ψ is assumed to have slow variation in space, then the integral involving the effective medium Green function $\mathcal{G}(\mathbf{r}, \mathbf{x})$ can be simplified. In general, for a function $f(\mathbf{x})$, after expanding $f(\mathbf{x})$ around \mathbf{r} :

$$\begin{aligned} \int d^d x' \psi(\mathbf{x} - \mathbf{x}') f(\mathbf{x}') &\approx M^{(0)} f(\mathbf{x}) + \sum_i M_i^{(1)} \frac{\partial f(\mathbf{x})}{\partial x_i} \\ &+ \frac{1}{2} \sum_{ij} M_{ij}^{(2)} \frac{\partial^2 f(\mathbf{x})}{\partial x_i \partial x_j} \end{aligned} \quad (5.41)$$

where

$$\begin{aligned} M^{(0)} &= \int d^d x' \psi(\mathbf{x} - \mathbf{x}') \\ M_i^{(1)} &= \int d^d x' \psi(\mathbf{x} - \mathbf{x}') (x'_i - x_i) \\ M_{ij}^{(2)} &= \int d^d x' \psi(\mathbf{x} - \mathbf{x}') (x'_i - x_i) (x'_j - x_j) \end{aligned}$$

The d -wave symmetry is implemented via the wave function $\psi(\mathbf{x} - \mathbf{x}')$. It is possible to factorise it in elementary functions:

$$\psi(\mathbf{x} - \mathbf{x}') = \psi_0(\mathbf{x}) \theta(x'_1) \dots \theta(x'_n)$$

where $\theta(x'_i) = -1$ for $x'_i < 0$ and $\theta(x'_i) = 1$ for $x'_i > 0$. Hence the only term which survives after integration is the crossed term. The constant and linear terms in r_i disappear: $M^{(0)} = M^{(1)} = 0$. In 2-dimension, we have

$$M_{12}^{(2)} = \int dx'_1 dx'_2 \psi_0 \theta(x'_1) \theta(x'_2) x'_1 x'_2 = c \psi_0(\mathbf{x}) \quad (5.42)$$

where c is a constant that can be set to 1. Hence the integral (5.41) becomes

$$\int d^d x' \psi(\mathbf{x} - \mathbf{x}') f(\mathbf{x}') = \psi_0(\mathbf{x}) \frac{\partial^2 f(\mathbf{x})}{\partial x_1 \partial x_2} \quad (5.43)$$

The field $\psi_0(\mathbf{x})$ still depends on the location \mathbf{x} like in the s -wave case. Using the Fourier transform (FT), in reciprocal space, the differential operator is:

$$\begin{aligned} FT \left[\frac{\partial^2}{\partial x \partial y} \right] &= -k_x k_y \delta(\mathbf{k}) \\ &= -k^2 \cos(\phi) \sin(\phi) \delta(\mathbf{k}) \\ &= -\frac{1}{2} k^2 \cos(2\theta) \delta(\mathbf{k}) \end{aligned} \quad (5.44)$$

where the angle $\theta = \phi - \pi/4$ has been rotated by a factor $\pi/4$ with respect to ϕ . Using result (5.43), we can simplify the x' integral in equation (5.45) to the matrix:

$$\begin{aligned} \mathcal{A}(\mathbf{r}, \mathbf{x}) &= \int dx' \tilde{\mathbf{V}}(\mathbf{x} - \mathbf{x}') \mathcal{G}(\mathbf{r}, \mathbf{x}') \\ &= \int dx' \begin{pmatrix} -\mathcal{G}_{11}(\mathbf{r}, \mathbf{x}') \Sigma_{11}(z) \delta(x - x') & \mathcal{G}_{11}(\mathbf{r}, \mathbf{x}') \psi(\mathbf{x} - \mathbf{x}') \\ \mathcal{G}_{22}(\mathbf{r}, \mathbf{x}') \psi^*(\mathbf{x} - \mathbf{x}') & -\mathcal{G}_{22}(\mathbf{r}, \mathbf{x}') \Sigma_{22}(z) \delta(x - x') \end{pmatrix} \\ &= \begin{pmatrix} -\mathcal{G}_{11}(\mathbf{r}, \mathbf{x}) \Sigma_{11}(z) & \psi(\mathbf{x}) \partial_{x_1} \partial_{x_2} \mathcal{G}_{11}(\mathbf{r}, \mathbf{x}) \\ \psi^*(\mathbf{x}) \partial_{x_1} \partial_{x_2} \mathcal{G}_{22}(\mathbf{r}, \mathbf{x}) & -\mathcal{G}_{22}(\mathbf{r}, \mathbf{x}) \Sigma_{22}(z) \end{pmatrix} \end{aligned} \quad (5.45)$$

The d -wave form of equation (5.45) is finally:

$$\boxed{\mathbf{g}(\mathbf{r}, \mathbf{r}') = \mathcal{G}(\mathbf{r}, \mathbf{r}') + \int dx \mathcal{A}(\mathbf{r}, \mathbf{x}) \mathbf{g}(\mathbf{x}, \mathbf{r}')} \quad (5.46)$$

5.2.3 The Effective Medium d -wave Green Function

The effective medium or mean field Green function is chosen in order to satisfy the translational invariance. However the self-energy should reflect the d -wave symmetry. The effective self-energy is chosen as:

$$\Sigma_i(\mathbf{k}, z) = k^4 \cos^2(2\theta) \sigma_i(z) \quad (5.47)$$

where $\sigma_i(z)$ does not depend on \mathbf{k} . The only space dependence has been put in the prefactor in front of the self-energy $\sigma_i(z)$. The effective medium Green function \mathcal{G} satisfies the equation

$$\begin{pmatrix} h_1(\mathbf{k}, z) - \Sigma_1(\mathbf{k}, z) & 0 \\ 0 & h_2(\mathbf{k}, z) - \Sigma_2(\mathbf{k}, z) \end{pmatrix} \mathcal{G}(\mathbf{k}, z) = \mathbb{I} \quad (5.48)$$

since $\Sigma = \mathcal{G}^{-1} - G_0^{-1}$ and the unperturbed solution G_0^{-1} is found when $\psi = 0$:

$$G_0^{-1} = \begin{pmatrix} h_1(\mathbf{k}, z) & 0 \\ 0 & h_2(\mathbf{k}, z) \end{pmatrix}$$

Since the CPA condition (5.20) is only valid in real space, one needs to compute the Fourier transform of the effective medium Green function. Following the same procedure as in the s -wave case, the local effective medium Green function is then given by:

$$\begin{aligned} \mathcal{G}(z) &= \int d^d k \mathcal{G}(\mathbf{k}, z) \\ &= \int d^d k \frac{1}{z + \xi_k - k^4 \cos^2(2\theta)\sigma(z)} \\ &= \int d\theta d\varepsilon \frac{D(\varepsilon)}{z + \varepsilon - \mu - c^2 \varepsilon^2 \cos^2(2\theta)\sigma(z)} \end{aligned} \quad (5.49)$$

The only change with respect to the s -wave symmetry, is the k -dependence of the self-energy.

5.2.4 The Field Dependent CPA d -wave Green Function

The field dependent local Green function $\mathbf{g}(\mathbf{r}, \mathbf{r}', z)$ is the solution of the one impurity problem in the presence of the local effective medium Green function $\mathcal{G}(\mathbf{r}, \mathbf{r}', z)$. The one impurity problem is introduced by requiring that the potential is only different from zero at the particular site \mathbf{r}' :

$$\tilde{\mathbf{V}}(\mathbf{x}) \rightarrow \delta(\mathbf{x} - \mathbf{r}') \tilde{\mathbf{V}}(\mathbf{x}) \quad (5.50)$$

This condition is then for the matrix $\mathcal{A}(\mathbf{r}, \mathbf{x})$:

$$\mathcal{A}(\mathbf{r}, \mathbf{x}) \rightarrow \delta(\mathbf{x} - \mathbf{r}') \mathcal{A}(\mathbf{r}, \mathbf{x}) \quad (5.51)$$

Introducing the replacement in equation (5.46), we have

$$\begin{aligned} \mathbf{g}(\mathbf{r}, \mathbf{r}') &= \mathcal{G}(\mathbf{r}, \mathbf{r}') + \int dx \mathcal{A}(\mathbf{r}, \mathbf{x}) \delta(\mathbf{x} - \mathbf{r}') \mathbf{g}(\mathbf{x}, \mathbf{r}') \\ &= \mathcal{G}(\mathbf{r}, \mathbf{r}') + \mathcal{A}(\mathbf{r}, \mathbf{r}') \mathbf{g}(\mathbf{r}, \mathbf{r}') \end{aligned} \quad (5.52)$$

The local Green function $\mathbf{g}(\mathbf{r}, \mathbf{r})$ is found by setting $\mathbf{r}' = \mathbf{r}$ and by solving the last equation with respect to it:

$$\boxed{\mathbf{g}(\mathbf{r}, \mathbf{r}) = \mathcal{G}(\mathbf{r}, \mathbf{r}) [\mathbb{I} - \mathcal{A}(\mathbf{r}, \mathbf{r}')|_{\mathbf{r}'=\mathbf{r}}]^{-1}} \quad (5.53)$$

where $\mathcal{A}(\mathbf{r}, \mathbf{x})$ is now from equation 5.52

$$\mathcal{A}(\mathbf{r}, \mathbf{r}) = \begin{pmatrix} -\mathcal{G}_{11}(\mathbf{r}, \mathbf{r})\Sigma_{11}(z) & \psi(\mathbf{x})\mathcal{B}_{11}(\mathbf{r}, \mathbf{r}) \\ \psi^*(\mathbf{r})\mathcal{B}_{22}(\mathbf{r}, \mathbf{r}) & -\mathcal{G}_{22}(\mathbf{r}, \mathbf{r})\Sigma_{22}(z) \end{pmatrix} \quad (5.54)$$

where the derivative of the effective local Green function is:

$$\mathcal{B}_{\alpha\alpha} = (\partial_x^2 - \partial_y^2) \mathcal{G}_{\alpha\alpha}(\mathbf{r}, \mathbf{r}')|_{\mathbf{r}=\mathbf{r}'} \quad (5.55)$$

for $\alpha = 1, 2$.

5.2.5 The CPA Condition

As for the s -wave case, our CPA condition will be for the Green function: the averaged local Green function $\langle \mathbf{g}(\mathbf{r}, \mathbf{r}) \rangle$ must be equal to the effective medium local Green function \mathcal{G} . This condition leads to the CPA equation

$$\langle \mathbf{g}(\mathbf{r}, \mathbf{r}) \rangle_\psi = \mathcal{G}(\mathbf{r}, \mathbf{r}) \quad (5.56)$$

and so to the important result:

$$\left\langle \left[\mathbb{I} - \mathcal{A}(\mathbf{r}, \mathbf{r}')|_{\mathbf{r}'=\mathbf{r}} \right]^{-1} \right\rangle_\psi = \mathbb{I} \quad (5.57)$$

Writing these equations in terms of the Green functions, we have:

$$\left\langle \frac{\begin{pmatrix} 1 + \mathcal{G}_2 \Sigma_2 & -\mathcal{B}_1 \psi_r \\ -\mathcal{B}_2 \psi_r^* & 1 + \mathcal{G}_1 \Sigma_1 \end{pmatrix}}{(1 + \mathcal{G}_1 \Sigma_1)(1 + \mathcal{G}_2 \Sigma_2) - \mathcal{B}_1 \mathcal{B}_2 |\psi_r|^2} \right\rangle_{\psi_r} = \mathbb{I} \quad (5.58)$$

where double indices are dropped ($\Sigma_1 := \Sigma_{11}$, etc). Solving the diagonal equations with respect to the self-energies Σ_1 and Σ_2 for the case where the amplitude is fixed leads to

$$\Sigma_1 = \frac{\langle |\psi|^2 \rangle \mathcal{B}_1 \mathcal{B}_2}{\mathcal{G}_1 (1 + \Sigma_2 \mathcal{G}_2)} \quad (5.59)$$

$$\Sigma_2 = \frac{\langle |\psi|^2 \rangle \mathcal{B}_1 \mathcal{B}_2}{\mathcal{G}_2 (1 + \Sigma_1 \mathcal{G}_1)} \quad (5.60)$$

5.3 CPA for Random Amplitudes

The amplitude is not fixed in general but it has a probability distribution. Since amplitudes are uncorrelated from site to site we can choose a site independent probability distribution $p_a(|\psi|)$ as for the phases. The form of the distribution resembles the probability distribution shown in figure 4.5 for high temperature, and it is of the form

$$p_1(|\psi|) \sim |\psi| e^{-|\psi|^2} \quad (5.61)$$

Here we would like in a first approach to study the influence of amplitude fluctuations on CPA equations.

5.3.1 Uniform Distribution

The simplest distribution is the uniform distribution:

$$p(|\psi|) = \begin{cases} \frac{1}{2b} & \text{if } |\psi_0| - b < |\psi| < |\psi_0| + b \\ 0 & \text{elsewhere} \end{cases} \quad (5.62)$$

where b is the fluctuation around the average value ψ_0 . In order that the first $\langle |\psi| \rangle$ and second momentum $\langle |\psi|^2 \rangle$ are equal with the one of distribution (5.61), b has to be set equal to: $b = 0.906$. The averaging of CPA equations (5.58) under $p(|\psi|)$ and random phases leads to the following equations:

$$\left\langle \frac{1 + \mathcal{G}_2 \Sigma_2}{(1 + \mathcal{G}_1 \Sigma_1)(1 + \mathcal{G}_2 \Sigma_2) - \mathcal{G}_1 \mathcal{G}_2 |\psi|^2} \right\rangle_p = 1 \quad (5.63)$$

$$\left\langle \frac{1 + \mathcal{G}_1 \Sigma_1}{(1 + \mathcal{G}_1 \Sigma_1)(1 + \mathcal{G}_2 \Sigma_2) - \mathcal{G}_1 \mathcal{G}_2 |\psi|^2} \right\rangle_p = 1 \quad (5.64)$$

Using the uniform distribution p from equation (5.62) leads to

$$\frac{1 + \mathcal{G}_{1,2} \Sigma_{1,2}}{\mathcal{G}_1 \mathcal{G}_2} \int_{|\psi_0|-b}^{|\psi_0|+b} d|\psi| \frac{1}{A - |\psi|^2} = 1 \quad (5.65)$$

where the symmetric coefficient A is:

$$A = \frac{(1 + \mathcal{G}_1 \Sigma_1)(1 + \mathcal{G}_2 \Sigma_2)}{\mathcal{G}_1 \mathcal{G}_2} \quad (5.66)$$

The primitive of the integral

$$\int dx \frac{1}{A - x^2} = \text{ArcTan} \left(\frac{x}{\sqrt{A}} \right) \frac{1}{\sqrt{A}}$$

leads to the two final equations:

$$\boxed{\begin{aligned} \frac{1 + \mathcal{G}_1 \Sigma_1}{\mathcal{G}_1 \mathcal{G}_2} \left[\frac{1}{\sqrt{A}} \text{ArcTan} \left(\frac{|\psi|}{\sqrt{A}} \right) \right]_{|\psi_0|-b}^{|\psi_0|+b} &= 1 \\ \frac{1 + \mathcal{G}_2 \Sigma_2}{\mathcal{G}_1 \mathcal{G}_2} \left[\frac{1}{\sqrt{A}} \text{ArcTan} \left(\frac{|\psi|}{\sqrt{A}} \right) \right]_{|\psi_0|-b}^{|\psi_0|+b} &= 1 \end{aligned}} \quad (5.67)$$

These two equations reduce to the CPA equations (5.26) and (5.27) when the fluctuation parameter b goes to zero.

This model distribution shows that a larger parameter $|\psi_0|$ (i.e. a stronger attraction) is needed in order to open a gap in the density of states when amplitude fluctuations are taken into account. The latter also round the edge of the density of states. One can see the effect of amplitude fluctuations in figure 5.4: amplitude fluctuations smooth out the energy landscape.

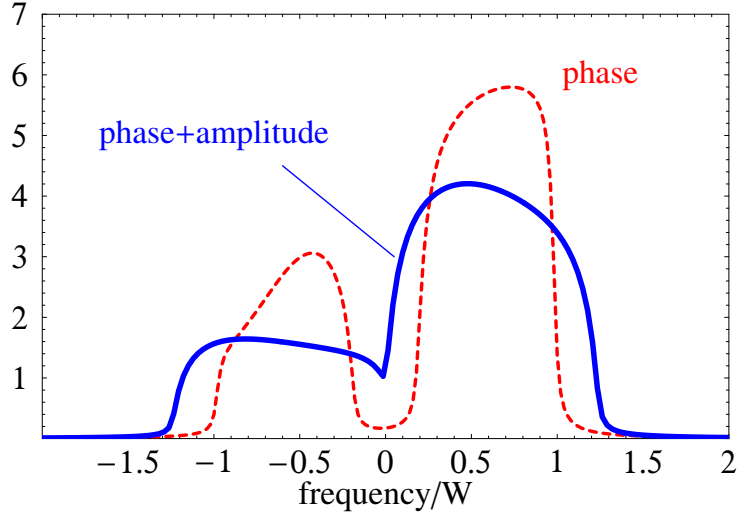


Figure 5.4: Density of states in the CPA approach for $\psi = 0.5W$ and $\mu = 0.25W$. Blue: phase and uniform amplitude fluctuations. Red: density of states from equations (5.26) and (5.27) where the amplitude is fixed.

5.3.2 Gaussian Distribution

The main problem of the uniform distribution approach is the presence of the fluctuation parameter: one has to set by hand the value of fluctuations. As already mentioned in the beginning of this section, the amplitude distribution for a disordered system (see 4.5) can be very well approximated by the analytical expression:

$$p(|\psi|) = 2b |\psi| e^{-b|\psi|^2} \quad (5.68)$$

The average amplitude is then related to the parameter b :

$$\begin{aligned} \langle |\psi| \rangle &= \int_0^\infty d|\psi| |\psi| p(|\psi|) \\ &= \frac{\sqrt{\pi}}{2\sqrt{b}} \end{aligned} \quad (5.69)$$

Contrary to the uniform distribution, the gaussian distribution has then only one free parameter which is the average value of the amplitude $\langle |\psi| \rangle$. The absolute size of this average value, i.e. the ratio to the band width is then given by the self-consistent amplitude equation (5.32). Inserting the gaussian distribution $p(|\psi|)$ from equation (5.68) into CPA equations (5.58) leads to

$$\frac{1 + \mathcal{G}_{1,2}\Sigma_{1,2}}{\mathcal{G}_1\mathcal{G}_2} \int_0^\infty d|\psi| 2b |\psi| e^{-b|\psi|^2} \frac{1}{A - |\psi|^2} = 1 \quad (5.70)$$

where the symmetric coefficient A is give by formula (5.66). The primitive of the integral

$$2b \int_0^\infty dx x e^{-bx^2} \frac{1}{A - x^2} = -be^{-bA} \tilde{\Gamma}_0(-bA)$$

where $\Gamma_0(z)$ is the incomplete gamma function:

$$\tilde{\Gamma}_a(z) := \int_z^\infty t^{a-1} e^{-t}$$

This leads to the two CPA equations:

$$\begin{aligned} -b e^{-bA} \frac{1 + \mathcal{G}_1 \Sigma_1}{\mathcal{G}_1 \mathcal{G}_2} \tilde{\Gamma}_0(-bA) &= 1 \\ -b e^{-bA} \frac{1 + \mathcal{G}_2 \Sigma_2}{\mathcal{G}_1 \mathcal{G}_2} \tilde{\Gamma}_0(-bA) &= 1 \end{aligned} \quad (5.71)$$

These two equations reduce to the CPA equations (5.26) and (5.27) when the fluctuation parameter b goes to zero.

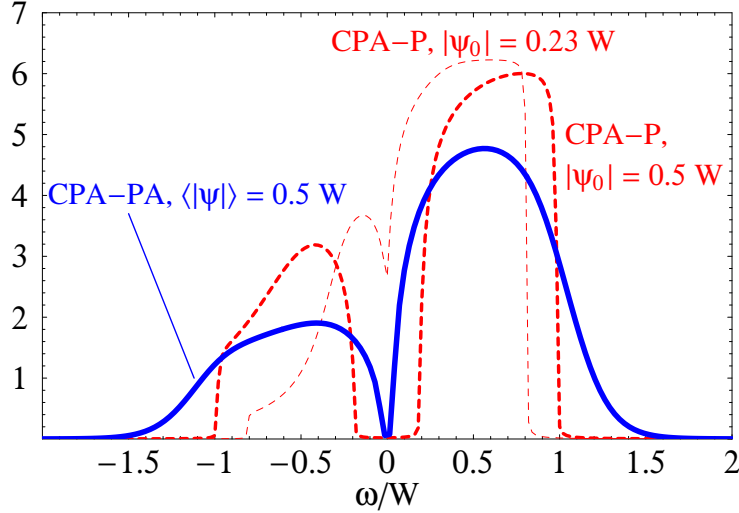


Figure 5.5: Density of states for CPA gaussian amplitude fluctuations approach for $\mu = 0.25W$. Thick: phase and amplitude fluctuations (CPA-PA). Thin dashed: density of states from equations (5.26) using the phase only approach (CPA-P). Thick dashed: same quantity but for the gapped phase for $\psi = 0.5W$.

5.3.3 Comparison with DMFT

Dynamic Mean Field Theory (DMFT) is method similar to CPA. The main difference is that the usual DMFT [50] treat the one site Hubbard model. There is no decoupling of the interaction term like in our CPA where an auxiliary pairing field is introduced. DMFT [50] yields similar results as CPA for the critical attraction at $\mu = 0$: $U_c \approx 0.6$. However the phase diagram is not the same, especially near half-filling, U_c in CPA with phase fluctuations only is approximately 0.2 although it should be of the order

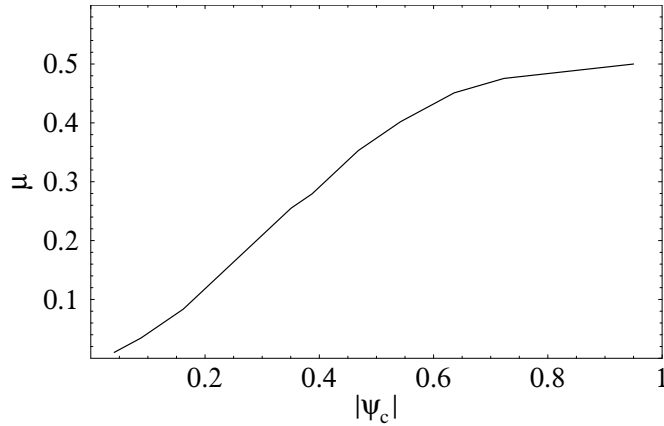


Figure 5.6: Minimal amplitude $|\psi_c|$ necessary to open a gap in the density of states. The filling is $n = 2\mu$ since we work at zero temperature. (in units of the bandwidth W)

of 1.5 as in DMFT and other methods. This problem can be overcome by solving the CPA problem in presence of amplitude fluctuations. This has been done in the previous section. The effect of amplitude fluctuations is that a larger U is needed in order to establish a gap in the density of states. Hence the phase diagram of CPA with amplitude fluctuations resembles much more to the phase diagram of DMFT. Using a gaussian distribution for the amplitude and an absolute size of the average amplitude $\langle|\psi|\rangle$ given by the BCS formula (see [44]):

$$U = \frac{-1}{\log\left(\frac{\langle|\psi|\rangle}{\sqrt{\langle|\psi|\rangle^2 + 4n - 2n^2}}\right)} \quad (5.72)$$

where $n = 2\mu$ is the filling at $T = 0$. In figure 5.6, the minimal amplitude $|\psi_c|$ needed to open a full gap in the density of states is shown. Contrary to BCS approach, where the critical amplitude is zero since the gap in the density of states is equal to the amplitude, here there is a pseudogap domain where a finite amplitude produces only a partial suppression of spectral weight. In figure 5.7, the phase diagram for the pairing attraction U and filling n is shown. Using DMFT, [50] found a first order phase transition between the metallic phase and the pairing phase. In the amplitude fluctuations CPA, we can identify a transition between a pseudogap phase and a full gap phase. The latter can be interpreted as a "pairing phase" like in DMFT results. Both results show a critical point at $U_c \approx 0.6$ and a transition at half-filling $U_c \approx 1.6$. However at half-filling, the amplitude CPA transition seems to have a cusp which is not present in DMFT.

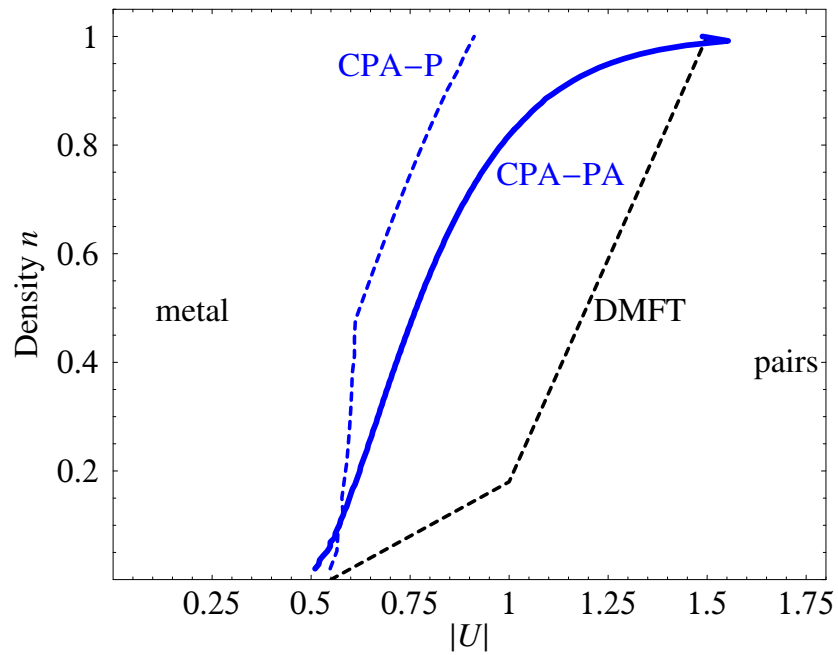


Figure 5.7: CPA with phase and amplitude fluctuations (CPA-PA)(thick) compared to DMFT first order transition (dashed). For small U , there is no full gap in the density of states although a finite amplitude is always present. The gap only opens when fluctuations are overcome by a sufficiently large U . The CPA with phase fluctuations only (CPA-P) is shown by the thin line. (in units of the bandwidth W)

Chapter 6

SUPERCONDUCTORS WITH SHORT RANGE CORRELATIONS

In this chapter we present an extension of the CPA method for computing the density of states of the attractive Hubbard model below and above the critical temperature. Since the CPA method assume that the amplitude of the paring field is not correlated with other sites, we can speak of short range correlations.

6.1 CPA below in Superconducting State

In the previous chapter, we have derived the CPA equations (5.26) and (5.27) in the presence of a field ψ where phase are random and the amplitude is fixed. Hence no superconductivity is present is the CPA calculations and application could be made for the pseudogap regime of high T_c superconductors or in a high magnetic field where superconductivity is suppressed.

Now the question arises whether a homogenous superconducting order parameter, i.e. a non-zero expectation value ψ_s independent of the position,

$$\psi_s := \langle \psi \rangle \neq 0,$$

is compatible with CPA calculations. In other words, is it possible that a CPA pseudogap and superconductivity coexist together. A first approach to give an answer to this problem, is to take the CPA self-energies from equations (5.26) and (5.27) and put them in BCS Gorkov equations. In k -space, we have:

$$\begin{pmatrix} z - \xi - \Sigma_{11}^{cpa} & \psi_s \\ \psi_s^* & z + \xi - \Sigma_{22}^{cpa} \end{pmatrix} \mathbf{G}(\mathbf{k}, z) = \mathbb{I} \quad (6.1)$$

where Σ_{11}^{cpa} and Σ_{22}^{cpa} are solutions of normal CPA equations (5.26) and (5.27). The solutions of equations (6.1) are then easily obtained by inverting the matrix and one

finds the following equations:

$$\mathbf{G}(\mathbf{k}, z) = \frac{\begin{pmatrix} z + \xi - \Sigma_{22}^{cpa} & -\psi_s \\ -\psi_s^* & z - \xi - \Sigma_{11}^{cpa} \end{pmatrix}}{(z - \xi - \Sigma_{11}^{cpa})(z + \xi - \Sigma_{22}^{cpa}) - \psi_s \psi_s^*} \quad (6.2)$$

The Green functions $G_{11}(\mathbf{k}, z)$ is therefore:

$$G_{11}(\mathbf{k}, z) = \frac{z + \xi - \Sigma_{22}^{cpa}}{(z - \xi - \Sigma_{11}^{cpa})(z + \xi - \Sigma_{22}^{cpa}) - \psi_s \psi_s^*} \quad (6.3)$$

If we introduce the CPA Green functions

$$G_{11}^{cpa} = \frac{1}{z - \xi - \Sigma_{11}^{cpa}}$$

and

$$G_{22}^{cpa} = \frac{1}{z + \xi - \Sigma_{22}^{cpa}},$$

we get the compact notation for the Green function $G_{11}(\mathbf{k}, z)$:

$$G_{11}(\mathbf{k}, z) = \frac{G_{11}^{cpa}}{1 - \psi_s \psi_s^* G_{11}^{cpa} G_{22}^{cpa}} \quad (6.4)$$

6.2 Spectral Properties

In figure 6.1, we show the density of states for different temperatures. The temperature is introduced as a parameter which parameterizes the amplitude and the order parameter. Hence the order parameter should be non-zero below T_c and zero above T_c . In order to have a more physical description, a complex damping term $i\Gamma$ can be added to the self-energy in the CPA calculations. We would like to compare these results with scanning tunneling experiments [11] or intrinsic tunneling experiments [12, 13]. However, there are two drawbacks with our method:

1. If we look at the low temperatures data, i.e. when $T/T_c = 0.1$, the difference between the pure CPA result and the CPA+superconducting Gap result, is not represented by two coherence peaks like in intrinsic tunneling experiments [12, 13]. The difference is that the gap is more pronounced.
2. A second drawback is that the amplitude and the order parameter form a gap in the density of states which is approximately equal to their sum. However, in experiments, the pseudogap width seems to be constant from high temperatures to low temperatures, i.e. it does not seem to be produced by addition of the different quantities.

What do we learn?

1. The coherence peaks seen in intrinsic tunneling experiments cannot be produced by the presence of an order parameter coexisting with a pseudogap. The peaks are presumably due to phase correlations and could be found in $d = 2$ as well where the order parameter must be zero due to Mermin-Wagner theorem.
2. One cannot have a coexistence of two gaps, here an amplitude and an order parameter, if one wants to reproduce experiments since the latter add themselves in calculations. Moreover, the pseudogap at high temperature must become a full gap at low temperature. In some sense, it is the same if one calculates specific heat like in chapter 4: the wide hump seen in specific heat of underdoped cuprate transforms to a BCS peak upon doping. Since for our calculations increasing doping is almost equivalent to decrease temperature, the high temperature CPA density of states should transform into a BCS density of states upon decreasing the temperature.

In figure 6.2, the average amplitude entering into the CPA calculation has been replaced by the average amplitude fluctuation:

$$\langle \delta|\psi| \rangle = \sqrt{\langle |\psi|^2 \rangle - \langle |\psi| \rangle^2}$$

In this scenario, the problem of the addition of the two parameters ψ_s and $\langle |\psi| \rangle$ is removed except in a small region below T_c where the order parameter is non zero and amplitude fluctuations are still large. However the correspondence between the BCS low temperature properties and the pseudogap regime is lost, i.e. the pseudogap vanishes at low temperature instead of being transformed into the BCS superconducting gap like in specific heat (see chapter 4) where the pseudogap hump transforms into the BCS gap when increasing the doping.

The fact that in our calculations the superconducting gap modifies strongly the density of states is in contradiction with intrinsic tunneling experiments [12, 13] where the difference between the superconducting state and the normal state is in two thin coherence peaks. This has been shown experimentally by turning on a magnetic field.

However if one replaces the superconducting gap ψ_s by the average amplitude $\langle |\psi| \rangle$ at low temperatures, then the correspondence between low temperatures and overdoped doping is preserved. The contradiction with intrinsic tunneling experiments would also be removed since magnetic field used in these experiments do not reduce the amplitude.

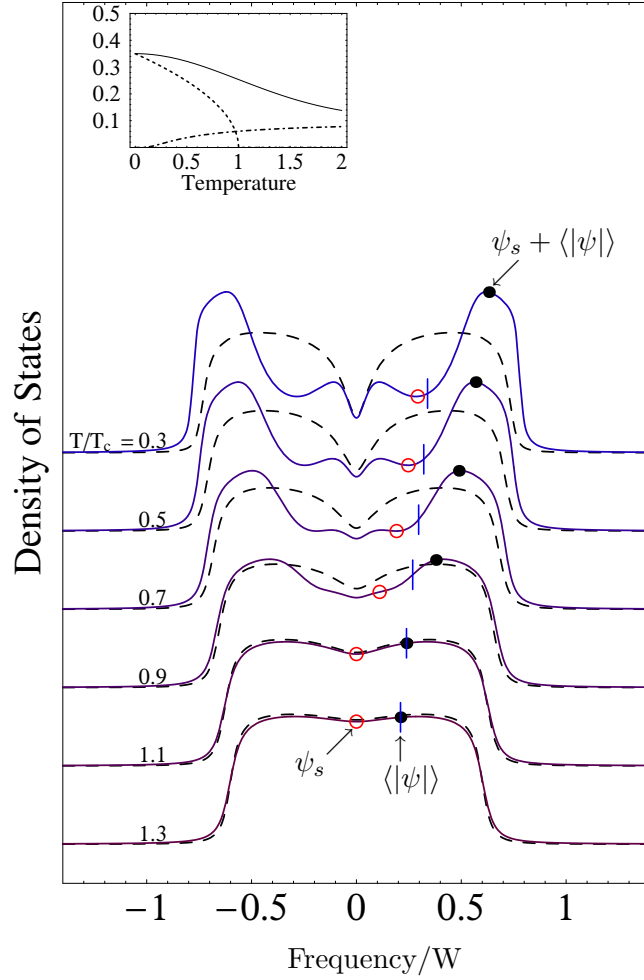


Figure 6.1: Density of states in the CPA approach in the presence of an order parameter. Dashed lines: density of states from equations (5.26) and (5.27). The distance between the zero frequency and the vertical dash represents the value of the average amplitude for the corresponding density of states. The distance between zero frequency and the circle shows the order parameter, and points are for the sum of the amplitude and the order parameter. **Inset:** the upper thick curve is the average amplitude $\langle |\psi| \rangle$ that enters in the CPA calculations. The dashed curve is the order parameter ψ_s and the dotted-dashed line is represents the damping term Γ . Note that the amplitude is now large at low temperature.

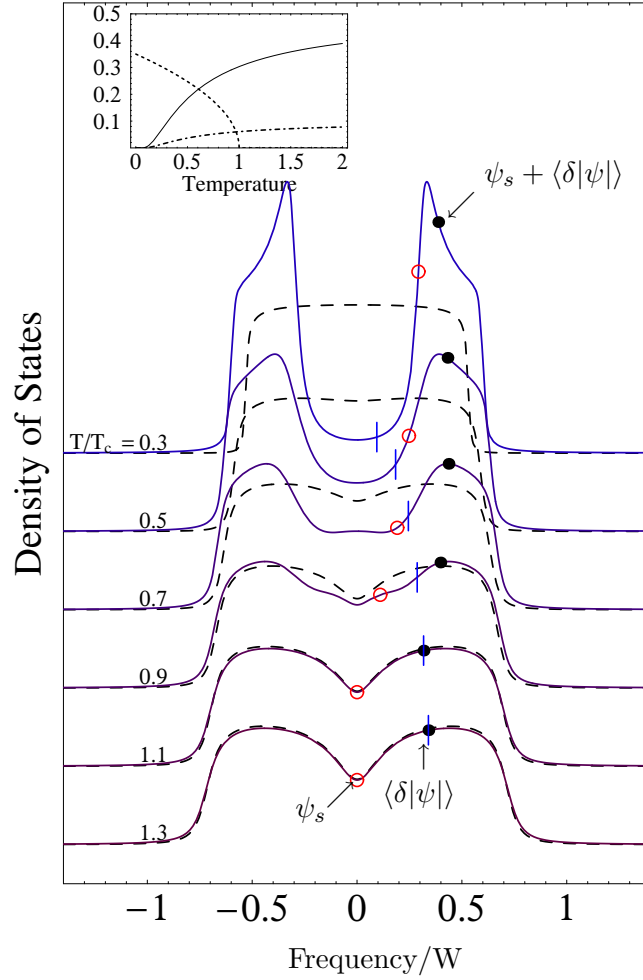


Figure 6.2: Density of states in the CPA approach in the presence of an order parameter. Dashed lines: density of states from equations (5.26) and (5.27). The points, lines and circles have the same signification as in previous figure. **Inset:** the thick curve is the average amplitude fluctuations $\langle \delta|\psi| \rangle$ that comes in the CPA calculations. The dashed curve is the order parameter ψ_s and the dotted-dashed line represents the damping term $i\Gamma$.

Chapter 7

SUPERCONDUCTORS WITH LONG RANGE CORRELATIONS

In this chapter, we derive an effective theory based on the Hubbard-Stratonovich transformation (see section 2.3.5 and 2.3.6). Contrary to the CPA shown in the last chapter, the Hubbard-Stratonovich transformation and the derivation of the self-energy allows to take into account long range correlations: the same effective amplitude pairing field influence a large region, whereas in CPA, the amplitude pairing field is considered to be decorrelated from all other sites.

7.1 The Electronic Self-Energy

We start again from the attractive Hubbard model whose hamiltonian is

$$H = - \sum_{\langle i,j \rangle \sigma} t_{ij} c_{i\sigma}^\dagger c_{j\sigma} - U \sum_i c_{i\uparrow}^\dagger c_{i\downarrow}^\dagger c_{i\uparrow} c_{i\downarrow} \quad (7.1)$$

We would like to derive an analytical expression for the self-energy $\Sigma(\mathbf{k}, \omega_n)$ in the presence of a pairing field ψ . This derivation is done in the framework of the Hubbard-Stratonovich transformation (see section 2.3.5 and 2.3.6). The matrix self-energy is defined by its relation to the matrix Green function:

$$\mathbf{G}(\mathbf{k}, \omega_n) = \left(\mathbf{G}_{0,k}^{-1} + \Sigma(\mathbf{k}, \omega_n) \right)^{-1} \quad (7.2)$$

The form of the self-energy can be derived by comparing equations (2.94) and (7.2). First we expand equation (7.2) in a Dyson form:

$$\mathbf{G}(\mathbf{k}, \omega_n) = \mathbf{G}_{0,k} + \mathbf{G}_{0,k} \Sigma(\mathbf{k}, \omega_n) \mathbf{G}_{0,k} + \dots \quad (7.3)$$

Expanding equation (2.94) is more complicated since the function \mathbf{g} appears on both side of the equation. Hence the equation has to be solve self-consistently by replacing

\mathbf{g} on the right side by its full expression:

$$\begin{aligned} \mathbf{g}_{k-q,k'}(\omega_n - \omega_m) &\rightarrow \mathbf{G}_{0,k-q}(\omega_{nm})\delta_{k-q,k'} \\ &\quad - \mathbf{G}_{0,k-q}(\omega_{nm}) \sum_{q',\omega_{m'}} \mathbf{V}_{q'}(\omega_{m'}) \mathbf{g}_{k-q-q',k'}(\omega_{nm} - \omega_{m'}) \end{aligned} \quad (7.4)$$

where $\omega_{nm} = \omega_n - \omega_m$. Equation (2.94) is then

$$\begin{aligned} \mathbf{g}_{kk'}(\omega_n) &= \mathbf{G}_{0,k}(\omega_n)\delta_{kk'} - \mathbf{G}_{0,k}(\omega_n) \sum_{q,\omega_m} \mathbf{V}_q(\omega_m) \\ &\quad \left[\mathbf{G}_{0,k-q}(\omega_{nm})\delta_{k-q,k'} - \mathbf{G}_{0,k-q}(\omega_{nm}) \sum_{q',\omega_{m'}} \mathbf{V}_{q'}(\omega_{m'}) \mathbf{g}_{k-q-q',k'}(\omega_{nm} - \omega_{m'}) \right] \end{aligned}$$

Expanding and simplifying this expression leads to

$$\begin{aligned} \mathbf{g}_{kk'}(\omega_n) &= \mathbf{G}_{0,k}(\omega_n)\delta_{kk'} - \mathbf{G}_{0,k}(\omega_n) \sum_{\omega_m} \mathbf{V}_{k-k'}(\omega_m) \mathbf{G}_{0,k'}(\omega_{nm}) \\ &\quad - \mathbf{G}_{0,k}(\omega_n) \sum_{q,\omega_m} \sum_{q',\omega_{m'}} \mathbf{V}_q(\omega_m) \mathbf{G}_{0,k-q}(\omega_{nm}) \mathbf{V}_{q'}(\omega_{m'}) \mathbf{g}_{k-q-q',k'}(\omega_{nm} - \omega_{m'}) \end{aligned}$$

Now we can replace the last Green function $\mathbf{g}_{k-q-q',k'}(\omega_{nm} - \omega_{m'})$ by its zero order approximation, i.e. by $\mathbf{G}_{0,k-q-q',k'}(\omega_{nm} - \omega_{m'})\delta_{k-q-q',k'}$, and we average the equation over the field ψ :

$$\begin{aligned} \mathbf{G}_{kk'}(\omega_n)\delta_{kk'} &= \mathbf{G}_{0,k}(\omega_n)\delta_{kk'} - \mathbf{G}_{0,k}(\omega_n) \sum_{\omega_m} \langle \mathbf{V}_{k-k'}(\omega_m) \rangle \mathbf{G}_{0,k'}(\omega_n - \omega_m) \\ &\quad - \mathbf{G}_{0,k}(\omega_n) \sum_{q,\omega_m,\omega_{m'}} \langle \mathbf{V}_q(\omega_m) \mathbf{G}_{0,k-q}(\omega_{nm}) \mathbf{V}_{k-k'-q}(\omega_{m'}) \rangle \mathbf{G}_{0,k'}(\omega_{nm} - \omega_{m'}) \end{aligned}$$

This equation can be simplified if we assumed the system is translational invariant:

$$\langle \psi_q^*(\omega_m) \rangle = \langle \psi_0^*(0) \rangle \delta_{q,0} \delta_{\omega_m,0} \quad (7.5)$$

where $q = 0, \omega_m = 0$ is a particular state chosen as reference. The pairing correlation does not depend on the location of measurement as well. Hence we have:

$$\langle \psi_q^*(\omega_m) \psi_{k-k'-q}(\omega_{m'}) \rangle = \delta_{q,k-k'-q} \delta_{\omega_m\omega_{m'}} \quad (7.6)$$

The Green function can simplified then as:

$$\begin{aligned} \mathbf{G}_{kk'}(\omega_n)\delta_{kk'} &= \mathbf{G}_{0,k}(\omega_n)\delta_{kk'} - \mathbf{G}_{0,k}(\omega_n) \langle \mathbf{V}_0(0) \rangle \mathbf{G}_{0,k'}(\omega_n) \\ &\quad - \mathbf{G}_{0,k}(\omega_n) \sum_{q,\omega_m} \langle \mathbf{V}_q(\omega_m) \mathbf{G}_{0,k-q}(\omega_{nm}) \mathbf{V}_q(\omega_m) \rangle \mathbf{G}_{0,k'}(\omega_n) \end{aligned} \quad (7.7)$$

Comparing equations (7.3) and (7.7) allows to identify a expression for the self-energy in first order approximation:

$$\Sigma^{(1)} = \langle \mathbf{V}_0(0) \rangle \quad (7.8)$$

The average of $\Sigma^{(1)}$ is zero above T_c since the order parameter $\langle\psi\rangle$ is zero above T_c . The self-energy in second order approximation is

$$\Sigma_k^{(2)}(\omega_n) = \sum_{q\omega_m} \langle \mathbf{V}_q(\omega_m) \mathbf{G}_{0,k-q}(\omega_n - \omega_m) \mathbf{V}_q(\omega_m) \rangle \quad (7.9)$$

The components of the self-energy can be expressed it in a matrix equation:

$$\begin{pmatrix} \Sigma^{11} & \Sigma^{21} \\ \Sigma^{21} & \Sigma^{22} \end{pmatrix} = \sum_{q\omega_m} \begin{pmatrix} \langle |\psi|^2 \rangle G^{22} & \langle \psi\psi \rangle G^{21} \\ \langle \psi^*\psi^* \rangle G^{21} & \langle |\psi|^2 \rangle G^{11} \end{pmatrix} \quad (7.10)$$

where all indices, except matrix indices, have been dropped for clarity.

The diagonal matrix elements of the self-energy are then

$$\begin{aligned} \Sigma_k^{11}(\omega_n) &= \sum_{q\omega_m} \langle |\psi_q(\omega_m)|^2 \rangle G_{0,k-q}^{22}(\omega_n - \omega_m) \\ \Sigma_k^{22}(\omega_n) &= \sum_{q\omega_m} \langle |\psi_q(\omega_m)|^2 \rangle G_{0,k-q}^{11}(\omega_n - \omega_m) \end{aligned} \quad (7.11)$$

where we dropped the exponent ⁽²⁾ for clarity. If we neglect the Matsubara bosonic frequency summation, i.e. we work at zero frequency, the self-energy is then:

$$\begin{aligned} \Sigma_k^{11}(\omega_n) &= - \sum_q \langle |\psi_q|^2 \rangle G_{0,k-q}^{11}(-\omega_n) \\ \Sigma_k^{22}(\omega_n) &= - \sum_q \langle |\psi_q|^2 \rangle G_{0,k-q}^{22}(-\omega_n) \end{aligned} \quad (7.12)$$

where we used the relation $G_{11}(\omega_n) = -G_{22}(-\omega_n)$. Since $G_{0,k}^{11}(\omega_n) = (\omega_n - \varepsilon_k + \mu)^{-1}$ and $G_{0,k}^{22}(\omega_n) = (\omega_n + \varepsilon_k - \mu)^{-1}$ (where μ is the chemical potential), we have

$$\begin{aligned} \Sigma_k^{11}(\omega_n) &= \sum_q \langle |\psi_q|^2 \rangle \frac{1}{\omega_n + \varepsilon_{k-q} - \mu} \\ \Sigma_k^{22}(\omega_n) &= \sum_q \langle |\psi_q|^2 \rangle \frac{1}{\omega_n - \varepsilon_{k-q} + \mu} \end{aligned} \quad (7.13)$$

7.2 Phase Correlations Below and Above T_c

Now we are interested in the Green function in the presence of a superconducting order parameter

$$\psi_s = \langle\psi\rangle$$

The derivation of the Green function is similar to derivation of section 6.1 where we have found the Green function in the presence of a superconducting gap with a self-energy coming from CPA calculations. Here the self-energy comes from the expansion in the Hubbard-Stratonovich transformation. Hence, following a similar development as in section 6.1 and result of equation (6.4) the desired Green function is

$$G_{11}(\mathbf{k}, z) = \frac{\bar{G}_{11}}{1 - \psi_s \psi_s^* \bar{G}_{11} \bar{G}_{22}} \quad (7.14)$$

where

$$\bar{G}_{11} = \frac{1}{z - \varepsilon_k + \mu - \Sigma_k^{11}}, \quad \text{and} \quad \bar{G}_{22} = \frac{1}{z + \varepsilon_k - \mu - \Sigma_k^{22}}$$

are the Green function corresponding to the self-energy (7.12), and the complex Matsubara frequency z is

$$z = i\omega_n.$$

Using this Green function, we can express (7.14) in term of the self-energy:

$$G_{11}(\mathbf{k}, z) = \frac{1}{z - \varepsilon_k + \mu - \Sigma_k^{11} - |\psi_s|^2 \frac{1}{z + \varepsilon_k - \mu - \Sigma_k^{22}}} \quad (7.15)$$

Until now we did not take into account other scattering processes like fermion-fermion scattering, fermion-phonon scattering. To take into account these processes, we add an imaginary damping term $i\Gamma$ to the self-energy. All these scattering should not be physically important for the superconductivity itself. This is why we "summerize" their influence in the damping $i\Gamma$. The effect of a complex damping term on the Green function is to smooth the curves, but the essential physics remains similar. Inserting results from equations (7.13) into (7.15), and adding the damping term $i\Gamma$ to Σ_{11} and Σ_{22} gives:

$$G_{11}(\mathbf{k}, z) = \frac{1}{z - \xi_k + i\Gamma - \sum_q \frac{\langle |\psi_q|^2 \rangle}{z + \xi_{k-q}} - |\psi_s|^2 \frac{1}{z + \xi_k - i\Gamma - \sum_q \frac{\langle |\psi_q|^2 \rangle}{z - \xi_{k-q}}} \quad (7.16)$$

where the reduced energy is $\xi_k = \varepsilon_k - \mu$.

7.2.1 $T \gg T_c$

Above T_c The average amplitude in q space can simplified as:

$$\langle |\psi_q|^2 \rangle = \int d^3r \int d^3r' \langle \psi(\mathbf{r}) \psi^*(\mathbf{r}') \rangle e^{i\mathbf{k}(\mathbf{r}-\mathbf{r}')} = \langle |\psi|^2 \rangle \quad (7.17)$$

since the correlation function is only non zero at high temperature for the "self-correlation", i.e. $\langle \psi(\mathbf{r}) \psi^*(\mathbf{r}) \rangle > 0$ and $\langle \psi(\mathbf{r}) \psi^*(\mathbf{r}') \rangle = 0$ if $\mathbf{r} \neq \mathbf{r}'$. Since the order parameter ψ_s is zero above T_c , we have:

$$G_{11}(\mathbf{k}, z) = \frac{1}{z - \xi_k + i\Gamma - \langle |\psi|^2 \rangle \sum_q \frac{1}{z + \xi_{k-q}}} \quad (7.18)$$

7.2.2 $T \ll T_c$

Well below the critical temperature, the correlation function is almost constant: $\langle \psi(\mathbf{r}) \psi^*(\mathbf{r}') \rangle = \langle |\psi(\mathbf{r})|^2 \rangle$. The average amplitude in q space can simplified as:

$$\langle |\psi_q|^2 \rangle = \langle |\psi|^2 \rangle \delta(q) \quad (7.19)$$

$$G_{11}(\mathbf{k}, z) = \frac{1}{z - \xi_k + i\Gamma - \frac{\langle |\psi|^2 \rangle}{z + \xi_k} - |\psi_s|^2 \frac{1}{z + \xi_k - \frac{\langle |\psi|^2 \rangle}{z - \xi_k}}} \quad (7.20)$$

The density of states $D(\omega)$ has been calculated by using the standard formula

$$D(\omega) = -\frac{1}{W} \int_{-\mu}^{W-\mu} d\xi \operatorname{Im} (G_{11}(\mathbf{k}, z))$$

where W is the bandwidth. The non-perturbed density of states is assumed to be constant and equal to $1/W$.

In figure 7.1, the density of states $D(\omega)$ is presented for temperature dependent parameters $\psi_s(T)$, $\langle |\psi| \rangle(T)$, $\Gamma(T)$ in units of the bandwidth W . The chemical potential is $\mu = 0.5W$. The temperature dependence of $\psi_s(T)$ $\langle |\psi|^2 \rangle(T)$ can be taken from Ginzburg-Landau simulations, see chapter 4. The scattering $\Gamma(T)$ is zero at zero temperature, and increases with temperature.

Above T_c , we have a pseudogap in the density of states due to the presence of a finite amplitude $\langle |\psi| \rangle(T)$. Below the critical temperature, a superconducting gap opens inside the pseudogap region. The width between the superconducting peaks is of the order of ψ_s whereas the amplitude gap becomes much wider and has a width of the order of $\psi_s + \langle |\psi| \rangle(T)$. This result is very similar to the one found for the CPA calculation in the presence of an order parameter ψ_s shown in figure 6.1: the pseudogap width is not constant and becomes too wide at low temperature. We are confronted to the situation where both parameter ψ_s and $\langle |\psi| \rangle(T)$ opens a full gap in the density of states. However, in experiments the pseudogap width is almost constant from low to high temperatures and superconductivity produces only additional peaks, not a full gap. With respect to the pseudogap shape, it seems that CPA results are closer to experiments, since the pseudogap is smoother than in the self-energy expansion.

In figure 7.2, the density of states $D(\omega)$ is shown for $\psi_s(T)$, $\langle \delta |\psi| \rangle(T)$, $\Gamma(T)$ in units of the bandwidth W . The parametrisation is identical to figure 6.2. One can see that the lowest parameter between $\psi_s(T)$ and $\langle \delta |\psi| \rangle(T)$ produces additional peaks in the inner of the gap.

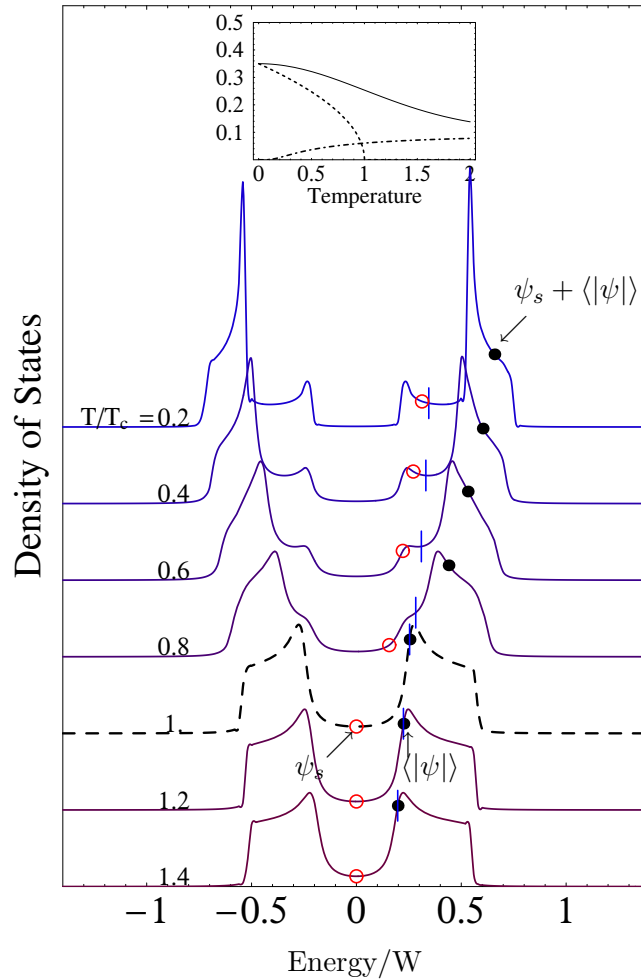


Figure 7.1: Density of states in the presence of an order parameter and an average amplitude. The points have the same significance as in CPA figures (6.1) and (6.1). **Inset:** the upper curve is the amplitude that comes in the CPA calculations. The dashed curve is the order parameter ψ_s and the dotted-dashed line represents the damping term Γ . Note that this parametrisation is identical to the one of figure (6.1) but the vertical scale is different.

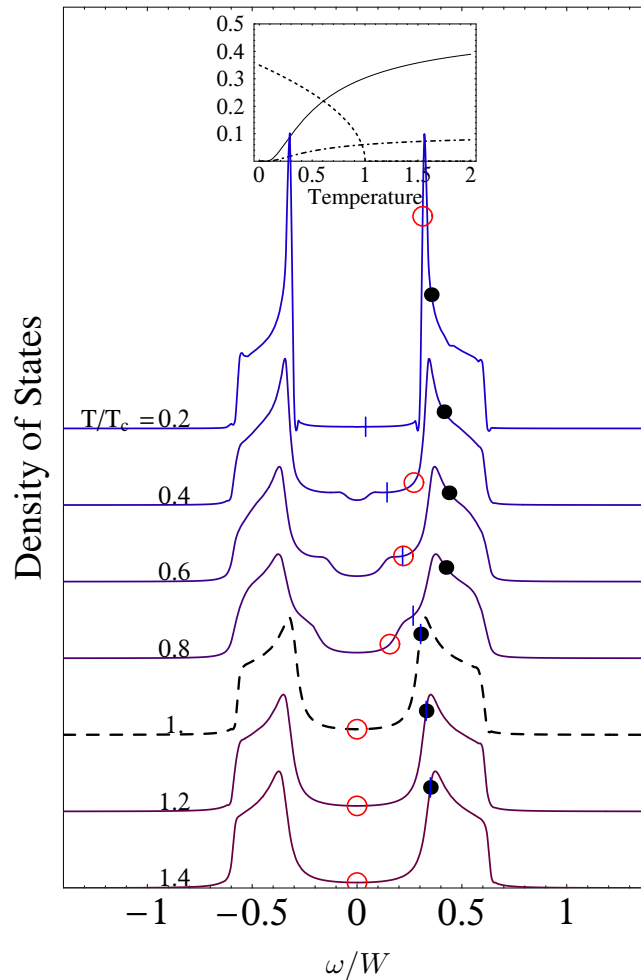


Figure 7.2: Density of states in the presence of an order parameter and amplitude fluctuations. The points have the same significance as in CPA figures (6.1). **Inset:** the thick curve is the average amplitude. The dashed curve is the order parameter ψ_s and the dotted-dashed line represents the damping term $i\Gamma$. Note that this parametrisation is identical to the one of figure (6.2) but the vertical scale is different.

Appendix A

EXPECTATION VALUE OF $\log \mathbf{R}$

The problem of computing the expectation value of $\langle \log R \rangle$ is solved using an approximation that conserves the *log* behaviour (as the cumulant expansion conserves the *exp* behaviour). In order to compute $\langle \log 1 + x \rangle$ with a gaussian distribution of x . First, we expand the *log*. Second, we take the *log exp* of this expression and then expand the *exp*, keeping always terms up to the fourth power:

$$\begin{aligned}\langle \log 1 + x \rangle &\approx -\langle x^2 \rangle / 2 - \langle x^4 \rangle / 4 = \log \exp(-\langle x^2 \rangle / 2 - \langle x^4 \rangle / 4) \\ &\approx \log \left(1 - \langle x^2 \rangle / 2 - \langle x^4 \rangle / 4 + 1/8 \langle x^2 \rangle^2 \right) \\ &= \log \left(1 - \frac{1}{2} \langle x^2 \rangle - \frac{5}{8} \langle x^2 \rangle^2 \right)\end{aligned}$$

where we use the identity

$$\langle x^{2n} \rangle = (2n - 1)!! \langle x^2 \rangle^n$$

See [51] for a demonstration.

Therefore, when amplitude fluctuations η are small compared to the average amplitude R_0 , we can write:

$$\langle \log R \rangle = \langle \log(R_0 + \eta) \rangle \approx \log(R_0) + \log \left[1 - \frac{1}{2} \frac{\langle \eta^2 \rangle}{R_0^2} - \frac{5}{8} \left(\frac{\langle \eta^2 \rangle}{R_0^2} \right)^2 \right] \quad (\text{A.1})$$

Appendix B

GL MODEL AND QUANTUM CHAIN

Starting with a classical hamiltonian H with nearest neighbour interaction in d dimension and a potential on site U , a transfer integral operator is used to transform the partition function of H to an eigenvalue problem. The latter is equivalent to a $d - 1$ Schroedinger equation with a potential U . To the continuum limit, the mapping is shown to be exact.

The transformation of quantum system in a classical model has been studied mainly with the formalism of the Feynman integral. With this transformation, one can show that a quantum model in $d - 1$ dimensions is formally equivalent to statistical system in d dimensions. There are many proofs of this transformation, but all start from the quantum system. However, in one case, the $1d$ Ginzburg-Landau model (a classical model), Scalapino, Sears and Ferrell (SSF) [34] have shown that this model is equivalent to the quantum double-well oscillator.

Here, we want to show the equivalence between a classical statistical system in d dimensions and a quantum model in $d - 1$ dimensions by using a transfer integral operator. Our calculation is a generalisation of the method used by SSF in 1 dimension to the d dimensional case of a n -component vector field.

We define the classical hamiltonian functional by

$$H[\psi] = \int d^d r \left[U(\psi) + \frac{\gamma}{2} |\nabla \psi|^2 \right] \quad (\text{B-1})$$

where U is a potential on site (U can be, for example, the Landau potential $U_L = -|\psi|^2 + 1/2|\psi|^4$). γ is a constant. The field ψ has n components: $\psi = \{\psi^{(1)}, \dots, \psi^{(n)}\}$. On the lattice, with lattice spacing ε , we separate H in hyperplanes of dimension $d - 1$ that are labeled by the indice μ . The indice $i = i_\mu$ runs over all spins of the hyperplane μ . (for $d = 2$ a hyperplane is a straight line, a hyperplane in $d = 3$ is a plane, etc)

$$H = \varepsilon^d \sum_{\mu, i} \left[U_i + \frac{\gamma}{2\varepsilon^2} (|\psi_{i\mu} - \psi_{i+1, \mu}|^2 + |\psi_{i\mu} - \psi_{i, \mu+1}|^2) \right]$$

where N is the number of site in a line and $U_i := U(\psi_i)$. We have also $N^d = S/\varepsilon^d$ where S is the surface of the hyperplane. The first interaction term $|\psi_{i\mu} - \psi_{i+1,\mu}|^2$ contains all interactions lying in the hyperplane whereas $|\psi_{i\mu} - \psi_{i,\mu+1}|^2$ contains interaction only for one direction between two hyperplanes. We define a multi-indices I_μ by

$$I_\mu = \{i_1, \dots, i_N\}_\mu$$

where μ is the indices of the hyperplane μ . The hamiltonian becomes then

$$H[\psi] = \sum_{\mu=1}^N [g(\mu) + f(\mu, \mu + 1)] \quad (\text{B-2})$$

where

$$g(\mu) = \varepsilon^d \sum_i \left[U_i + \frac{\gamma}{2\varepsilon^2} |\psi_{i\mu} - \psi_{i+1,\mu}|^2 \right]$$

and

$$f(\mu, \mu + 1) = \varepsilon^d \sum_i \frac{\gamma}{2\varepsilon^2} |\psi_{i\mu} - \psi_{i,\mu+1}|^2$$

$g(\mu)$ contains only interactions between spins in a single hyperplane μ , whereas $f(\mu, \mu + 1)$ contains interactions between two hyperplanes. The partition function is the trace over all configurations of the spins

$$Z = \int_{-\infty}^{+\infty} D\psi_{I_1} \dots D\psi_{I_N} e^{-\beta \sum_{\mu=1}^N [g(\mu+1) + f(\mu, \mu+1)]}$$

where $\int D\psi_{I_\mu} = \int d\psi_{1\mu} \dots d\psi_{N\mu}$ is the integral over one single hyperplane, and $\beta = 1/(k_B T)$.

B.1 The Transfer Operator

Following the same method for the one-dimensional case [34], we will now introduce a complete set of normalized eigenstates and derive the transfer operator integral. In order to break the periodic nature of our array, that is the bond between ψ_N and ψ_1 , we formally introduce a new field ψ'_1 and the complete set of normalized eigenstates χ_m :

$$\delta(\psi_{I_1} - \psi'_{I_1}) = \sum_m \chi_m^*(\psi'_{I_1}) \chi_m(\psi_{I_1}) \quad (\text{B-3})$$

where $\psi_{I_1} = \{\psi_1, \dots, \psi_N\}$. The function δ is the standard multidimensional Dirac *delta* function. The integral or trace of the partition function is then

$$\int D\psi_{I_1} \dots D\psi_{I_N} = \int \delta(\psi_{I_1} - \psi'_{I_1}) D\psi'_{I_1} D\psi_{I_1} \dots D\psi_{I_N}$$

Taking this new trace in the partition function yields

$$Z = \sum_m \int D\psi'_{I_1} \chi_m^*(\psi'_{I_1}) \int D\psi_{I_N} e^{-\beta[g(1') + f(N, 1')]} \dots \int D\psi_{I_1} e^{-\beta[g(2) + f(2, 1)]} \chi_m(\psi_{I_1})$$

where $1'$ is the hyperplane of vectors ψ'_{I_1} . We define the transfer integral operator by

$$\int D\psi_{I_\mu} e^{-\beta[g(\mu+1)+f(\mu+1,\mu)]} \chi_m(\psi_{I_\mu}) = e^{-\beta\varepsilon^d \lambda_m} \chi_m(\psi_{I_{\mu+1}}) \quad (\text{B-4})$$

The partition function is then

$$Z = \sum_m e^{-\beta N \varepsilon^d \lambda_m} = \sum_m e^{-\beta \sqrt{S} \lambda_m} \quad (\text{B-5})$$

For a thermodynamic system, we have $S \rightarrow \infty$, then only the lowest eigenvalue λ_0 contributes to the free energy density:

$$f = -k_B T \log Z = \lambda_0 \varepsilon / \sqrt{S} \quad (\text{B-6})$$

B.2 Reduction to a $d - 1$ Quantum Problem

The problem is now to find an equation that gives the eigenvalues λ_m of the transfer operator integral. To simplify our notation, we note respectively all vectors of hyperplanes μ and $\mu + 1$ by ψ and ϕ . The transfer integral operator (B-4) becomes:

$$e^{-\beta\varepsilon^d g(\phi)} \int D\psi e^{-\beta\varepsilon^2 f(\phi,\psi)} \chi_m(\psi) = e^{-\beta\varepsilon^d \lambda_m} \chi_m(\phi) \quad (\text{B-7})$$

In order to perform the integral, we will expand the function $\chi_m(\psi)$ about the nearest neighbours using the fact that the field is varying slowly over one bond:

$$\chi_m(\psi) = \chi_m(\phi) + \sum_{i=1}^N \frac{\partial \chi_m(\phi)}{\partial \phi_i} (\psi_i - \phi_i) + \frac{1}{2} \sum_{i=1, j=1}^N \frac{\partial^2 \chi_m(\phi)}{\partial \phi_i \partial \phi_j} (\psi_i - \phi_i) (\psi_j - \phi_j)$$

Integrals over odd terms are zero, such that the transfer integral is:

$$e^{-\beta\varepsilon^2 g(\phi)} \left(A \chi_m(\phi) + \frac{1}{2} \sum_{i=1}^N B \frac{\partial^2 \chi_m(\phi)}{\partial \phi_i^2} \right) = e^{-\beta\varepsilon^2 \lambda_m} \chi_m(\phi) \quad (\text{B-8})$$

where

$$A = \int D\psi e^{-\beta\varepsilon^2 f(\phi,\psi)} = \prod_{i=1}^N \int d\psi_i e^{-\beta\frac{\gamma}{2}(\psi_i - \phi_i)^2}$$

and

$$B = \int D\psi e^{-\beta\frac{\gamma}{2} f(\phi,\psi)} (\psi_i - \phi_i)^2 = \prod_{j \neq i}^N \int d\psi_j e^{-\beta\frac{\gamma}{2}(\psi_j - \phi_j)^2} \int d\psi_i e^{-\beta\frac{\gamma}{2}(\psi_i - \phi_i)^2} (\psi_i - \phi_i)^2$$

Keeping in mind that the field ψ has n components, we can evaluate these gaussian integrals:

$$A = \left(\frac{2\pi}{\beta\gamma} \right)^{nN/2} \quad B = A \frac{1}{\beta\gamma}$$

The transfer integral (B-8) is then

$$e^{-\beta\varepsilon^2 g(\phi)} A/\varepsilon^2 \left(\varepsilon^2 + \frac{\varepsilon^2}{2\beta\gamma} \sum_{i=1}^N \frac{\partial^2}{\partial\phi_i^2} \right) \chi_m(\phi) = e^{-\beta\varepsilon^2 \lambda_m} \chi_m(\phi) \quad (\text{B-9})$$

By rescaling the fields χ with the constant A/ε^2 , which changes only the origin of the energy, this last equation can be exponentiated and recombined to the same order in ε , such that the transfer integral (B-4) becomes then

$$e^{-\beta H_Q} \chi_m(\phi) = e^{-\beta\varepsilon^2 \lambda_m} \chi_m(\phi) \quad (\text{B-10})$$

where the quantum hamiltonian H_Q is defined as

$$H_Q = \varepsilon^2 \sum_{i=1}^N \left[-\frac{1}{2\beta^2\gamma} \frac{\partial^2}{\partial\phi_i^2} + U_i + \frac{\gamma}{2\varepsilon^2} |\phi_i - \phi_{i+1}|^2 \right] \quad (\text{B-11})$$

The case with $n = 2$ corresponds to a chain where the atoms have two degrees of freedom. For $n = 1$, oscillations remains strictly in one dimension. This is result seems to be reasonable. Indeed, we have change a 2d classical system in a 1d quantum system. This correspondence is well-known when using the formalism of path integrals to express a quantum system with classical variables. The second point is that the 1d GL model corresponds to the single quantum double-well oscillator, such that this principle of correspondence is preserved in both case.

Appendix C

REMERCIEMENTS :-)

J'aimerais remercier toutes les personnes qui ont permis l'élaboration de ce travail de thèse:

En premier lieu, j'aimerais mentionner mon directeur de thèse Hans Beck qui a toujours été disponible pour le dialogue malgré ses nombreuses tâches. Il a su également apporter l'expérience et les idées de la physique théorique sans lesquelles ce travail n'aurait pas pu aboutir.

Les experts, Piero Martinoli, Pierbiago Pieri et Nicolas Macris, qui ont pris la peine de lire ce travail.

et dans le désordre, Maxime (fancy headers), Alain (Valais), Luca (de D.), Romain (tunnel), Natascia (Italia), Sergei (Prosper!), et tous ceux que j'oublie...

Les gens du personnel technique notamment Daniel Varidel sans qui je n'aurais pas pu maintenir en vie les ordinateurs du réseau de la physique théorique.

Hubert Schneuwly qui m'a encouragé lors de mes études en physique, et qui m'a initié à la critique scientifique.

ma famille et mon amie Corina ♡.

Appendix D

LA RECHERCHE ACADÉMIQUE EN SUISSE: QUEL AVENIR?

Durant mon doctorat, j'ai pu constater de nombreuses différences entre les instituts dans les universités suisses concernant les conditions de travail. Elles sont bonnes dans certains instituts comme en physique à Neuchâtel, mais peuvent se révéler scandaleuses dans d'autres instituts. Il existe un institut dans une université suisse que je ne nommerai pas où les doctorants sont engagés à 50% mais doivent travailler 100% de leur temps pour le projet de recherche et l'assistantat.

De plus, dans le même institut, il existe certains doctorants payés deux fois plus que les autres. La seule raison est qu'ils ont suivi d'autres études. Mais ces doctorants, qui ont un traitement honorable au demeurant, font exactement le même travail que leurs autres collègues.

Toutes ces inégalités de traitements sont scandaleuses et contreproductives. Elles conduisent les collaborateurs à la frustration et à la démotivation. Comment encourager les gens à poursuivre une carrière dans la recherche académique dans de telles conditions?

Une conséquence de ce dumping salariale est que de plus en plus d'étrangers sous qualifiés entament des doctorats en Suisse. Dans le même institut mentionné plus haut, une place de doctorat est restée vacante six mois! Après ce temps, la première personne qui s'est présentée et a été prise. On peut douter de la qualité d'une telle procédure de recrutement...

Les assistants-doctorants ne sont plus des étudiants, et ne font pas de la recherche pour leur compte personnel. Ils accomplissent un travail de recherche nécessaire et approuvé par le fond national de la recherche scientifique et les universités. La formation qu'ils reçoivent est dirigée vers une plus grande efficacité dans le travail comme dans toute entreprise qui assure la formation continue de ses cadres.

En conclusion, la Suisse doit absolument réformer en profondeur son système académique pour que les instituts, qui propagent les inégalités et ne payent pas leur employés correctement, retrouvent la capacité d'attirer les meilleurs scientifiques. Le cadre intermédiaire des universités doit enfin être considéré à sa juste valeur. Le respect des conditions d'engagement, un cahier des charges précis et un salaire attractif doivent être établis partout. C'est à ce prix là seulement que la Suisse pourra reprendre la place qui était la sienne dans la science il y a vingt ans.

Bibliography

- [1] P. Curty and H. Beck, Phys. Rev. Lett. **85**, 796 (2000).
- [2] P. Curty and H. Beck, Phys. Rev. Lett. **91**, 257002 (2003).
- [3] H. Beck, P. Curty, A. Sewer, N. Andrenacci and S. Sharapov, Ukrainian J. Phys. **48**, 829 (2002).
- [4] J. Bardeen, L. Cooper and J. Schrieffer, Phys. Rev. **108**, 1175 (1957).
- [5] J. Bednorz and A. Mueller, Zeitschrift fuer Physik B **64**, 189 (1986).
- [6] Gao *et al.*, Phys. Rev. B **50**, 4260 (1994).
- [7] W. Warren and *et al*, Phys. Rev. Lett. **62**, 1193 (1989).
- [8] R. Walstedt, Phys. Rev. B **41**, 9574 (1990).
- [9] J.W. Loram *et al* , Phys. Rev. Lett. **71**, 1740 (1993).
- [10] M. Tinkham, *Introduction to Superconductivity* (McGraw-Hill, 1996).
- [11] Ch. Renner *et al*, Phys. Rev. Lett. **80**, 149 (1997).
- [12] V. Krasnov, A. Yurgens, D.Winkler, P. Delsing and T. Claeson, Phys. Rev. Lett. **86**, 2657 (2001).
- [13] V. Krasnov, A. E. Kovalev, A. Yurgens and D. Winkler, Phys. Rev. Lett. **86**, 2657 (2001).
- [14] T. Timusk and S. Bryan, Rep. Prog. Phys. **62**, 61 (1999).
- [15] Y. Wang *et al*, Phys. Rev. B **64**, 224519 (2001).
- [16] N. Goldenfeld, *Lectures on Phase Transitions and Renormalisation Group* (Addison-Wesley, 1992).
- [17] N. Nagaosa, *Quantum Field Theory in Condensed Matter Physics* (Springer, 1999).
- [18] P. G. de Gennes, *Superconductivity of Metals and Alloys* (Benjamin New York, 1966).

- [19] L. P. Gor'kov, Sov. Phys. JETP **7**, 505 (1958).
- [20] U. Wolff, Phys. Rev. Lett. **62**, 361 (1989).
- [21] R. C. Brower and P. Tamayo, Phys. Rev. Lett. **62**, 1087 (1989).
- [22] L. P. Gorkov, Zh. Eksperim. i Teor. Fiz. **36**, 1918 (1959).
- [23] M. Randeria, *Bose Einstein Condensation* (Cambridge UP, 1995).
- [24] E. Simanek, *Inhomogeneous Superconductors* (Oxford UP, 1994).
- [25] R. A. Pelcovits, PhD thesis, Harvard University, 1978.
- [26] J. J. Toner, PhD thesis, Harvard University, 1981.
- [27] K. G. Wilson, Rev. Mod. Phys. **55**, 583 (1983).
- [28] K. G. Wilson and M. E. Fisher, Phys. Rev. Lett. **28**, 240 (1972).
- [29] D. Bormann and H. Beck, J. Stat. Phys. **76**, 361 (1994).
- [30] P. Minnhagen and M. Wallin, Phys. Rev. B **28**, 5378 (1994).
- [31] B. I. Halperin, T. C. Lubensky and S.-K. Ma, Phys. Rev. Lett. **32**, 292 (1974).
- [32] V. J. Emery and S. A. Kivelson, Nature **374**, 4337 (1995).
- [33] H. Kleinert, *Gauge Fields in Condensed Matter* (, 1980).
- [34] D. J. Scalapino, M. Sears and R. A. Ferrell, Phys. Rev. B **6**, 3409 (1972).
- [35] N. Morozov, E. Zeldov, D. Majer and M. Konczykowski, Phys. Rev. B **54**, R3784 (1996).
- [36] J. W. Loram, K. A. Mirza, J. M. Wade, J. R. Cooper and W. Y. Liang, Physica C **134**, 235 (1994).
- [37] M. Capezzali and H. Beck, Physica B **259-261**, 501 (1999).
- [38] J. Schmalian *et al*, Phys. Rev. B **41**, 6399 (1990).
- [39] P. Lee, Physica C **317-318**, 194 (1999).
- [40] S.Sachdev, *Quantum Phase Transition* (Physics World, 1999).
- [41] T. Takigawa, *et al*, Phys. Rev. B **43**, 247 (1991).
- [42] P. Pieri *et al*, Phys. Rev. Lett. **89**, 127003 (2002).
- [43] P. Devillard *et al*, Phys. Rev. Lett. **84**, 5200 (2000).
- [44] B. L. Gyorffy *et al*, Phys. Rev. B **44**, 5190 (1991).

-
- [45] M. Kugler *et al*, Phys. Rev. Lett. **86**, 4911 (2001).
- [46] A. Sewer and H. Beck, Phys. Rev. B **64**, 15410 (2001).
- [47] T. Eckl, 2001, cond-mat/0110377.
- [48] J. Tallon and J. Loram, 2000, cond-mat/0005063.
- [49] D. Matthey *et al*, Phys. Rev. B **64**, 24513 (2001).
- [50] M. Capone *et al*, Phys. Rev. Lett. **88**, 126403 (2002).
- [51] M. Lebellac, *Des phénomènes critiques aux champs de jauges* (Editions du CNRS, 1990).

Index

- T^* , 51
- T_ϕ , 51
- Γ , 98
- ξ_k , 98
- \mathbb{I} , 72

- amplitude, 1, 49
- amplitude fluctuations, 43, 51, 53, 57, 82
- antiferromagnetism, 5, 52
- average value method, 57

- BCS, 3, 39
- Bogoliubov inequality, 43
- Bogoliubov-de Gennes, 25

- cluster, 32
- CPA, 71

- d-wave, 62, 78
- damping, 98
- detailed balance, 30
- diamagnetic susceptibility, 66
- differential conductance, 7, 67
- doping, 5, 51

- effective action, 55
- ergodicity, 29

- first order transition, 43
- fluctuations, 10
- Fourier-Matsubara transformation, 22
- frequency z , 98

- Ginzburg-Landau, 9, 30, 37, 57
- Green function, 17, 72

- Hall effect, 69

- harmonic approximation, 11
- high temperature superconductors, 3

- imaginary time, 15
- interaction representation, 15
- Ising, 29, 32

- Matsubara, 17
- Metropolis, 27
- Monte Carlo, 27, 42

- Nernst effect, 8, 69
- NMR, 6, 66

- pairing, 5
- phase diagram, 6, 68
- phase fluctuations, 43, 51
- phase stiffness, 40, 56
- phase transition, 9
- photoemission, 8
- pseudogap, 6, 51

- quantum critical point, 52

- renormalisation group, 14, 48

- s-wave, 63
- self-consistent, 37
- self-energy, 25, 95
- simulations, 45
- specific heat, 6, 61
- spin susceptibility, 66
- super-exchange, 5
- superconductivity, 3
- sweep, 31

- thermodynamics, 55
- tunneling, 7, 67

variational method, 56

vortex, 49

YBCO, 4, 62